

Systemic Amyloidosis – Insights by Cardiovascular Magnetic Resonance

By

Dr Sanjay M. Banypersad

MD (Res) Thesis

UCL

2015

1. Declaration

I, Sanjay Mahesh Banypersad, confirm that the work presented in this thesis is my own.
Where information has been derived from other sources, I confirm that this has been indicated in the thesis

Signature: Sanjay Banypersad
Sanjay Banypersad
(electronically signed)

Name: **Sanjay M. Banypersad**

Date: 13th April 2015

2. Abstract

Systemic amyloidosis is the exemplar infiltrative, extracellular disease. Although it is a multi-organ disorder, cardiac involvement drives prognosis. Survival is worst in the AL amyloidosis subtype. It can affect any age and any race. There is no direct test for amyloid burden and there is no treatment for amyloidosis, there is only treatment for the underlying condition. Earlier diagnosis permits prompt treatment and improves survival.

A number of imaging modalities exist to non-invasively detect cardiac disease but all have limitations. Cardiovascular magnetic resonance (CMR) with late gadolinium enhancement (LGE) imaging provides the highest sensitivity for early detection. However, this also has its shortcomings. There is currently no non-invasive method of directly measuring amyloid burden in the extracellular space. New therapies are pending – but their development needs new surrogate endpoints and new tests are therefore desperately needed. T1 mapping permits tissue abnormalities to be directly visualised in a simple scan – the colour changes being instantly recognisable, either before contrast (pre contrast or native T1 mapping) or after, when the myocardial extracellular volume (ECV) can be measured.

In a collaboration between the National Amyloidosis Centre and the Heart Hospital, I explored the possibility and potential that T1 mapping might measure cardiac (and other organ) involvement in systemic amyloidosis using EQ-MRI.

In early clinical exploration in systemic AL amyloid, I showed that native myocardial T1 was elevated in cardiac amyloidosis and tracked disease, particularly early disease. Mean pre contrast myocardial T1 as measured by ShMOLLI was higher in patients at 1086 ± 90 msec, compared to healthy volunteers of 958 ± 20 msec ($P<0.001$). Myocardial T1 times showed a stepwise elevation as the probability for cardiac involvement increased: 1009 ± 31 msec without cardiac involvement, 1048 ± 48 msec with possible cardiac involvement, 1140 ± 61 msec with definite cardiac involvement ($P<0.001$).

Using contrast to measure the ECV, I was able to non-invasively and directly measure the amyloid burden in the heart for the first time. Mean cardiac ECV was greater in patients compared to healthy volunteers with a wider range (0.44 ± 0.12 vs 0.25 ± 0.02 , $P<0.001$) and

tracked pre-test probability of cardiac involvement by conventional parameters ($P<0.001$). ECV also tracked conventional measures of disease severity and correlated with survival with a median ECV of 0.45 being the best model for assessing survival: HR 3.84 (1.53 – 9.61), $P=0.004$. I demonstrated good reproducibility of the technique with an ICC of > 0.9 for both the FLASH IR and ShMOLLI techniques of T1 mapping and good agreement of ECV derived from both techniques. In pilot studies, I also demonstrated by serial scanning that changes (including regression) over time could be measured.

In other organs, I showed that the amyloid burden could be measured and was higher in amyloidosis compared to healthy volunteer: ECV 0.32 vs 0.29 ($P<0.001$) for liver, 0.39 vs 0.34 ($P<0.001$) for spleen and 0.16 vs 0.09 ($P<0.001$) for skeletal muscle. These ECVs also tracked current conventional measures of disease severity by nuclear scintigraphy.

These results demonstrate that the interstitial volume in patients with systemic AL amyloidosis can be measured non invasively in the heart, liver, spleen and skeletal muscle and that this correlates with existing markers of disease and survival. Pre contrast myocardial T1 was a good alternative measure for the heart.

In conclusion, the work in this thesis has enabled a deeper understanding of cardiac amyloidosis, disease processes and stages. It has pioneered a new prognostic marker that is also able to identify some patients with cardiac involvement that were previously unrecognised. Novel subtypes are now recognised (e.g. cardiac amyloidosis with no LVH) and it has also allowed direct quantification of the liver and spleen. ECV is a new and powerful biomarker that has already been adopted by industry allowing development of new therapies and providing hope that an end to the scourge of this disease is near.

3. Abbreviations

6MWT	6 Minute Walking Test
AA	Amyloid (serum amyloid A)
ACE-i	Angiotensin Converting Enzyme inhibitor
AF	Atrial Fibrillation
AFD	Anderson Fabry's disease
AHA	American Heart Association
AL	Amyloid Light-chain
ANOVA	Analysis of Variance
ANP	Atrial Natriuretic Peptide
ApoA1	Apolipoprotein A1
ARB	Angiotensin Receptor Blocker
AS	Aortic stenosis
ASCT	Autologous Stem Cell Transplant
ATTR	Amyloid Transthyretin
AV	Atrioventricular
AVR	Aortic Valve Replacement
BCS	British Cardiovascular Society
BHF	British Heart Foundation
BNP	Brain Natriuretic Peptide
BP	Blood Pressure
CI	Confidence Intervals
CMR	Cardiovascular Magnetic Resonance
CPHPC	R-1-[6-[R-2-carboxy-pyrrolidin-1-yl]-6-oxo-hexanoyl] pyrrolidine-2-carboxylic acid
CR	Complete (light chain) Response
CSF	Cerebrospinal Fluid
CT	Computed Tomography
CTD	Cyclophosphamide, Thalidomide (and) Dexamethasone
CVD	Cyclophosphamide, Velcade (and) Dexamethasone
DCM	Dilated Cardiomyopathy
DNA	Deoxyribonucleic Acid

DOTA	1,4,7,10-tetraazacyclododecane-1,4,7,10-tetraacetic acid
DPD	3,3-diphosphono-1,2-propanodicarboxylic acid
ECG	Electrocardiogram
ECOG	Eastern Cooperative Oncology Group
ECV	Extracellular Volume
ECV _b	Extracellular Volume (bolus only method)
ECV _i	Extracellular Volume (infusion method)
EF	Ejection Fraction
eGFR	Estimated Glomerular Filtration Rate
EMG	Electromyogram
EQ-CMR	Equilibrium (contrast) Cardiovascular Magnetic Resonance
FAP	Familial Amyloid Polyneuropathy
FISP	Fast Imaging with Steady State Precession
FLASH (IR)	Fast Low Angle Shot (Inversion Recovery)
FOV	Field of View
GAGS	Glycosaminoglycans
GE	General Electric
GI	Gastrointestinal
GSK	Glaxo Smith Kline
HCM	Hypertrophic Cardiomyopathy
HR	Hazard Ratio
IBM	International Business Machine (Corporation)
ICC	Intraclass Correlation Coefficient
ICD	Implantable Cardioverter Defibrillator
IQ	Interquartile (range)
IVRT	Isovolumic Relaxation Time
KM	Kaplan Meier
LA	Left Atrium
LAA	Left Atrial Area
LBBB	Left Bundle Branch Block
LGE	Late Gadolinium Enhancement
Ln	Natural logarithm
LV	Left Ventricle
LVEDV(i)	Left Ventricular End Diastolic Volume (indexed)

LVESV(i)	Left Ventricular End Systolic Volume (indexed)
LVH	Left Ventricular Hypertrophy
MAPSE	Mitral Annular Plane Systolic Excursion
MGUS	Monoclonal Gammopathy (of) Undetermined Significance
MI	Myocardial Infarction
MOLLI	Modified Look Locker Inversion (recovery)
MRI	Magnetic Resonance Imaging
msec	Milliseconds
mV	Millivolts
NAC	National Amyloidosis Centre
NHS	National Health Service
NNE	Nearest Neighbour Estimator
NT-proBNP	Nitrogen-Terminal Brain Natriuretic Peptide
NYHA	New York Heart Association
PET	Positron Emission Tomography
PR	Partial (light chain) Response
PSIR	Phase Sensitive Inversion Recovery
REDCap	Research Electronic Data capture
RF	Radiofrequency
RNA	Ribonucleic acid
ROC	Receiver Operating Characteristic
ROI	Region of Interest
RV	Right Ventricle
SAA	Serum Amyloid A
SAP	Serum Amyloid P
SASHA	Saturation-recovery Single-shot Acquisition
SCMR	Society (of) Cardiovascular Magnetic Resonance
SD	Standard Deviation
ShMOLLI	Shortened Modified Look Locker Inversion (recovery)
SPECT	Single Photon Emission Computed Tomography
SPSS	Statistical Package (for the) Social Sciences
SSA	Senile Systemic Amyloidosis
SSFP	Steady State Free Precession
TAPSE	Tricuspid Annular Plane Systolic Excursion

TD	Trigger delay
TDI	Tissue Doppler Imaging
TE	Echo Time
TI	Inversion Time
TNF	Tumour Necrosis Factor
TR	Repeat Time
TTR	Transthyretin
VIF	Variance Inflation Factor
VT	Ventricular Tachycardia

4. Contents

<u>Chapter</u>		<u>Page</u>
1	Declaration	2
2	Abstract	3
3	Abbreviations	5
4	Contents	9
	4.1 Figures	15
	4.2 Tables	17
5	Aims and Objectives	18
6	Introduction	19
	6.1 What is Amyloidosis?	19
	6.2 What is Systemic Amyloidosis?	20
	6.3 Cardiac Disease in Amyloidosis	23
	6.3.1 AL Amyloidosis	23
	6.3.2 Hereditary (ATTR) Amyloidosis	24
	6.3.3 Senile Systemic Amyloidosis	25
	6.3.4 Other types of cardiac amyloidosis	26
	6.4 Diagnosis	26
	6.4.1 ECG	26
	6.4.2 Echocardiography	28
	6.4.3 Cardiac biomarkers	29
	6.4.4 Radionuclide Imaging	30
	6.4.5 Cardiac MRI	31
	6.4.6 Endomyocardial biopsy	33

6.5	Liver and Spleen in Systemic Amyloidosis	34
6.6	Skeletal muscle in Systemic Amyloidosis	35
6.7	Prognosis	35
6.8	Treatment	36
6.8.1	Non Amyloid Specific	36
6.8.1.1	<i>Heart Failure Therapy</i>	36
6.8.1.2	<i>Device Therapy</i>	36
6.8.1.3	<i>Cardiac Transplantation</i>	37
6.8.2	Amyloid Specific	37
6.8.2.1	<i>Reducing Amyloid Fibril Precursor Protein Production</i>	37
6.8.2.2	<i>Inhibition of Amyloid Formation</i>	39
6.8.2.3	<i>Targeting Amyloid Deposits by Immunotherapy</i>	40
6.9	Measuring Interstitial Expansion using MRI	41
6.9.1	MRI General Physics	41
6.9.2	T1 mapping	43
6.10	Equilibrium cardiovascular magnetic resonance	45
7	Methods	52
7.1	Ethical approval	52
7.2	Patients	52
7.3	Healthy Volunteers	54
7.4	CMR	54
7.4.1	Pilot Images	54
7.4.2	Cine Imaging	55
7.4.3	Pre contrast T1 assessment	55
7.4.3.1	<i>FLASH Heart</i>	55

7.4.3.2 <i>FLASH Liver, Spleen and Skeletal Muscle</i>	56
7.4.3.3 <i>ShMOLLI Heart, Liver and Spleen</i>	57
7.4.4 LGE Imaging	57
7.4.5 Post Contrast T1 Evaluation	58
7.4.6 Off line Analysis	58
7.5 Blood pressure and ECG	58
7.6 Blood Tests	59
7.7 6 minute walk testing	59
7.8 Echocardiography	59
7.9 SAP scintigraphy	59
7.10 DPD scintigraphy	60
7.11 Statistical Analysis	60
8 Results: Myocardial ECV as measured by EQ-CMR in Systemic AL Amyloidosis	63
8.1 Introduction	63
8.2 Hypotheses	64
8.3 Methods	64
8.4 Results	66
8.5 Discussion	72
8.6 Conclusion	74
9 Results: Extracardiac ECV as measured by EQ-CMR in Systemic AL Amyloidosis	75
9.1 Introduction	75
9.2 Hypotheses	76
9.3 Methods	76
9.4 Results	76
9.5 Discussion	78

9.6	Conclusion	81
10	Results: Technical Development – Refining Clinical Applicability	82
10.1	Introduction	82
10.2	Hypotheses	84
10.3	Methods	84
10.4	Results	84
10.5	Discussion	87
10.6	Conclusion	88
11	Results: Pre Contrast T1 Mapping in Systemic AL Amyloidosis	89
11.1	Introduction	89
11.2	Hypotheses	90
11.3	Methods	90
11.4	Results	91
11.5	Discussion	95
11.6	Conclusion	97
12	Results: T1 Mapping and Survival in Systemic AL Amyloidosis	98
12.1	Introduction	98
12.2	Hypotheses	98
12.3	Methods	99
12.4	Results	100
12.5	Discussion	108
12.6	Conclusion	110
13	Results: Pilot Study – Follow up in AL Amyloid	111
13.1	Introduction	111
13.2	Hypotheses	111

13.3	Methods	112
13.4	Results	112
13.5	Discussion	115
13.6	Conclusion	117
14	Discussion and Conclusions	118
14.1	Background and hypothesis explored	118
14.2	Technical development	119
14.3	ECV	120
14.4	Native T1 mapping	120
14.5	Clinical insights	121
14.6	Future work	122
14.7	Conclusions	123
15	References	124
16	Appendix	143
16.1	Acknowledgements	143
16.2	List of original findings	145
16.3	Location of research	145
16.4	Personal contribution	145
16.5	Supervision	146
16.6	Funding	146
16.7	Prizes / Awards	146
16.8	Publications	146
16.9	Abstract presentations	149
16.9.1	Oral Presentations	149
16.9.2	Poster Presentations	149

Figures & Tables

4.1 Figures

	<u>Page</u>
Figure 1: Cardiac biopsy in AL Amyloidosis	20
Figure 2: ECG appearances in cardiac amyloidosis	27
Figure 3: Speckle tracking in cardiac amyloidosis	28
Figure 4: DPD imaging in ATTR amyloidosis	31
Figure 5: Global subendocardial LGE in cardiac amyloidosis	32
Figure 6: Alternative LGE appearances on CMR in cardiac amyloidosis	32
Figure 7: Post gadolinium T1 scout appearances in cardiac amyloidosis	33
Figure 8: SAP scan image in AL and ATTR amyloidosis	34
Figure 9: SAP scan image in AA amyloidosis	35
Figure 10: Diagram illustrating mode of action of CPHPC and antibody	41
Figure 11: MRI recovery curve demonstration T1 times	42
Figure 12: Graph showing changes in gadolinium concentration with time in myocardium and blood	43
Figure 13: Pre contrast T1 scout in cardiac amyloidosis	43
Figure 14: Schematic showing recovery curves in ShMOLLI	44
Figure 15: ShMOLLI image in normals and amyloidosis	45
Figure 16: FLASH T1 measurement for heart	46
Figure 17: Graph showing change in signal intensity with T1	46
Figure 18: Graph showing change in T1 with time with and without infusion	47
Figure 19: Graph showing change in signal intensity with T1 for myocardium and blood pre and post contrast administration	48
Figure 20: Graph showing correlation of ECV with collagen in AS	49
Figure 21: Mean ECV in various cardiac diseases	50
Figure 22: FLASH T1 measurement for liver, spleen and muscle	56
Figure 23: Pie chart of biopsies for AL amyloidosis patients	65
Figure 24: Difficulty avoiding LGE when drawing ROI in T1 measurement	66
Figure 25: Relationship of ECV with pre-test probability of cardiac amyloidosis	68

Figure 26: Graphs showing relationship of ECV with LV structure	69
Figure 27: Graphs showing relationship of ECV with LV function	69
Figure 28: Graphs showing relationship of ECV with ECG and biomarkers	70
Figure 29: Graphs showing ECV of liver, spleen and muscle	77
Figure 30: Liver, spleen and muscle ECV with SAP grade	78
Figure 31: FLASH vs ShMOLLI reproducibility for cardiac ECV	85
Figure 32: FLASH vs ShMOLLI reproducibility for liver ECV	85
Figure 33: FLASH vs ShMOLLI reproducibility for spleen ECV	86
Figure 34: ECV_i vs ECV_b correlation and agreement	86
Figure 35: Interstudy reproducibility for cardiac ECV using ShMOLLI	87
Figure 36: Pie chart of biopsies for AL amyloidosis patients in native myocardial T1 chapter	90
Figure 37: Relationship of T1 with pre-test probability of cardiac amyloidosis	92
Figure 38: ROC curve analysis for T1 and amyloidosis	93
Figure 39: Typical appearances of T1 map and LGE in amyloidosis	94
Figure 40: Relationship of T1 with markers of cardiac amyloidosis	95
Figure 41: Pie chart of biopsies for AL amyloidosis patients in T1 mapping and survival chapter	99
Figure 42: Dot plot showing correlation between ECV and late gadolinium enhancement	103
Figure 43: Kaplan Meier survival curve for ECV_i	105
Figure 44: Kaplan Meier survival curve for ECV_b and T1	105
Figure 45: Time-dependent ROC curves for ECV and pre contrast myocardial T1 at 12 and 24 months using the NNE method	106
Figure 46: Time-dependent ROC curves for ECV and pre contrast myocardial T1 at 24 months using the KM method	107
Figure 47: Scatter plot of changes for ECV with treatment	114

4.2 TABLES:

Table 1: Pathology, presentation and management of different amyloid types	22
Table 2: Patient baseline characteristics for ECV using FLASH EQ-CMR chapter	67
Table 3: Pearson's correlations for myocardial ECV (FLASH) with cardiac measures	71
Table 4: Patient baseline characteristics for native myocardial T1 chapter	91
Table 5: Native myocardial T1 results and diastolic measures for AL patients	95
Table 6: Patient baseline characteristics for T1 mapping and survival chapter	101
Table 7: Correlations for ECV, native & post contrast T1 with cardiac measures	102
Table 8: Hazard ratios and Harrell's C statistic for ECV, native & post contrast T1	104
Table 9: Hazard ratios from univariate analyses of multiple variables with mortality	107
Table 10: Hazard ratios from multivariable analysis	108
Table 11: ECV and other parameter changes from baseline to follow up	113
Table 12: Difference in amyloid mass and cell mass from baseline to follow up	115

5. Aims & Objectives

This thesis investigates the use of novel methods in cardiovascular magnetic resonance (CMR) for the investigation of the extracellular space of multiple organs in systemic amyloidosis. As in all science, it is built on the work of others – key methods were developed at Heart Hospital by my colleagues: (a) Dr Andrew Flett (UCL MD (Res), 2012) who designed and validated the use of EQ-CMR to measure myocardial fibrosis in aortic stenosis and hypertrophic cardiomyopathy; and (b) Dr. Daniel Sado (UCL MD (Res), 2013) who explored the role of ECV measurement (again for fibrosis) across a variety of cardiac diseases. My thesis built on this, but in amyloidosis.

The aims are:

- 1) To investigate new potential markers of myocardial abnormality - ECV and native myocardial T1 measurement in cardiac amyloidosis, comparing the results to other clinical markers of disease severity.
- 2) To translate these methods to other organs - the liver, spleen and skeletal muscle in patients with systemic amyloidosis.
- 3) To improve ECV and T1 measurement techniques in CMR allowing quicker, more reproducible assessment for clinical delivery and as a surrogate endpoint for clinical trials
- 4) To create new hypotheses and aid in the recruitment and training of new researchers to continue this work, concurrently presenting and publishing the results, with the overall aim of bringing therapy and understanding of amyloid a step closer for patients; a step closer to improved outcomes for patients.

6. Introduction

This chapter is based on the publication below:¹

Banypersad SM, Moon JC, Whelan C, Hawkins PN, Wechalekar AD. *Updates in cardiac amyloidosis: a review.* *J Am Heart Assoc.* 2012 Apr;1(2):e000364

My contribution was to research the material and write the paper.

6.1 WHAT IS AMYLOIDOSIS?:

Amyloidosis is a generic term that refers to the extracellular deposition of autologous protein in an abnormal, insoluble β -pleated sheet, fibrillary conformation i.e. as amyloid fibrils. More than 30 proteins are known to be able to form amyloid fibrils *in vivo*, which cause disease by progressively damaging the structure and function of affected tissues.² Amyloid deposits also contain minor non-fibrillary constituents including serum amyloid P component (SAP), apolipoprotein, connective tissue components such as glycosaminoglycans (GAGS) and collagen, and basement membrane components such as fibronectin and laminin.³⁻⁷ Amyloid deposits can be massive and cardiac or other tissues may become substantially replaced.

Amyloid fibrils bind Congo red stain, yielding the pathognomonic apple-green birefringence under cross-polarized light microscopy that remains the gold standard for identifying amyloid deposits. Further staining with immunohistochemistry is performed to subtype into the 2 main types which affect ventricular myocardium, light chain amyloid (AL) and transthyretin amyloid (ATTR) (see figure 1).

Data regarding the molecular mechanisms at work in the extracellular space is rapidly accumulating. Autopsy studies of ventricular myocardium reveal homogeneous, eosinophilic deposits separating the muscle fibres and amorphous hyaline deposits that are predominantly seen in the expanding extracellular space.⁸ Molecular chaperones, such as clusterins, have been found to be over-represented in electron-microscopy analysis of cardiac biopsies in both AL and ATTR Amyloidoses.⁹

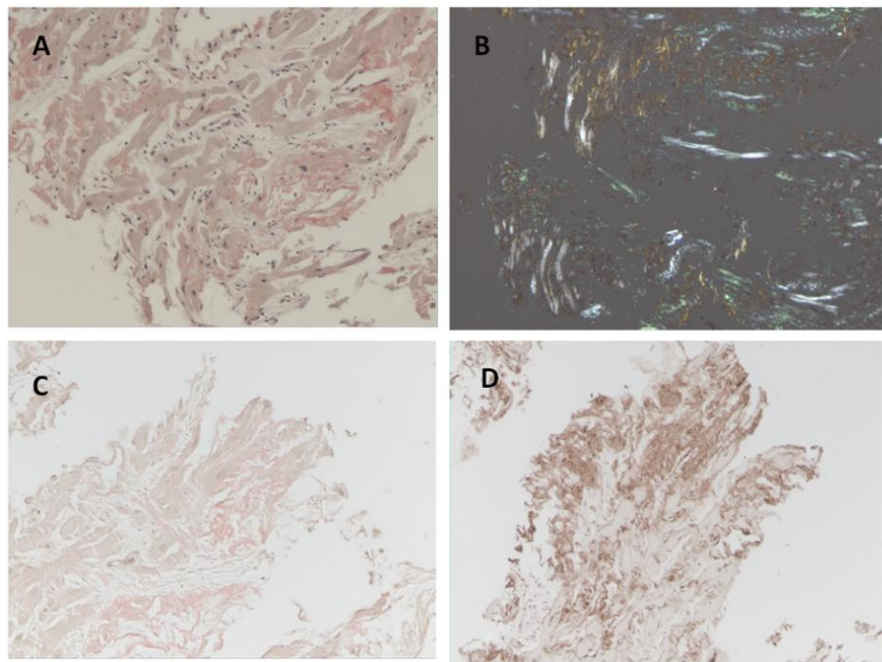


Figure 1: An endomyocardial biopsy of a patient with cardiac AL amyloidosis stained as follows: (A) Congo Red only; (B) Apple-green birefringence under cross-polarized light; (C) Congo Red with lambda overlay (negative); (D) Congo Red with kappa overlay (positive).

Studies of matrix metalloproteinases and their tissue inhibitors have suggested a direct effect of the activation of proteolysis in the extracellular matrix by circulating immunoglobulin light chains.¹⁰ This may explain the long recognised observation that in primary AL amyloidosis, even mild to moderate ventricular thickening can cause significantly debilitating symptoms whereas the patient with an equivalent wall thickness in ATTR amyloid is often asymptomatic.¹¹

6.2 WHAT IS SYSTEMIC AMYLOIDOSIS?:

Systemic amyloidosis is the exemplar of a purely extracellular disease; it is a relatively rare multisystem disease caused by the deposition of misfolded protein in various tissues and organs, causing organ dysfunction through interstitial expansion. It may present to almost any specialty and diagnosis is frequently delayed.¹² There are several different types of amyloid. As previously mentioned, the ventricles are primarily affected by AL and ATTR types; ATTR amyloid is further sub-divided into Senile Systemic Amyloidosis (SSA) and variant ATTR (see sections 6.3.2 and 6.3.3 later in this thesis).

Clinical phenotype varies greatly between different types of amyloidosis, and even the cardiac presentation has a great spectrum. The incidence of amyloidosis is uncertain, but it is thought that the most frequently diagnosed type, AL amyloidosis, has an annual incidence of 6-10 cases per million population in the UK and US. Wild type transthyretin (TTR) amyloid deposits, which predominantly accumulate in the heart, are very common at autopsy in the elderly and whilst the associated clinical syndrome known as senile systemic amyloidosis is diagnosed rarely in life,¹³ there is increasing evidence that this disorder is much under-diagnosed, and that with increasing longevity and improved diagnostic methods, it may be identified as a substantial public health problem.

Key ‘red flags’ to the diagnosis of possible systemic amyloidosis include: nephrotic syndrome, autonomic neuropathy (postural hypotension, diarrhoea), soft tissue infiltration (macroglossia, carpal tunnel syndrome), cutaneous bleeding (periorbital, gastrointestinal), malnutrition/cachexia and genetic predisposition (family history/ethnicity). Other organ involvement, particularly in AL amyloidosis, may cloud the cardiac presentation (nephrotic syndrome, autonomic neuropathy, pulmonary or bronchial involvement). Table 1 on the next page gives an outline of the clinical phenotype of the common amyloid subtypes.

Amyloid type	Precursor protein	Typical decade of presentation	Cardiac involvement	Other organ involvement	Treatment	Prognosis (median survival)
Primary (AL) Amyloidosis	Monoclonal light chain	6 th to 7 th decade (but can be any)	40-50%	Renal, liver, soft tissue, neuropathy	Chemotherapy or ASCT	48 months but 8 months for advanced stage disease.
Transthyretin Amyloidosis: consisting of:						
Senile Systemic (SSA)	Wild-type TTR	70 years	Almost all cases	carpal tunnel syndrome	Supportive	7-8 years
ATTR (V30M)	Variant TTR	3 rd or 4 th decade	Uncommon	Peripheral and autonomic neuropathy	Liver transplantation	Good with liver transplant for V30M
ATTR (T60A)	Variant TTR	6 th decade	Up to 90% by diagnosis	Peripheral and autonomic neuropathy	Liver transplant possible in selected	Variable with liver transplant
ATTR Ile 122	Variant TTR	6 th – 7 th decade	Almost all cases	carpal tunnel syndrome	Supportive	7-8 years
Apolipoprotein A1 (ApoA1)	Variant apolipoprotein	6 th – 7 th decade	Rare	Predominantly renal	Renal (+/- liver) transplant	Usually slowly progressive (years)
Secondary (AA) amyloidosis	Serum amyloid A (SAA)	Any	Rare	Renal, liver	Treat underlying condition	Good
Atrial natriuretic peptide (ANP)	ANP	70 years or older	All cases (uncertain significance)	None reported	Not needed	-

Table 1: summarising the pathology, presentation and management of different amyloid types

6.3 CARDIAC DISEASE:

Ventricular cardiac involvement is a leading cause of morbidity and mortality, especially in primary (AL) amyloidosis and in both wild type and hereditary transthyretin amyloidosis. The heart is also occasionally involved in acquired AA amyloidosis, other rare hereditary types, and there is a specific atrial subtype (ANP).

Cardiac amyloidosis affecting the ventricles, irrespective of type, presents as a restrictive cardiomyopathy caused by interstitial expansion due to the amyloid and is characterized by progressive diastolic and subsequently systolic biventricular dysfunction and arrhythmia.¹² Initial presentations may be cardiac with progressive exercise intolerance and heart failure. Pulmonary oedema is not common early in the disease process,¹⁴ but pleural and pericardial effusions and atrial arrhythmias are often seen.^{15, 16} Syncope is common and a poor prognostic sign.¹⁷ It is typically exertional or post-prandial as part of either restrictive cardiomyopathy, sensitivity to intravascular fluid depletion from loop diuretics combined with autonomic neuropathy, or conduction tissue involvement (AV or sinus nodes) or ventricular arrhythmia.¹⁸⁻²⁰ The latter may rarely cause recurrent syncope.

Disproportionate septal amyloid accumulation mimicking hypertrophic cardiomyopathy (HCM) with dynamic left ventricular outflow tract obstruction²¹⁻²⁴ is rare, but well documented. Myocardial ischaemia can result from amyloid deposits within the microvasculature.^{25, 26} Atrial thrombus is common, particularly in AL amyloidosis, sometimes before atrial fibrillation (AF) occurs.²⁷ Intracardiac thrombus can embolise, causing transient ischaemic attacks or strokes and may be an early or even presenting feature.²⁸ Anticoagulation is therefore important in the appropriate clinical situation but careful consideration has been given in patients with extensive systemic AL amyloidosis who may have an elevated bleeding risk seen due to Factor X deficiency or in some cases with GI involvement.²⁹

6.3.1 AL Amyloidosis:

AL amyloidosis is caused by deposition of fibrils composed of monoclonal immunoglobulin light chains, and is associated with clonal plasma cell or other B-cell dyscrasias. The fibrils in AL amyloidosis are derived from the variable region of lambda light

chains in approximately 75% of cases, and kappa in the remainder.³⁰ In approximately 10% of cases, the disorder overlaps with overt multiple myeloma.

The spectrum and pattern of organ involvement is very wide, but cardiac involvement occurs in half of cases and is sometimes the only presenting feature.³¹ Cardiac AL amyloidosis may be rapidly progressive. Low QRS voltages, particularly in the limb leads are common. Thickening of the left ventricular wall is typically mild to moderate, and is rarely greater than 18mm, even in advanced disease. Cardiac AL amyloid deposition is accompanied by marked elevation of the biomarkers brain natriuretic peptide (BNP, specifically NT-proBNP) and cardiac troponin, even at an early stage. The right heart failure is often exacerbated by the co-presence of nephrotic syndrome in 30-50% of cases.¹² The hypoalbuminaemia of nephrotic syndrome is itself exacerbated by concomitant liver disease. Hypotension can be present not only because of a “low-output” state, but also because of associated autonomic neuropathy.

Involvement of the heart is the commonest cause of death in AL amyloidosis, and a major determinant of prognosis; without cardiac involvement, AL amyloidosis has a median survival of around 4 years³² but the prognosis among affected patients with markedly elevated BNP and cardiac troponin (Mayo stage III disease)³³ is in the order of 6-8 months.

6.3.2 Hereditary Amyloidoses:

Mutations in a number of genes, such as TTR, fibrinogen, apolipoprotein A1 and A2 can be responsible for hereditary amyloidosis but by far the most common cause is variant ATTR amyloidosis, caused by point mutations in the TTR gene leading to neuropathy and often, cardiac involvement.

TTR is synthesised in the liver and a number of point mutations are described (see table 1) but the most common is the Val122Ile mutation.^{34, 35} In a large autopsy study that included individuals with cardiac amyloidosis, the TTR Val122Ile allele was present in 3.9% of all African Americans and 23% of African Americans with cardiac amyloidosis. Penetrance of the mutation is not truly known and is associated with a late-onset cardiomyopathy that is indistinguishable from SSA. Although the prevalence of disease caused by this mutation is unknown, recent evidence suggests it is almost certainly underdiagnosed,³⁶ since the wall thickening is often incorrectly attributed to hypertensive heart disease. The male to female

ratio is around 50:50, in contrast to a slight male predilection in AL amyloid with cardiac involvement.²³

Over 100 genetic variants of TTR are associated with amyloidosis. Most present as the clinical syndrome of progressive peripheral and autonomic neuropathy. Unlike wild type ATTR or variant ATTR Val122Ile, the features of other variant ATTR include, vitreous amyloid deposits or rarely deposits in other organs. Cardiac involvement in variant ATTR varies by mutations and can be the presenting, or indeed the only clinical feature.³⁷ For example, cardiac involvement is rare in variant ATTR associated with Val30Met (a common variant in Portugal or Sweden), but is almost universal and develops early in individuals with variant ATTR due to Thr60Ala mutation (a mutation common in Ireland).

Mutations in apolipoprotein A1 gene can cause systemic amyloidosis, typically causing renal and hepatic involvement - although cardiac involvement is well recognised.³⁸

6.3.3 Senile Systemic Amyloidosis:

Wild type TTR amyloid deposits are found at autopsy in about 25% of individuals older than 80 years, but their clinical significance has not been clear³⁹⁻⁴¹ The epidemiological studies assessing the prevalence of wild type TTR deposits, leading to the clinical syndrome of wild type ATTR cardiac amyloidosis, remains to be ascertained but is distinct and clearly far rarer. Wild Type ATTR is a predominant cardiac disease and the only other significant extracardiac feature is a history of carpal tunnel syndrome, often preceding heart failure by 3-5 years.^{42, 43} Extracardiac involvement is most unusual.

Both wild type ATTR as well as ATTR due to Val122Ile are diseases of the over 60 year old age group and are often misdiagnosed as hypertensive heart disease.¹⁴ Wild Type ATTR has a strong male predominance and the natural history remains poorly understood, but studies suggest a median survival of about 6-7 years from presentation.^{39, 40} The true incidence of wild type ATTR is probably underestimated³⁶ and recent developments in CMR, which have greatly improved detection of cardiac amyloid during life, suggest that wild type ATTR is more common than previously thought – it accounted for 0.5% of all patients seen at the UK amyloidosis centre until 2001 but now accounts of 7% of 1100 cases with amyloidosis seen since end of 2009.⁴⁴ This observation is also in part explained by the ageing population.

There appears to be an association between wild type ATTR and history of myocardial infarction (MI), G/G (Val/Val) exon 24 polymorphism in the alpha2-macroglobulin (alpha2M), and the H2 haplotype of the tau gene;⁴⁵ the association of tau with Alzheimer's disease raises interesting questions as both are amyloid-associated diseases of ageing. Whilst the echocardiographic manifestations of cardiac ATTR may be indistinguishable from advanced AL amyloidosis, patients with the former typically have fewer symptoms and better survival.⁴⁶

6.3.4 Other types of cardiac amyloidosis:

Localised atrial amyloid deposits derived from atrial natriuretic peptide (ANP), are associated with AF, notably post operatively^{14, 47} and become ubiquitous with age, being present at autopsy in 80% of over 70s.^{48, 49} The significance and causality of ANP amyloid deposits remain unknown. Amyloid of as yet unknown fibril type is also common in explanted cardiac valves.^{50, 51} Systemic AA amyloidosis complicating chronic inflammatory diseases, in which the amyloid fibrils are derived from the acute-phase reactant, serum amyloid A (SAA) protein, involves the heart in about 2% of cases with systemic AA amyloidosis. Incidence of AA amyloidosis is generally in decline, likely reflecting better treatment for rheumatological disorders with biological agents.

6.4 DIAGNOSIS AND EVALUATION OF CARDIAC AMYLOIDOSIS:

6.4.1 Electrocardiography (ECG):

Low QRS voltages (all limb leads <5 mm in height) with poor R wave progression in the chest leads (pseudoinfarction pattern) occur in up to 50% of patients with cardiac AL amyloidosis.⁵² The combination of low ECG voltage with concentrically increased wall thickness is highly suspicious for cardiac amyloidosis (see figure 2), but voltage criteria for left ventricular hypertrophy (LVH) can nevertheless sometimes occur.⁵³⁵⁴

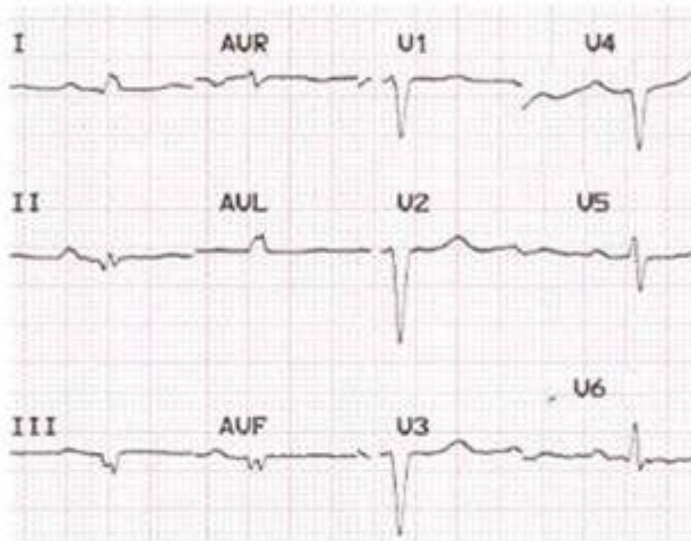


Figure 2: ECG of a patient with Cardiac AL Amyloidosis showing small QRS voltages (defined as $\leq 6\text{mm}$ height), predominantly in the limb leads and pseudoinfarction pattern in the anterior leads.

A recent, small evaluation of ECGs in cardiac AL amyloidosis⁵² supported the findings of the largest reported ECG series of 127 patients with AL amyloidosis and biopsy-proven cardiac involvement seen at the Mayo Clinic. The 2 most common abnormalities were low voltage (particularly in the limb leads) and a pseudoinfarction pattern, which were seen in 45-50% of cases. The mechanisms, however, are poorly understood.

Other findings include first degree atrioventricular (AV) block (21%), nonspecific intraventricular conduction delay (16%), second or third degree AV block (3%), AF/flutter (20%), and ventricular tachycardia (VT) (5%).⁵³ Left (LBBB) and right bundle branch block can also occur.²³ ECG patterns can provide clues to differentiate between AL and ATTR amyloidosis: LBBB is seen in 40% of patients with wild type ATTR but is rare in AL (4%), while typical low QRS voltages are seen in 40% wild type ATTR vs 60% AL.⁵⁵

There has been little recent study of ECG correlation with cardiac biomarkers, treatment toxicity and mortality. Progressive ECG changes may be useful in assessing silent cardiac progression.⁵⁶ Changes in ECG abnormalities after treatment in AL amyloidosis remain poorly studied, but can occur – more often, little improvement is seen. Holter ECG monitoring identifies asymptomatic arrhythmias in >75% of cardiac AL patients (mainly supraventricular tachyarrhythmias and some non-sustained VT).⁵⁷

6.4.2 Echocardiography:

All patients with suspected amyloidosis should undergo echocardiography. Findings are characteristic in advanced disease, but harder to elicit earlier on, and have prognostic as well as diagnostic significance.⁵⁸⁻⁶⁰ Typical findings include concentric LVH with right ventricular (RV) involvement, poor biventricular long axis function with (near) normal ejection fraction (EF)^{61, 62} and valvular thickening (particularly in wild type or variant ATTR).⁵⁵ Diastolic dysfunction is the earliest echocardiographic abnormality and may occur before cardiac symptoms develop.^{63, 64} As with all investigations, echocardiography must be interpreted within the clinical context; a speckled or granular myocardial appearance, although characteristic of amyloid, is an inexact finding which is dependent on machine gain settings. Biatrial dilatation in presence of biventricular, valvular and interatrial septal thickening⁶³ are useful clues to the diagnosis.

Advanced echocardiographic techniques are beginning to reveal more about the underlying pathology and functional abnormalities, such as the twisting and untwisting cardiac motion that may be augmented through compensatory mechanisms before reversing to impairment later in the course of the disease.^{65, 66} Strain and strain rate imaging, derived from speckle tracking (see figure 3), may help differentiate cardiac amyloidosis from hypertrophic cardiomyopathy.^{67, 68}

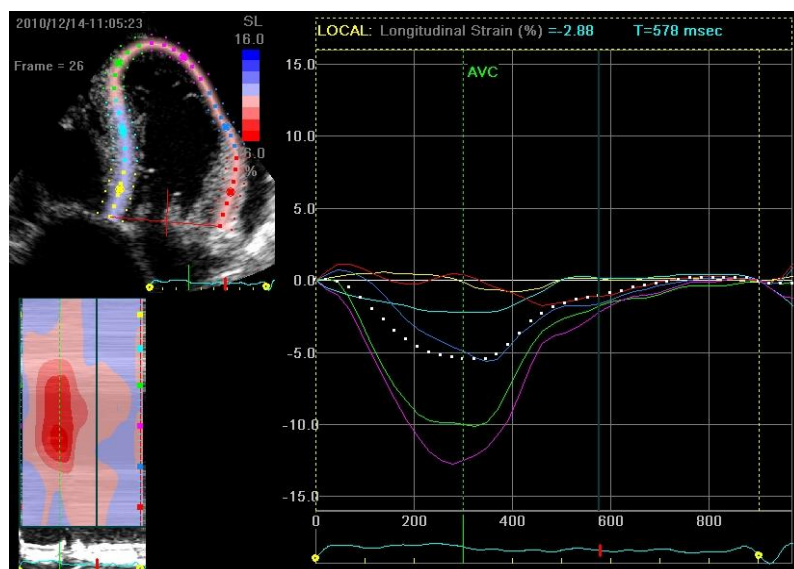


Figure 3: Transthoracic echocardiogram with speckle tracking: The red and yellow lines represent longitudinal motion in the basal segments while the purple and green lines represent apical motion. This shows loss of longitudinal ventricular contraction at the base compared to apex.

Typically, there is much greater restriction of basal compared to apical movement. Mean LV basal strain is an independent predictor of both cardiac and overall deaths. Contrast echocardiography using transpulmonary bubble contrast can show microvascular dysfunction in AL amyloidosis.⁶⁹ Although transoesophageal echo may help detect atrial appendage thrombus in a third of cases, of AL amyloid – translation of this into routine clinical practice for this frail and unwell patient population needs further study.^{63, 70}

6.4.3 Cardiac Biomarkers

Measurements of BNP, its more stable N-terminal fragment (NT-proBNP), and cardiac troponins are extremely informative in AL amyloidosis, which is the only type in which they have been systematically studied to date. Their value in ATTR amyloidosis is yet to be determined. BNP/NT-proBNP are cleared by the kidneys (BNP also partially cleared by the liver), confounding evaluation of patients with kidney involvement. Elevated NT-proBNP levels in systemic AL amyloidosis are a sensitive marker of cardiac involvement, with a cut-off >152pmol/L being associated with higher mortality (72% vs 7.6% per year).⁷¹ Abnormal NT-proBNP is predictive of clinically significant cardiac involvement developing in future.⁷² BNP/NT-proBNP, in general, reflects high filling pressures, but amyloid deposits may have a local effect – BNP granules are found in higher quantities in myocytes adjacent to amyloid deposits.⁷³

Increased troponin concentrations are a marker of poor prognosis⁷⁴ but the mechanism remains unclear. In a study of 261 patients with newly diagnosed AL amyloidosis, median survival for patients with or without detectable levels of Troponin T was 6 months and 22 months, respectively.⁷⁴ Indeed more recently, high-sensitivity Troponin T has been shown to correlate with morbidity and mortality after patients with renal impairment were excluded.⁷⁵ High-sensitivity Troponin is abnormal in more than 90% of cardiac AL patients,⁷⁶ and the combination of BNP/NT-proBNP plus troponin measurements are used to stage and risk-stratify patients with AL amyloidosis at diagnosis.^{33, 77}

Interestingly, the concentration of BNP/NT-proBNP in AL amyloidosis may fall dramatically within weeks following chemotherapy that substantially reduces the production of amyloidogenic light chains.⁷⁸ The basis for this very rapid phenomenon, which is not

mirrored by changes on echocardiography or CMR remains uncertain, but a substantial fall is associated with improved outcomes.⁷⁹ An early transient increase in BNP/NT-proBNP may occur after treatment with the immunomodulatory drugs thalidomide and lenalidomide, which are frequently used in the management of AL amyloidosis (see later), but the significance and cause is unclear.^{80, 81}

6.4.4 Radionuclide Imaging:

Serum amyloid P component (SAP) scintigraphy uses purified human SAP radiolabelled with ¹²³I, which is injected into patients. The tracer localises to target organs rich in amyloid and an image captured with a gamma camera. SAP scans enable visceral amyloid deposits, including those in the liver, kidneys, spleen, adrenal glands and bones to be imaged serially in a specific and qualitative manner.⁸² It does not adequately image the moving heart, in part because the high atomic mass of SAP (125kDa) prevents movement across myocardial capillary endothelium and thus has no role in assessing cardiac amyloidosis. SAP scans are described further and illustrated in section 6.5 “Liver and Spleen,” later in this chapter.

Numerous case reports over the past 30 years have indicated that various commonly used diphosphonate bone seeking radionuclide tracers occasionally localise to cardiac amyloid, and this approach has lately been investigated systematically. It transpires that technetium-labelled 3,3-diphosphono-1,2-propanodicarboxylic acid bone scanning agent (^{99m}Tc-DPD), a particular tracer that has been little used of late for bone scintigraphy, appears to localise to cardiac amyloid deposits very sensitively, especially in patients with ATTR type (see figure 4), where it has become the gold standard imaging test for cardiac ATTR amyloid. Indeed, asymptomatic cardiac ATTR deposits can be identified through ^{99m}Tc-DPD scintigraphy at an early stage when echocardiography, serum cardiac biomarkers and perhaps even CMR remain normal.⁸²

By contrast, uptake of ^{99m}Tc-DPD occurs in about one third of patients with cardiac AL amyloidosis, and ^{99m}Tc-DPD-SPECT-CT can help to distinguish the two types.⁸³ The sensitivity of DPD scintigraphy for detecting cardiac amyloidosis of ATTR type would appear to have considerable potential for diagnosis and screening.⁸⁴ Early work using N-[methyl-(¹¹C)]2-(4'-

methylamino-phenyl)-6-hydroxybenzothiazole ((¹¹C-PIB) PET imaging for cardiac amyloidosis is promising.⁸⁵

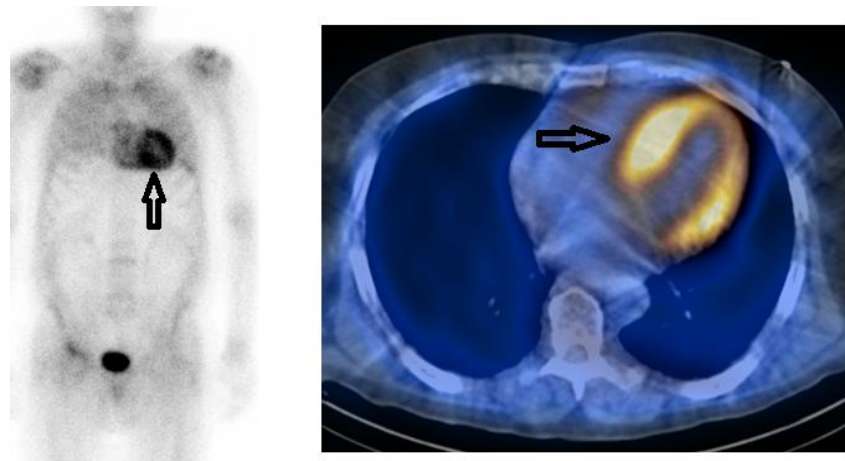


Figure 4: A positive ^{99m}Tc-DPD scan for ATTR cardiac amyloid (left), showing uptake in the heart (arrow) and reduced bone uptake. The right hand panel showed a fused CT/SPECT image showing myocardial uptake with greater uptake in the septum.

In reality, because of the much lower sensitivity of DPD scintigraphy in AL compared with ATTR amyloidosis, a multimodality imaging approach is adopted using radionuclide scintigraphy as described above, along with cardiac MRI as described below.

6.4.5 Cardiac MRI:

CMR provides functional and morphological information on cardiac amyloid in a similar way to echocardiography, though the latter is superior for evaluating and quantifying diastolic abnormalities. An advantage of CMR is in myocardial tissue characterisation. Amyloidotic myocardium reveals subtle (but see later with the new methods) pre-contrast abnormalities (T₁, T₂)^{86, 87} but extravascular contrast agents based on chelated gadolinium provided key information. The appearance (see figure 5) of global, subendocardial LGE, is highly characteristic of cardiac amyloid^{88, 89} and correlates with prognosis,^{90, 91} although other LGE patterns are also recognised (see figure 6). These factors are explored in more detail later in this thesis. CMR is especially useful in patients with other causes of LVH, since it can differentiate amyloidosis from hypertension, which may not be possible by routine echocardiography.

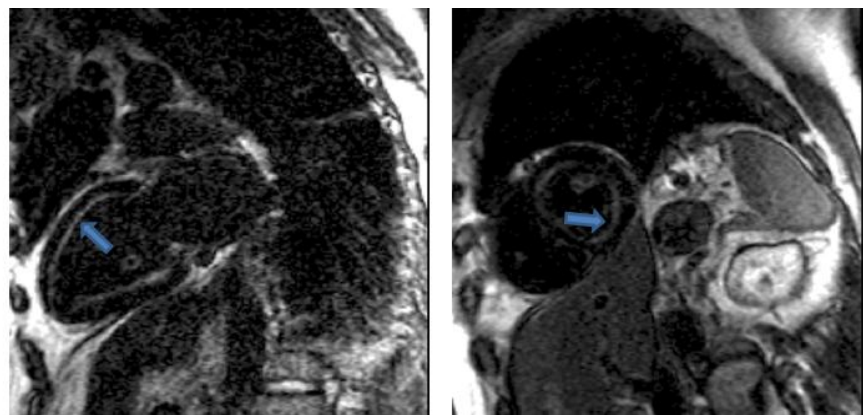


Figure 5: CMR with the classic amyloid global, subendocardial late gadolinium enhancement pattern in the left ventricle with blood and mid-/epi-myocardium nulling together.

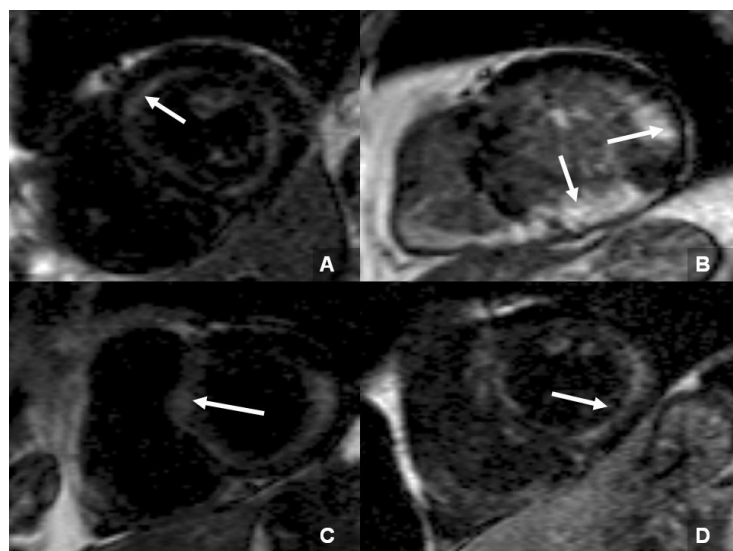


Figure 6: LGE patterns: (A) Characteristic global, subendocardial; (B) patchy; (C) extensive and (D) LGE in a patient without hypertrophy (maximum wall thickness in this individual was 10mm)

Difficulties are however often encountered, for example arrhythmias, particularly AF and ectopic beats, degrade image quality during CMR, and increasing experience of the technique in clinical practice has shown that the pattern of LGE can be atypical and patchy, especially in early disease.⁹² LGE imaging in amyloidosis is inherently challenging since amyloid infiltration within the interstitium of the heart reduces the differences in contrast signal between blood and myocardium such that the two compartments may null together or even be reversed and effusions may cause considerable ghosting artefact, although these both can be a strong clue to the underlying diagnosis (see figure 7).^{89, 93, 94}

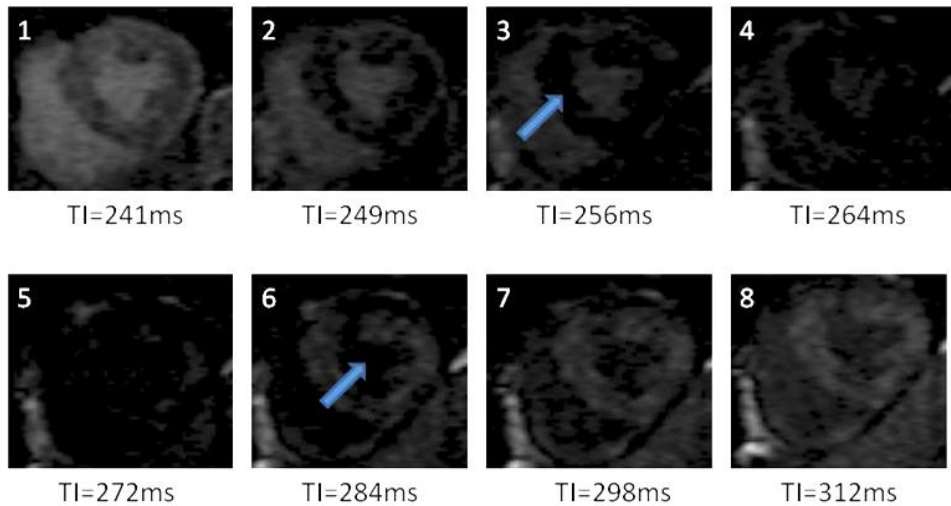


Figure 7: Sequential static images from a CMR TI scout sequence after gadolinium administration. As the inversion time (TI) increases, myocardium nulls first (arrow in image 3), followed by blood afterwards (arrow in image 6), implying that there is more gadolinium contrast in the myocardium than blood

6.4.6 Endomyocardial biopsy:

Endomyocardial biopsy has been considered to be the gold standard for demonstrating cardiac amyloid deposition.⁹⁵ Although cardiac involvement can reasonably be inferred in a patient with proven systemic amyloidosis through a combination of clinical features, ECG, echocardiography and biomarkers etc., endomyocardial biopsy is required when suspected cardiac amyloidosis is an isolated feature and/or when identification of the cardiac amyloid fibril type cannot be defined by other means. In practice, endomyocardial biopsies are most commonly required to differentiate between AL and ATTR in older patients, some 5% of whom have a monoclonal gammopathy of undetermined significance (MGUS),⁹⁶ and should be considered in patients with LV thickening by echocardiography where hypertension, valvular disease and a family history of HCM have been excluded, particularly if the patient is young.

Complications such as perforation remain a small but real risk and may not be well tolerated in restrictive cardiomyopathy.^{97, 98} The presence of amyloid deposition should be confirmed by Congo red staining, and immunohistochemistry can usefully identify fibril type in about 60-70% cases. Electron microscopy to confirm or refute the presence of amyloid fibrils has an occasional role when Congo red stains fail to produce definitive results.^{99, 100} Proteomic typing of amyloid by mass spectrometry using tiny samples obtained through laser

capture micro-dissection of tissue sections usually provides definitive results,¹⁰¹ and is critical when immunohistochemistry has not done so.

6.5 LIVER AND SPLEEN:

The liver is affected in around 25-30% with Systemic AL Amyloidosis. It presents either as hepatomegaly or as previously undetected liver enzyme derangement.³¹ Rarely, it can present with life threatening hepatic rupture,¹⁰² which is also seen in some other hereditary, non-TTR amyloid types.¹⁰³

SAP scintigraphy is the gold standard for assessing disease burden within the liver. As mentioned earlier, its high atomic mass of 125kDa favours evaluation of tissues with a fenestrated endothelium, such as the liver and spleen. A qualitative assessment is made ranging from the “congested” appearance seen in ATTR type amyloid, to the small, moderate and large loads seen in AL and some other hereditary, non-ATTR amyloids (see figure 8).

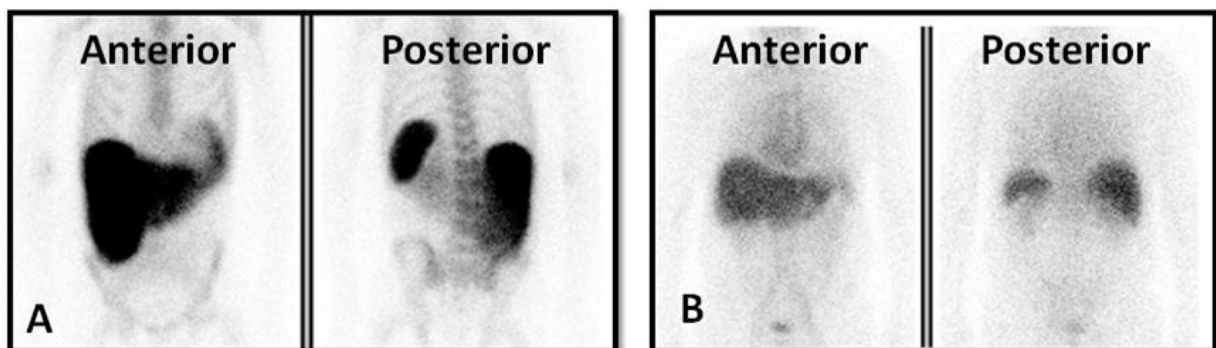


Figure 8: SAP scans showing (A) Large amyloid load in liver and spleen in a patient with AL Amyloidosis; (B) Congested liver and spleen in a patient with TTR amyloid

Splenic amyloid is seldom of clinical significance and is most commonly involved in AA Amyloidosis, but some cases of AL Amyloid also show uptake on SAP scintigraphy (see figure 9).

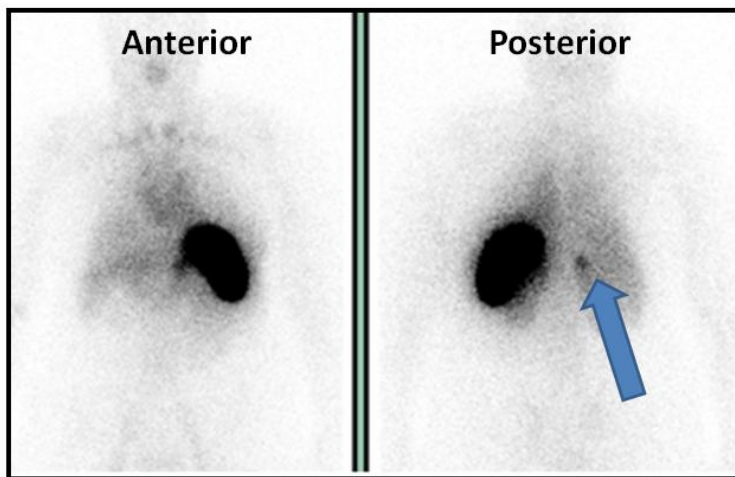


Figure 9: SAP scan showing moderate load in the spleen and the right adrenal gland (arrow) in a patient with AA Amyloidosis

6.6 SKELETAL MUSCLE:

Skeletal muscle amyloidosis is rare and little is known about it. It has been described in hereditary Apo A2¹⁰⁴ and senile amyloidosis¹⁰⁵ in mice. Primary (AL) Amyloidosis can however also present with myopathy (e.g. dropped head syndrome)¹⁰⁶ and there are a number of case reports of patients with myeloma / lymphoma who have amyloid deposits in skeletal muscle histologically, with confirmed myopathic changes on EMG.¹⁰⁷⁻¹⁰⁹ There is no good non-invasive imaging technique to diagnose this condition. CT scanning can reveal infiltrative changes but muscle biopsy remains the diagnostic gold standard.

6.7 PROGNOSIS:

In the absence of treatment, the natural history of AL amyloidosis is rapidly progressive, with death occurring within 2 years in about 80% of patients;¹⁴ it is much worse with cardiac involvement and heart failure. In a study of 18 patients with amyloid heart involvement due to SSA, the median survival was 60 months; over the same period, patients with AL amyloid heart disease at the same institution had a median survival of only 5.4 months.⁴⁰ Despite thicker walls and an older age, the senile amyloid patients had less severe heart failure and a much longer median survival (75 vs 11 months). Similar results have been recently reported in a large series comparing different forms of amyloid cardiomyopathy.⁵⁵

5.8 TREATMENT:

Cardiac amyloidosis in general has a poor prognosis, but this differs according to amyloid type, and availability and response to therapy. Treatment may be “amyloid-specific” or “non amyloid-specific” as detailed below:

6.8.1 Non Amyloid Specific:

6.8.1.1 Heart Failure Therapy:

Standard heart failure therapy may be of limited benefit or even detrimental in cardiac amyloidosis. There is scanty evidence for the use (or not) of ACE-i, ARBs and β-blockers. These may be poorly tolerated, worsen postural hypotension or renal function (ACE/ARBs). Restrictive cardiomyopathy leads to a heart-rate dependent cardiac output in some cases and such patients may find difficulty in tolerating beta-blockers. Digitalis and calcium channel blockers may be selectively concentrated in amyloidotic tissue and are relatively contraindicated on grounds of increased toxicity¹¹⁰⁻¹¹² especially the latter, which can lead to rapid worsening. Careful monitoring is needed to avoid significant drug interactions e.g. β-blockers with thalidomide used in chemotherapy of AL amyloidosis causing bradycardia.¹¹³

Maintenance of adequate filling pressures is vital due to the restrictive physiology; balancing peripheral oedema and renal impairment with salt/water restriction and judicious use of diuretics is also important. Patient education and participation, ideally with backup from heart-failure teams, is critical to successful management. Contrary to standard heart failure management, maintenance of adequate blood pressure with an α-agonist like midodrine may permit higher doses of loop diuretics especially in patients with autonomic neuropathy.¹¹⁴

6.8.1.2 Device therapy:

Pacemakers or implantable cardioverter-defibrillators (ICDs) may not prevent sudden cardiac death, since this is thought to often be due to electromechanical dissociation.¹¹⁵ In the absence of evidence, pacing indications remain within current standard guidelines. High defibrillator thresholds may be encountered and the benefits of such devices remain uncertain.^{115 116, 117} Biventricular pacing appears to play little role – but may be the ideal

pacing option of choice to avoid decompensation of the stiffened ventricle as a result of induced dyssynchrony from RV pacing.¹¹⁸

6.8.1.3 Cardiac transplantation in amyloidosis:

Cardiac transplantation has played a disappointingly small role, due to the multisystem nature of amyloidosis, advanced age, treatment related complications, and rapid disease progression. Furthermore, patients with AL amyloidosis must be deemed likely to be sufficiently fit to undergo chemotherapy afterwards, to address the underlying bone marrow disorder. As a result, only a few dozen cardiac transplants have ever been performed for amyloidosis. However, the long-term outcome can be good in highly-selected patients with AL amyloidosis.¹¹⁹ Cardiac transplantation followed by successful peripheral blood autologous stem cell transplantation (ASCT) was associated with better survival in selected patients as reported¹²⁰ from most major amyloidosis units in the UK,¹¹⁹ France,¹²¹ Germany¹²² and the USA.¹²³

A suitable patient with AL amyloidosis is likely to be young (<60 yrs), have isolated Mayo stage III cardiac amyloidosis, NYHA III or IV symptoms after adequate diuretics, good renal/liver function, no significant autonomic neuropathy, low level bone marrow plasma-cytosis and be eligible for ASCT after the heart transplant. Even in such patients, outcomes are probably inferior to other indications.¹²⁴ For variant ATTR, combined cardiac and liver transplantation has been performed in a few dozen cases throughout the world.^{119, 120, 125, 126} Although most patients with wild type ATTR are too elderly for cardiac transplantation, the absence of extra-cardiac involvement renders younger patients with wild type ATTR excellent candidates. The two patients with wild type ATTR who presented to the UK national amyloidosis centre before age 60, survived 10 and 20 years respectively following cardiac transplantation (unpublished data).

6.8.2 Amyloid Specific:

6.8.2.1 Reducing amyloid fibril precursor protein production:

Treatment of amyloidosis is currently based on the concept of reducing the supply of the respective amyloid fibril precursor protein. In AL amyloidosis, therapy is directed towards the clonal plasma cells using either cyclical combination chemotherapy or high dose

therapy with ASCT. Most chemotherapy regimes in AL amyloidosis comprise dexamethasone combined with an alkylator (oral melphalan or others).

Addition of thalidomide, for example in the risk-adapted cyclophosphamide, thalidomide and dexamethasone (CTD) regime used widely in the UK, improves response rates but probably at cost of greater toxicity.¹²⁷ Dexamethasone, although a very useful agent in all patients with AL amyloidosis including those with cardiac involvement, has to be used with great caution in patients with cardiac amyloidosis due to a high risk of fluid overload in the absence of adequate and rapid changes to diuretic therapy. Close coordination between the treating haematology and cardiology teams is critical to steer the patient successfully through the treatment course.¹²⁸ In a study of 75 AL patients, CTD (and attenuated dose CTD) produced a complete response (CR) in 21%. Estimated 3-year survivals for those achieving a CR, partial response (PR), or no response were 100%, 82%, and 0%, respectively (median survival 17 months).

High-dose melphalan followed by ASCT provides a more durable haematological response. In the largest published series of melphalan-primed ASCT (n=701), 312 AL patients were deemed eligible for high-dose chemotherapy, and the median survival of treated patients was 4.6 years. A CR was achieved in 40%, although the mortality rate in the first 100 days was 13%. Survival was poorer amongst patients with cardiac amyloidosis compared to those who had no evidence of heart involvement.¹²⁹ Although it has been argued that ASCT is the best treatment for suitable patients,¹³⁰⁻¹³² its role in the era of more novel agents (discussed below), is less certain.

The newer treatment options include bortezomib (a proteosome inhibitor)¹³³ and the newer immune-modulatory drugs, such as lenalidomide and pomalidomide. Bortezomib combinations appear to be especially efficient in amyloidosis with high rates of near CRs which appear to translate into early cardiac responses.¹³⁴⁻¹³⁶ Phase II (bortezomib in combination with cyclophosphamide or doxorubicin) and phase III (bortezomib, melphalan and dexamethasone compared to melphalan and dexamethasone as front line treatment) trials are underway.

AA amyloidosis is the only other type of amyloidosis in which production of the fibril precursor protein can be effectively suppressed by currently available therapies. Anti-inflammatory therapies, for example anti-TNF agents in rheumatoid arthritis, can substantially

suppress serum amyloid A protein production, but very little experience has been obtained regarding cardiac involvement which is very rare in this particular type of amyloidosis.

ATTR is produced almost exclusively in the liver. Liver transplantation has been used as a treatment for variant ATTR for 20 years, to remove genetically variant TTR from the plasma. Although this is a successful approach in ATTR Val30Met, it has had disappointing results in patients with other ATTR variants which often involve the heart. The procedure commonly results in progressive cardiac amyloidosis through on-going accumulation of wild-type TTR on the existing template of variant TTR amyloid.¹³⁷ The role of liver transplantation in non-Val30Met associated hereditary TTR amyloidosis thus remains very uncertain. Exercise training post surgery can be helpful however.¹³⁸

ATTR amyloidosis has lately become a focus for novel drug developments aimed at reducing production of TTR through silencing RNA and antisense oligonucleotide therapies. ALN-TTR01, a systemically delivered silencing RNA therapeutic¹³⁹ is already in phase I clinical trial.

6.8.2.2 Inhibition of amyloid formation:

Amyloid fibril formation involves massive conformational transformation of the respective precursor protein into a completely different form with a predominantly β-pleated sheet structure. The hypothesis that this conversion might be inhibited by stabilising the fibril precursor protein through specific binding to a pharmaceutical product has lately been explored in ATTR amyloidosis. A key step in TTR amyloid fibril formation is the dissociation of the normal TTR tetramer into a monomeric species that can auto-aggregate into a misfolded form. *In vitro* studies identified that diflunisal, a now little used non-steroidal anti-inflammatory analgesic, is bound by TTR in plasma, and that this enhances the stability of the normal soluble structure of the protein.^{140, 141} Studies of diflunisal in ATTR are in progress.

Tafamidis is a new compound without anti-inflammatory analgesic properties that has a similar mechanism of action. Tafamidis has just been licensed for neuropathic ATTR but its role in cardiac amyloidosis remains uncertain – clinical trial results are eagerly awaited. Higher affinity ‘superstabilizers’ are also in development.¹⁴²

Eprodisate is a negatively-charged, sulphonated molecule with similarities to heparin sulphate, which is being pursued as a treatment for AA amyloidosis. Eprodisate is thought to inhibit the pro-amyloidogenic interactions of GAGS with SAA during fibril formation in AA amyloidosis. A phase III trial showed benefits in terms of progression of AA amyloid associated renal dysfunction¹⁴³ and further studies are currently being conducted.

6.8.2.3 Targeting Amyloid Deposits by Immunotherapy:

Amyloid deposits are remarkably stable, but the body evidently has some limited capacity to remove them. Following treatment that prevents the production of new amyloid, e.g. successful chemotherapy in AL type, amyloid deposits are gradually mobilised in the majority of patients, though at different rates in different organs and between individuals. Unfortunately clearance of amyloid is especially slow in the heart, and echocardiographic evidence of improvement is rare, even over several years.

The challenge of developing a therapeutic monoclonal antibody that is reactive with all types of amyloidosis is currently being addressed by targeting SAP, since this is a universal constituent of all amyloid deposits and an excellent immunogen. Anti-SAP antibody treatment is clinically feasible because circulating human SAP can be depleted in patients by the bis-d-proline compound CPHPC, thereby enabling injected anti-SAP antibodies to reach residual SAP in the amyloid deposits (see figure 10 on the next page).³ The unprecedented capacity of this novel combined therapy to eliminate amyloid deposits in mice is encouraging and should be applicable to all forms of human systemic and local amyloidosis; trials are currently underway.

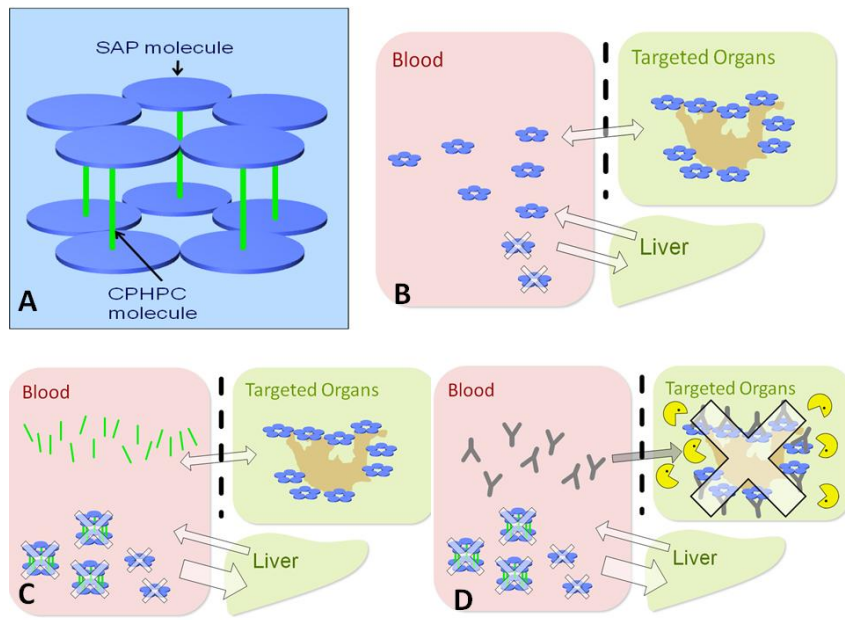


Figure 10: Showing (A) cross-linking of SAP by the R-1-[6-[R-2-carboxy-pyrrolidin-1-yl]-6-oxo-hexanoyl] pyrrolidine-2-carboxylic acid (CPHPC) molecule; (B) Circulating SAP in a patient with amyloidosis, showing the normal level of “coating” of amyloidotic organs by SAP and baseline low-level sequestration of circulating SAP by the liver; (C) Addition of CPHPC causing cross-linking of SAP in the blood and subsequent high level excretion of SAP from blood by the liver; (D) Addition of the anti-SAP antibody causing removal of SAP coating from amyloidotic organs, allowing immune system to destroy the amyloid in the target organ. Picture courtesy of Duncan Richards, GSK.

6.9 MEASURING INTERSTITIAL EXPANSION USING MRI:

6.9.1 MRI General Physics:

The majority of protons in the body align in the direction of the magnetic field B_0 when placed in the MRI scanner, as this is the lower energy state. A radiofrequency (RF) impulse at the Larmor frequency induces a higher energy state within the proton, causing it to spiral away from the B_0 alignment to an angle (flip angle) proportionate to the RF pulse. When the RF pulse stops, the proton slowly relaxes and energy is dissipated to the surrounding nuclei; this corresponds with the return of longitudinal magnetisation to the original B_0 alignment as calculated by $1 - e^{-t/T_1}$. The time constant of this exponential is known as the T1 relaxation time and represents the time taken for 63% of longitudinal magnetisation to recover after the RF impulse (see figure 11)

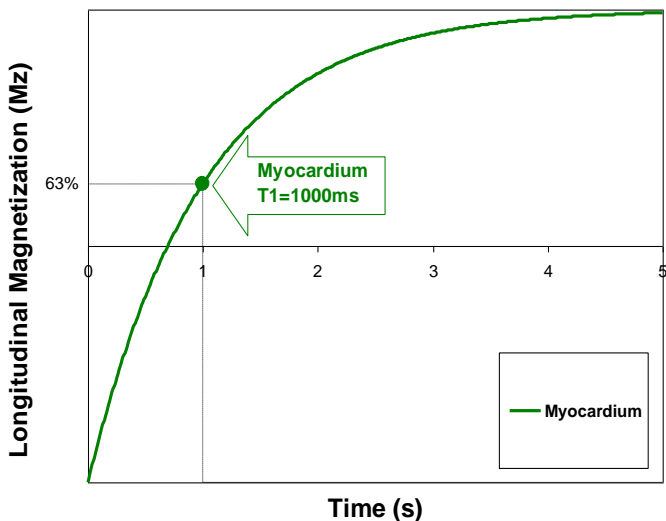


Figure 11: Magnetisation recovery curve plotted against time demonstrating T1 for myocardium.

T1 is therefore dependent on magnetic field strength. All tissues have an intrinsic T1 which is a composite signal representing cells and the interstitium. Any change in cell size or number will alter the T1. Similarly, any change in the interstitium such as scarring from MI or infiltration by amyloid will also change the T1 from normal. In general, the higher the water content, the higher the T1. The T1 of normal myocardium is approximately $960 \pm 30\text{ms}$. A high or low myocardial T1 can therefore give tissue characterisation and allow some inference as to the cause of the abnormal areas of myocardium in question. For example, the T1 varies widely from as low as 300-400ms in iron-loaded hearts to almost 2000ms in oedematous myocardium as seen in myocarditis.

T1 can be significantly lowered by administration of Gadolinium. There are many preparations, though cyclic, ionic compounds such as Gadoterate Meglumine (Dotarem) are thought to be the safest in terms of the lowest risk of nephrogenic systemic fibrosis. Gadolinium is a purely extracellular agent and produces a local environment in the interstitium that allows protons to relax by a factor of $\times 10^6$ faster than normal. In areas of gross interstitial expansion due to amyloid, gadolinium concentration is proportionately higher in these areas and causes the T1 in these areas to drop lower than compared to the surrounding or adjacent (normal) tissue (see figure 12), thus producing the contrast between black and white in the late gadolinium enhancement pictures shown in figures 6 and 7 earlier. This property of gadolinium is also the crux of the Equilibrium-CMR technique described shortly in section 6.10.

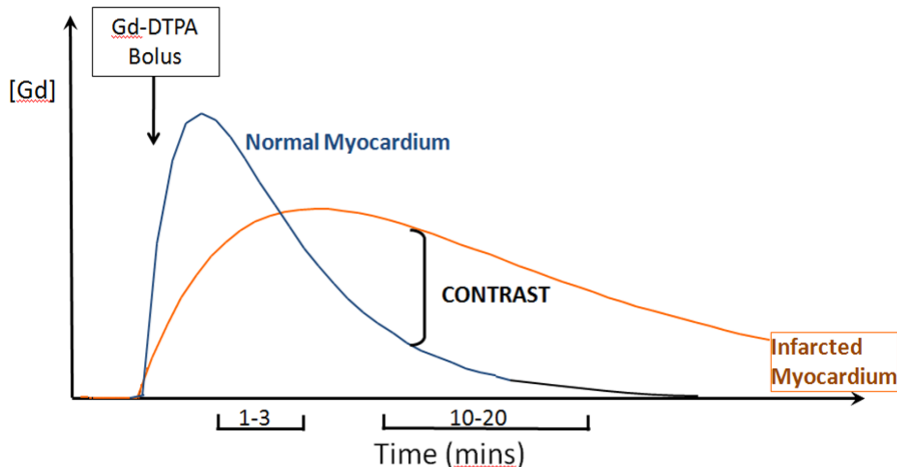


Figure 12: Graph showing change in concentration of gadolinium with time after IV bolus. Blue line shows concentrations in the interstitium of normal myocardium and the red line in abnormal (infarcted) myocardium. The difference in concentration at 10-20 mins (marked “contrast”) creates the standard LGE image with normal myocardium black and scar appearing as white. Picture courtesy of Dr. Daniel Sado, The Heart Hospital.

6.9.2 T1 Mapping:

A number of techniques are currently in widespread use in the CMR community to measure T1 values of tissues. The earliest method was using a Look Locker (T1 scout) sequence prior to the administration of gadolinium contrast (see figure 13), which took multiple images throughout several cardiac cycles after an RF pulse. From these, a region of interest (ROI) could be drawn and the signal intensities plotted against time on a recovery curve similar to figure 11 to determine the T1. This method had the disadvantage that it required a long breath hold from patients and also images were not acquired at the same point in the cardiac cycle.

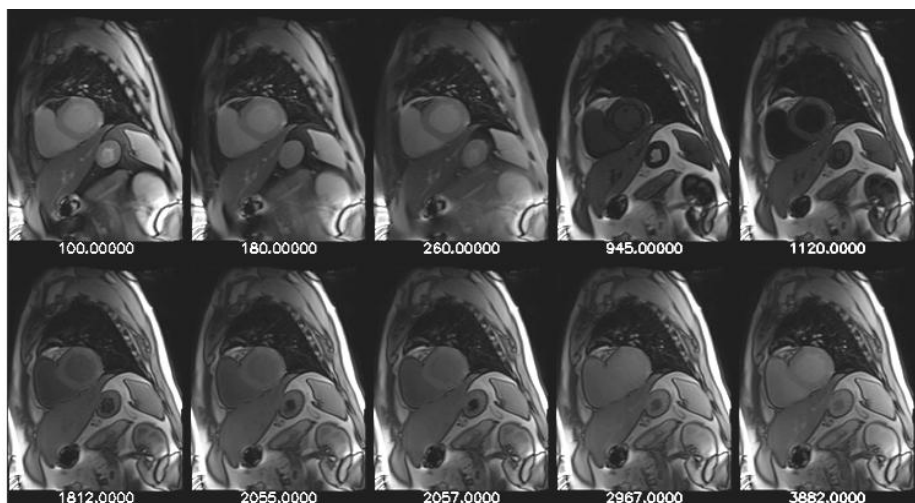


Figure 13: A pre contrast TI scout image showing the different signal intensities of the myocardium at increasing time points (100ms to 3882ms) after a RF impulse.

In 2004, the modified Look Locker T1 mapping (MOLLI)¹⁴⁴ sequence was developed. This sends out an RF impulse and reads out at 3 time-points along the T1 recovery curve. A further 2 RF impulses are applied to the selected tissue and read outs (3 and 5 respectively) along the recovery are taken after each RF impulse. Three recovery curves are then available to determine the tissue T1. The result is a pixel by pixel T1 map displayed as a graded colour image according to the T1 of each pixel. This is summarised in the schematic in figure 14.

MOLLI had the advantage of being more accurate than the Look Locker sequence because it samples at the same point in the cardiac cycle. But the breath hold is very long for most patients (around 20 seconds in some instances) and as such, is also more susceptible to heart rate changes and ectopics.

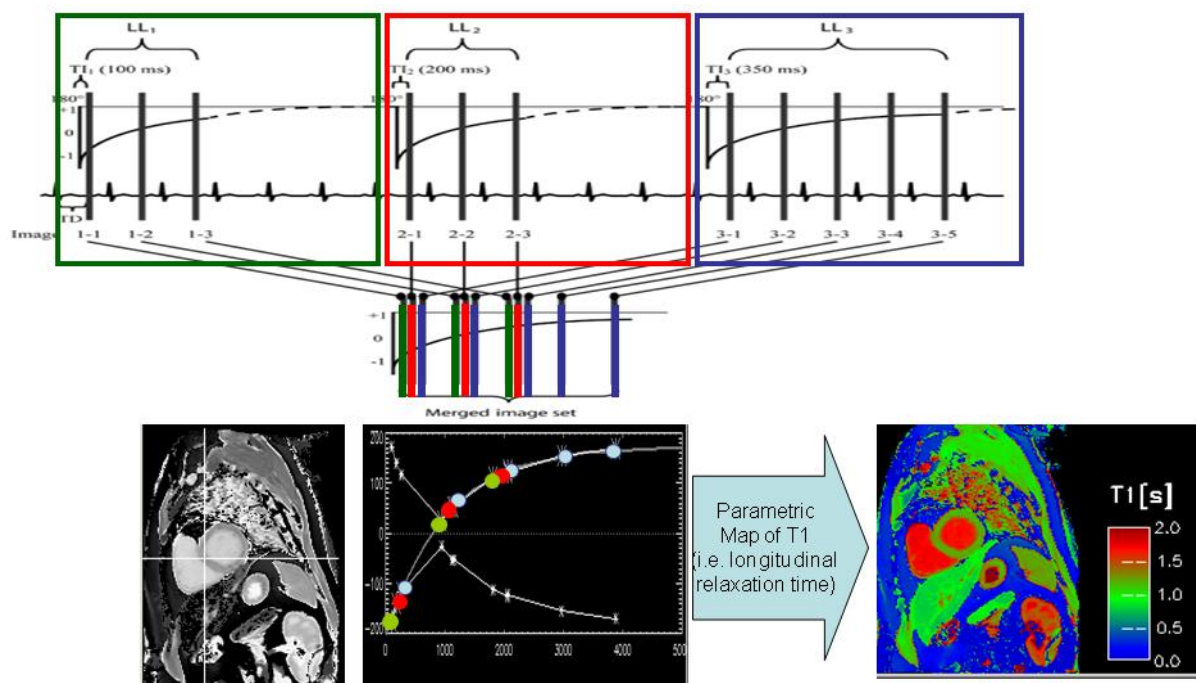


Figure 14: Schematic showing 3 RF impulses (boxes) and their subsequent readouts plotted on the recovery curve, coloured in green, red and blue respectively. This produces the colour, pixel by pixel T1 map. Courtesy of Dr. Stefan Piechnik, OCMR Unit, Oxford.

Later in 2010, in order to make the MOLLI more clinically applicable, it was shortened to become the ShMOLLI.¹⁴⁵ Certain assumptions needed to be made to achieve this, for example that the recovery periods after each RF impulse need not be as long as the MOLLI such that at heart rates with an R-R interval of approximately 1000 msec, even though 3 RF impulses were applied, only 1 recovery curve of 5 plots was required to determine the T1 of the myocardium; however, if the heart rate was particularly fast or the T1 of the tissue in

question was particularly low, information from the 2nd and 3rd recovery curves was then taken into consideration. The data obtained from the ShMOLLI experiment then undergoes automated mathematical correction and curve fitting performed by the Siemens computer which is used to control the scanner. This is used to calculate the T1 of each image pixel in the slice selected, which is then assigned a colour according to its value as shown below in figure 15.

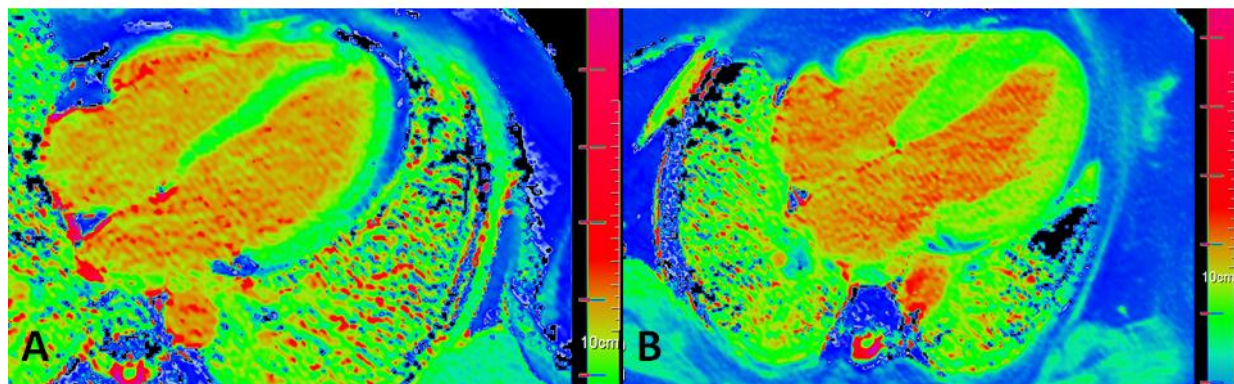


Figure 15: Pre-contrast ShMOLLI image showing (A) Normal myocardium appearing green, and (B) Amyloid myocardium appearing thickened with areas of red (high T1 signal) appearing in the otherwise green myocardium.

These assumptions meant the T1 map could now be taken in around 9 seconds. The ShMOLLI was also found to be more heart rate independent and T1 independent than the MOLLI as a result. Therefore, the pre-contrast T1 work presented in this thesis uses this ShMOLLI technique.

More recently, the MOLLI has been motion corrected to improve accuracy and newer techniques such as the saturation recovery, single-shot acquisition (SASHA) are entering the field,¹⁴⁶ but these are not considered in this thesis.

6.10 EQUILIBRIUM CMR (EQ-CMR):

Prior to the advent of ShMOLLI, our group in 2009 devised the first method of non-invasively quantifying in the interstitium of the heart using the technique of EQ-CMR.¹⁴⁷ There are 3 principles underlying this technique: (1) Gadolinium infusion to achieve equilibrium; (2) T1 measurement before and after gadolinium; (3) Haematocrit result.

Because of some of the limitations of T1 mapping at that time, it was felt that the most accurate method was T1 measurement using multiple, high resolution, fast, low-angle shot

(FLASH) inversion recovery images of a single, piloted view (usually the 4-chamber view) at specific inversion times (TI) ranging from 200ms to 100ms. This was done first of all prior to any gadolinium administration and gave the highest resolution images for ROIs to be drawn in the heart and blood pool to obtain the mean signal intensity at each TI, as shown in figure 16 below:

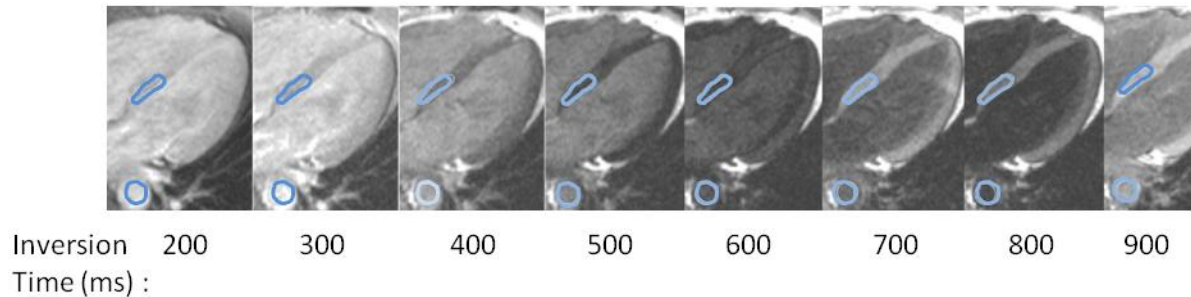


Figure 16: FLASH T1 measurement method for the heart. A 4-chamber slice is shown at different TIs with ROIs (blue) drawn in aorta and basal septum.

Mean tissue signal intensities were then plotted against TI. The TI producing the lowest signal intensity was identified and the magnitude of the signal intensities plotted to the left of this point were made negative. This allowed reconstruction of the full range of the T1 signal intensity inversion recovery curve. A second-order polynomial curve-fitting technique was used to find the null point (see figure 17). A previously validated algorithm was then used to correct for incomplete longitudinal recovery giving a corrected T1.

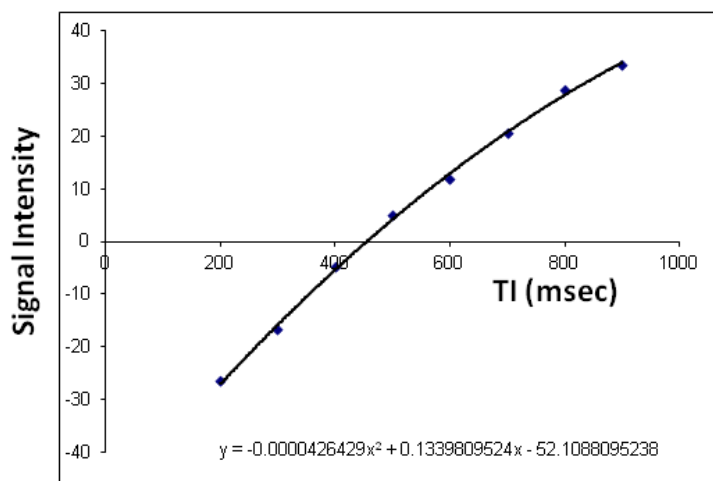


Figure 17: Graph showing signal intensity plotted against inversion time using a second-order, polynomial curve fitting technique to determine the null point and thus the T1 for myocardium.

Gadolinium was then administered as an intravenous bolus at a dose of 0.1mmol/kg, followed by a primed infusion of gadolinium at a rate of 0.0011mmol/kg/min. The infusion is necessary to create true equilibrium and eliminate the effect of gadolinium kinetics on the measured T1. If the infusion was not given, the T1 of both blood and myocardium would simply drop precipitously after the bolus injection of gadolinium before slowly returning to normal over the course of an hour or so (see figure 18A). Any T1 measurement in this situation would be affected by dynamic movement of gadolinium between extravascular compartments of blood and myocardium. Additionally, wash in and wash out is slower in abnormal myocardium compared to normal myocardium, and there is also the issue of renal excretion; hence, an infusion is required to achieve true equilibrium between blood and myocardium and thus eliminate any interference in T1 results from gadolinium kinetics (see figure 18B).

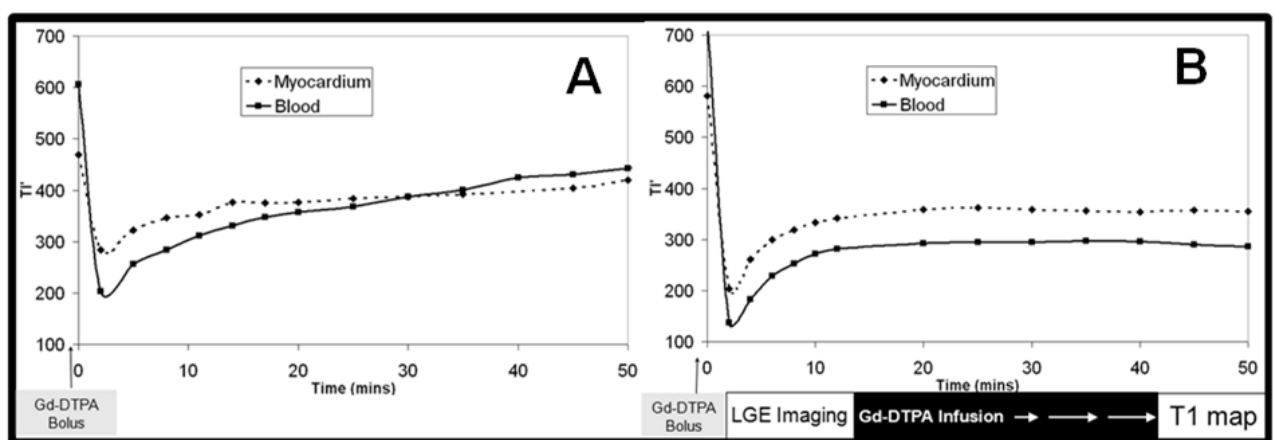


Figure 18: Graph showing change in inversion time for myocardium and blood, with time after an IV gadolinium bolus (time 0) and - (A) No infusion, allowing T1 to return to normal over 1 hour and (B) Primed gadolinium infusion commencing at $T = 15$ minutes holding T1 stable over the course of the infusion. Image courtesy of Dr. Andrew Flett.

Thirty minutes after the gadolinium infusion, equilibrium is reached. The T1 measurements are again taken in the manner described above. At this stage, the concentration of gadolinium in the interstitium of myocardium and plasma is the same. And as the rate of change of T1 (ΔT_1) is proportional to the concentration of gadolinium in the extracellular space (or volume i.e. ECV), then the following equation is true:

$$ECV = \lambda (1 - \text{haematocrit})$$

$$\text{where } \lambda = \frac{\Delta R_1 \text{ myocardium}}{\Delta R_1 \text{ blood}} \quad \text{and } R_1 = \frac{1}{T_1}$$

The end result is several signal intensity readings for myocardium and blood, before and after contrast, at multiple inversion times. These can be plotted on graphs as shown in figure 17 earlier, so that the rate of change of T1 for myocardium and blood can be calculated (see figure 19 below) and subsequently the ECV calculated.

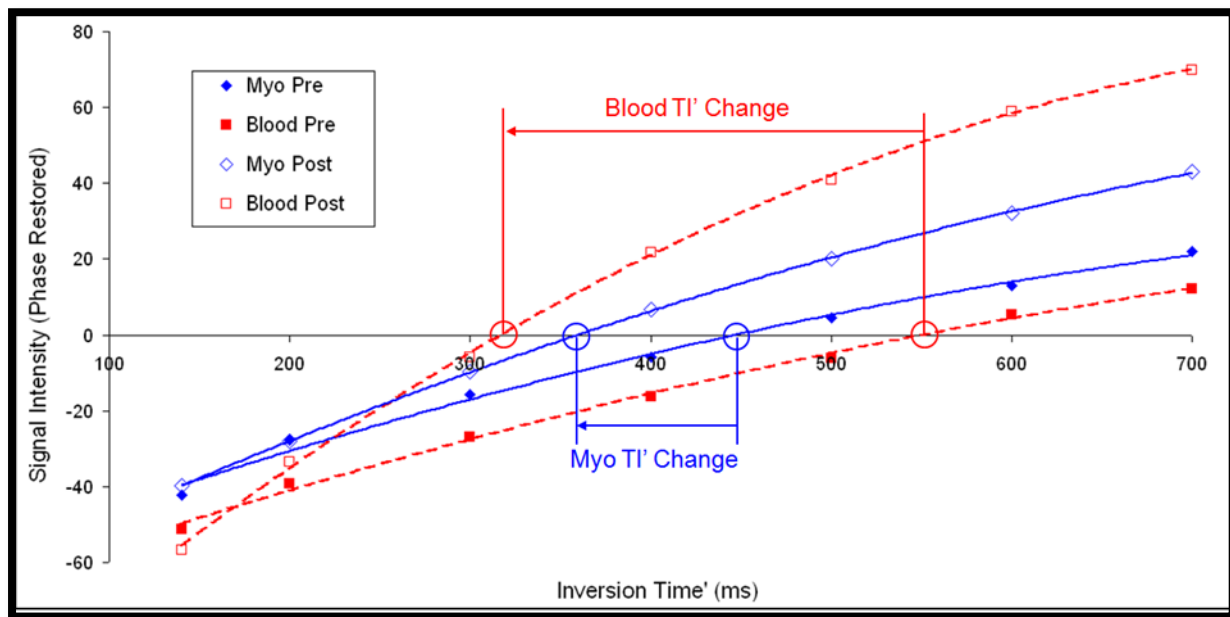


Figure 19: Graph showing typical changes in signal intensity plotted against inversion time for myocardium (blue) and blood (red), both pre- and post-contrast. Image courtesy of Dr. Andrew Flett.

Proof of principle was first demonstrated in 25 patients with severe aortic stenosis (AS) undergoing aortic valve replacement (AVR). The ECV was calculated using EQ-CMR and the results compared to histology from a septal biopsy performed during the AVR. There was a strong correlation of ECV with collagen volume fraction ($R^2 0.80, P<0.001$), suggesting ECV as assessed by EQ-CMR was quantifying diffuse fibrosis in the interstitium accurately (see figure 20 on the next page).¹⁴⁷

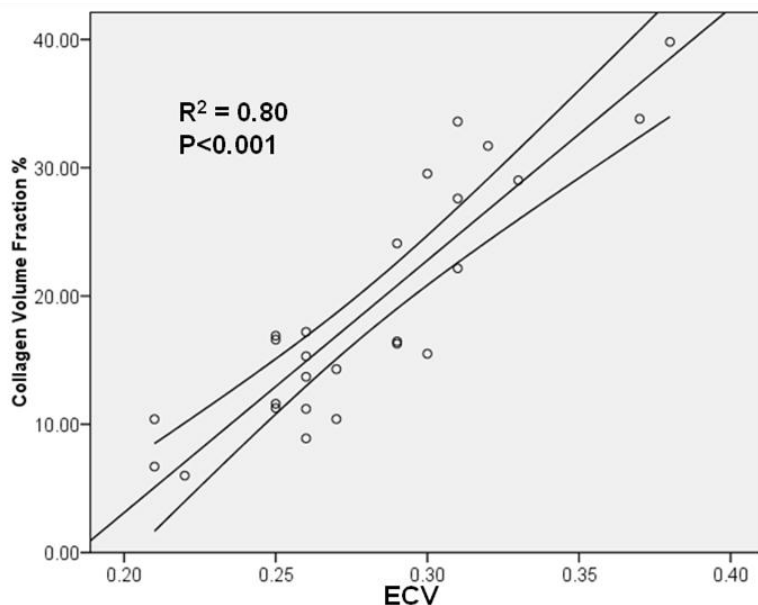


Figure 20: Scatter graph showing linear association of myocardial ECV with collagen volume fraction in aortic stenosis. Figure courtesy of Dr. Andrew Flett published in Circulation, 2010.¹⁴⁷

ECV was then assessed in a host of other cardiomyopathies and compared to normals. HCM (n=31), MI (n=20), familial dilated cardiomyopathy (DCM, n=31), severe AS (n=66) and Anderson Fabry's disease (AFD, n=17) were compared to 81 healthy volunteers. Mean ECV was statistically significantly higher in HCM (0.29), DCM (0.28) and AS (0.27) compared to healthy volunteers (0.25), $P < 0.001$. AFD did not show any rise in ECV as it is a predominantly intracellular disease process. Although there is overlap in these "low-ECV" diseases, the ECV of the infarct zone of an MI was massively raised at 0.59 compared to normals ($P < 0.001$) in keeping with net rise in extracellular space due to myocyte necrosis and scar formation (see figure 21).

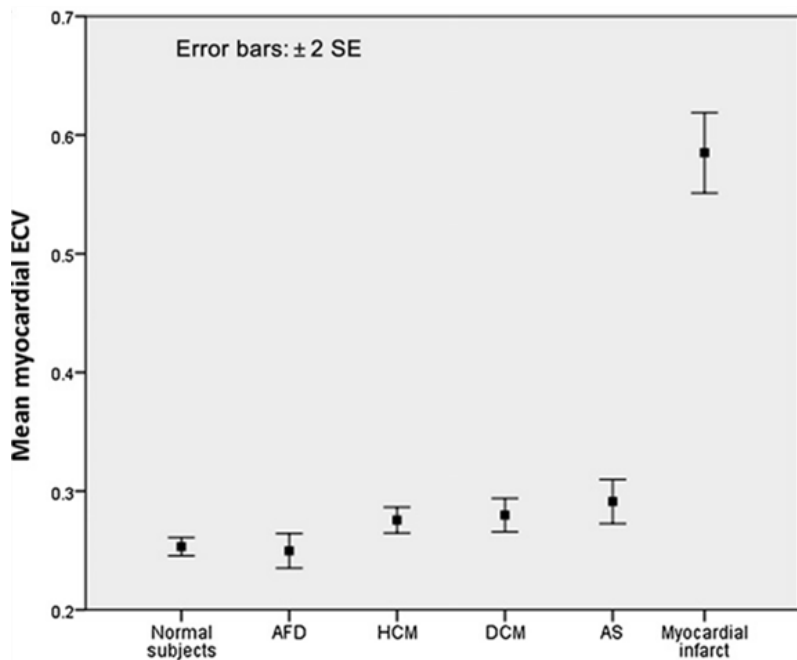


Figure 21: Graph showing relationship between myocardial ECV and various cardiac diseases as well as normal subjects. Figure courtesy of Dr. Daniel Sado published in Heart, 2012.¹⁴⁸

The work above in EQ-CMR led to the hypothesis that: as Amyloidosis is the exemplar of an interstitial disease process and as ECV is a purely extracellular measure, the 2 could be combined to produce a powerful tool to not only quantify cardiac amyloid burden more accurately, but also become a marker for treatment response and even prognosis. Current methods of assessment of cardiac amyloid burden are reliant on surrogate markers of the interstitial expansion rather than a true measure of it.

Wall thickness measured by echocardiography is non-specific due to other (more common) causes of LVH. Low voltage ECGs, as mentioned earlier, is not very sensitive and other pathologies e.g. pericardial effusions confound. Serum cardiac biomarkers such as NT-proBNP and Troponin T are not specific to amyloid and are also affected by renal impairment (a common mode of presentation in AL Amyloid) and chemotherapy. Cardiac biopsy is invasive and radioisotope scanning is either not useful in AL Amyloid (DPD scan) or simply does not image the heart at all (SAP scan).

Considering the poor prognosis carried by cardiac AL amyloidosis, any method of accurately and non-invasively quantifying the interstitial expansion seen in cardiac amyloidosis, detecting the disease earlier, detecting amyloid regression in cases that improve

and predicting survival optimally in order to reduce treatment-related mortality as well mortality due to the disease, is most welcome for these patients.

We hypothesise that T1 mapping and ECV measurement are able to achieve these outcomes and these hypotheses are now explored further in this thesis.

7. METHODS

7.1 ETHICAL APPROVAL:

Prior to this thesis, Dr. Andrew Flett had obtained ethical approval (ref 07/H0715/101) to study the EQ-CMR technique in patients with AS and HCM from the joint UCL/UCLH committee on ethics of human research. Dr. Daniel Sado then obtained 2 substantial amendments to this which granted permission to recruit and scan healthy volunteers (n=100) and patients with cardiac diseases (n unlimited) discussed in this thesis.

I was jointly appointed across the Heart Hospital and the National Amyloidosis Centre (NAC). I obtained 3 minor amendments to enable contact of patients by phone for recruitment because of the unavoidable necessity to coincide CMR scans with patients' existing appointments with the NAC, as many of them come from lengthy distances across the UK and Europe. The 2nd minor amendment was to create a second Patient information leaflet, changing it from the general subject of diffuse fibrosis in HCM, DCM and AS to interstitial expansion due to amyloid infiltration. The final amendment was to allow ethics to cover the National Amyloidosis Centre.

I subsequently helped with the requirements of setting up CMR as an endpoint for the first in man GSK study using my methods as a primary endpoint.

7.2 PATIENTS:

A total of 179 patients were scanned from the NAC over the course of 2010-2013. These patients were usually attending the NAC for a 24 hour period in order to have ECG, echo, SAP scan and a clinical consultation. All CMR scans were performed at the Heart Hospital and it was therefore necessary to transport patients from the NAC to the Heart Hospital and back in between their other numerous investigations. This was a limitation of the recruitment process.

Of these 179 patients, 26 were follow up scans (2nd scans) and 6 were interstudy reproducibility scans. The remaining 147 scans were of consecutive patients, either with a known diagnosis of amyloidosis (i.e. follow up patients) or an unknown diagnosis (i.e. new

referrals), attending the NAC between 2010-2013 with clinical indications for CMR and no contraindications to either MRI or gadolinium. Patients in AF on attending the NAC were also excluded.

Of these 147, 8 patients did not have EQ-CMR scans for the following reasons:

- eGFR <30ml/min (scan done on clinical grounds with patient's consent to gadolinium) (n=2)
- Poor pre-contrast T1 map (FLASH only patients) (n=2)
- Severely orthopnoeic (n=2)
- Patient refusal (n=1)
- Side effects (nausea & vomiting) on gadolinium infusion, therefore infusion terminated (n=1)

This left 139 patients who had full EQ-CMR; these are categorised as follows:

- AL 100
- ATTR 19
- AA 3
- Other hereditary 4
- Localised 2
- No amyloid 11

All patients had, as part of their routine clinical work up, tissue biopsy proof of amyloid except 2 patients in the AL cohort – 1 who died before a biopsy could be obtained and the other had a normal soft tissue biopsy but with a diagnostic SAP scan showing bone marrow uptake. Histology was performed with Congo red followed by immunohistochemical staining, these results are shown later in this thesis.

Before having their CMR scan, all patients were subgrouped into their pre-test probability of having cardiac involvement as follows:¹⁴⁹

Definite cardiac involvement – any of:

- Left ventricular wall thickness of $\geq 12\text{mm}$ by echocardiography in the absence of any other known cause
- RV free wall thickening co-existing with LV thickening by echocardiography in the absence of systemic or pulmonary hypertension

Possible cardiac involvement – any of:

- LV wall thickening by echocardiography in the presence of hypertension
- RV thickening by echocardiography in the presence of pulmonary hypertension
- Normal wall thickness by echocardiography with diastolic dysfunction and raised serum biomarkers³³

No suspected involvement

- Normal wall thickness by echocardiography with normal serum biomarkers

The majority of chapters in this thesis refer solely to the AL Amyloid cohort. Some chapters (e.g. reproducibility, pilot EQ-CMR in ATTR amyloidosis) also include the ATTR cohort.

7.3 HEALTHY VOLUNTEERS:

Over the course of the 2 year period, healthy volunteers (n=82) were recruited through advertising in hospital, University and general practitioner surgeries. All had no history or symptoms of cardiovascular disease or diabetes and were asked to fill in a health questionnaire on arrival for their CMR scan. No patient was on cardio-active medication except 4 on statins for primary prevention. These scans were performed and reported by Dr. Daniel Sado and Dr. Viviana Maestrini as a comparator group for ECV studies within our group.

Some were scanned before we had the ShMOLLI sequence available to us and therefore only 54 of the 82 healthy volunteers were scanned using the ShMOLLI T1 mapping sequence.

7.4 CMR:

All scans were performed on a 1.5 Tesla Siemens™ Avanto scanner and images always acquired during breath-hold at end expiration.

7.4.1 Pilot Images:

All studies started with single shot pilot images with the following settings: repeat time (TR): 3.39ms, echo time (TE): 1.7ms, slice thickness, 5mm, field of view (FOV) 360 x 360mm, read matrix 256 and flip angle 60°.

7.4.2 Cine Images:

After piloting, steady state free precession (SSFP) cine imaging was then undertaken, firstly in the long axis planes with a short axis cut through the aortic valve. A standard LV short axis stack was then acquired using a slice thickness of 7mm with a gap of 3mm. Retrospective ECG gating was used with 25 phases. Typical fast imaging with steady state precession (FISP) imaging parameters were TE: 1.6ms, TR: 3.2 ms, in plane pixel size 2.3 x 1.4mm, slice thickness 7mm, flip angle 60°. These settings were optimised accordingly if the subject was unable to breath-hold, or had an arrhythmia etc..

7.4.3 Pre Contrast T1 Assessment:

7.4.3.1 FLASH Heart:

Next, pre-contrast T1 assessment for the heart was performed using the method described in section 6.10 which is a multi-breath-hold, spoiled gradient echo, FLASH inversion recovery sequence with the following parameters: slice thickness 8mm, flip angle=21°, FOV 400x260mm and a TR and TE set according to the heart rate to avoid misgating. Images were taken at increasing TIs of 140 ms, then 200 to 1000 ms in 100ms increments subsequently corrected for heart rate.

A pre-saturation band was placed across the cerebrospinal fluid (CSF) to avoid ghosting onto the ventricular septum in the 4-chamber view, allowing a clean ROI to be drawn on the septum. All ROIs were drawn in the 4-chamber view as shown in figure 16 (on page 46) taking care to avoid the extremities of the blood:endocardial boundary. The signal intensity at each TI is then plotted on a pre-designed MS Excel® graph and the T1 calculated, as described in section 6.10.

For intrastudy reproducibility, scans were firstly analysed by myself before being anonymised and randomised by Dr. Viviana Maestrini and then subsequently re-analysed by myself within 24 hours; ECV results were collected by Dr. Maestrini. For interobserver reproducibility, scans analysed and reported by myself were anonymised; the second reporter was Dr. Maestrini and ECV results were collated by me within 7 days. For interstudy reproducibility, scans were performed no more than 14 days apart. These scans were anonymised and both reported by myself with ECV results collated by Dr. Maestrini.

7.4.3.2 FLASH Liver, Spleen and Skeletal Muscle:

For the liver, spleen and skeletal muscle, axial, sagittal and coronal plane localisers were used to plan an axial slice through the upper abdomen to include the greatest area of liver and spleen. Pre-contrast FLASH images were acquired at this location (as for the heart) for T1 measurement with inversion times increasing from 140 to 200ms and then to 1000ms in 100ms increments.

In the liver, a single, large, peripherally-based, wedge-shaped polygonal ROI was drawn in liver segment 6 and 7 so as to include the maximum area of liver tissue, but avoid visible hepatic and portal veins. These were non-gated acquisitions with a standard TR of 2000msec every time. A single image is shown as an example in figure 22.

Elliptical ROIs were also drawn in the spleen and paravertebral muscle to include the maximum area of tissue and avoid adjacent vessels and fat. A circular ROI was drawn in the abdominal aorta so as to include the greatest area of lumen, but not include aortic wall – frequently thickened by atheroma (see figure 22).

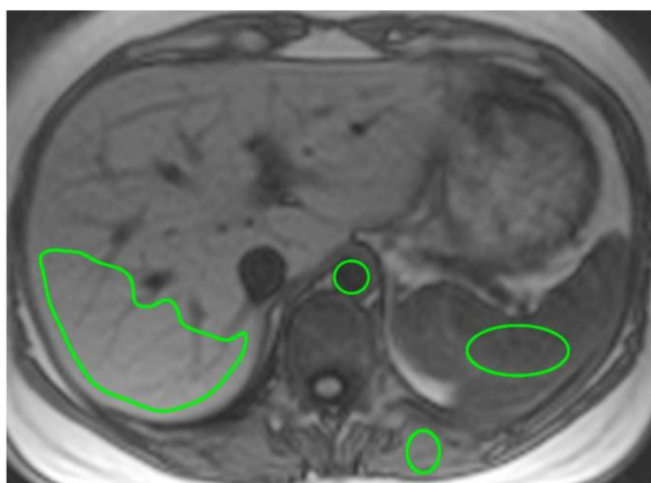


Figure 22: Pre contrast axial MR image (inversion time, 800 msec) shows sample ROIs drawn within the abdominal aorta, spleen, liver, and paravertebral muscle.

The 4 ROIs were then copied to the EQ phase FLASH images and mean signal intensity within each tissue at each TI recorded before being plotted on the MS Excel® graph as described above in section 6.10. Interstudy variability was tested for the liver and spleen as described on page 55 using Pearson's correlation coefficient and Bland-Altman analysis.

7.4.3.3 ShMOLLI Heart, Liver and Spleen:

In some AL amyloid patients (n=73) and healthy volunteers (n=54), ShMOLLI T1 mapping of the heart, liver and spleen were also performed in addition to FLASH T1 measurement. For the ShMOLLI mapping, typical setting were: FOV 340 x 340mm, FOV phase 69.8%, flip angle 35°, TR 1095msec, TE 1.05msec, slice thickness 8mm, 107 phase encoding steps, interpolated voxel size=0.9x0.9x8mm, base resolution 193 and phase resolution 100. Acquisition time was 206msec for a single image with a cardiac (trigger) delay time (TD) of 500ms; where necessary, to avoid misgating, the TD was decreased by 100ms for every 10 beats per minute above a resting heart rate of 80 beats per minute.

A ROI was then drawn in the basal septum on the 4-chamber view of the resulting parametric T1 map, 2 pixels away from the apparent blood:endocardial boundary and were drawn without reference to the LGE images.¹⁵⁰ This produced the T1 value which could then be converted to the ECV using the same equation described earlier in section 6.10.

7.4.4 LGE:

Intravenous Gadoterate meglumine (gadolinium-DOTA, marketed as Dotarem® Guerbet, S.A., France) was then administered as a 0.1mmol/kg dose via a pressure injector at a rate of 3ml/sec, with a 25ml normal saline flush. LGE assessment was then undertaken using a FLASH IR sequence with slice thickness 8 mm, TR: 9.8 ms, TE: 4.6ms, α: 21°, FOV 340 x 220 mm (transverse plane), sampled matrix size 256 x 115-135, 21 k-space lines acquired every other RR interval (21 segments with linear reordered phase encoding), spatial resolution 1.3 x 2.1 x 8 mm, no parallel imaging, pre-saturation bands over CSF and any pleural effusions.

These parameters were optimised according to individual patient characteristics. The TI was manually set to achieve nulling of the myocardium between 300 and 440 ms. When LGE was observed, images were acquired in phase swap and cross cut to ensure artefact elimination. Where the LGE distribution appeared particularly diffuse, a TI scout was used to ascertain the specific parts of myocardium with the highest concentration of gadolinium. If the participant was struggling with the breath-hold, FISP imaging or IR-SSFP imaging (single shot or segmented) was used as an alternative sequence.

7.4.5 Post contrast T1 evaluation:

In some studies, 15 minutes after the bolus was given, ShMOLLI T1 mapping was repeated, from which ECV_b was derived. In all studies, an infusion of gadolinium was then commenced at a rate of 0.0011mmol/kg/min. At this point, the participant was usually taken out of the scanner while the infusion ran over the next 30 minutes. They were then returned to the scanner with the infusion continuing to run. Repeat T1 assessment was performed using the FLASH IR sequence and in most cases, the ShMOLLI T1 mapping sequence as well, from which ECV_i was derived. Post contrast ShMOLLI required off-line post-processing before the T1 could be calculated.

7.4.6 Off line clinical analysis:

For LV volume and mass analysis, a thresholding technique was used. All of the amyloid patients in this thesis were analysed by myself; the healthy volunteers were analysed by Dr. Daniel Sado and Dr. Viviana Maestrini.

The healthy volunteer scans were reported by Dr. Daniel Sado and Dr. Viviana Maestrini, with authorisation by Dr. James Moon (primary supervisor to both); all patient studies were reported by myself and Dr. James Moon (primary supervisor and Reader in Cardiology) using international guidelines as the basis for all reporting.¹⁵¹

7.5 BLOOD PRESSURE AND 12 LEAD ECG:

All patients had their blood pressure (BP) measured at the National Amyloidosis Centre on a CareScape™ V100 machine by the nursing staff as part of their routine workup. In the healthy volunteer cohort, BP was measured after their CMR scan by Dr. Daniel Sado and Dr. Viviana Maestrini using a Mindray™ machine.

A 12 lead ECG was performed on all patients at the National Amyloidosis Centre on the same day as the CMR scan, as part of their clinical work up. The ECG was acquired using a calibration of 10 mm/mV and speed of 25 mm/s. Interpretation of the trace was performed by myself. Healthy volunteers followed an identical protocol.

7.6 BLOOD TESTS:

All participants had blood tests taken prior to the CMR scan at the National Amyloidosis Centre as part of their clinical workup. This included NT-proBNP and serum free light chain in all cases, with Troponin T in just over half the cases as this is only routinely performed on new patients.

7.7 SIX MINUTE WALKING TEST (6MWT):

This was performed at the Heart Hospital along a flat corridor in accordance with current guidelines.¹⁵² Patients were asked to walk a 30-metre length of the corridor at their own pace while attempting to cover as much ground as possible in the 6-minute period. Verbal encouragement was given using either of 2 standardised phrases: “You’re doing well” or “Keep up the good walk.” At the end of 6 minutes, participants were asked to stop and the distance covered was recorded. Any symptoms were recorded, as was the Borg score (on a scale of 1-10) to assess the degree of breathlessness.¹⁵³

7.8 ECHOCARDIOGRAPHY:

In all patients, transthoracic echocardiography was performed at the National Amyloidosis Centre on a Philips® IE33 machine as a part of the routine clinical work up. Echo studies, included tissue doppler just above the mitral valve annulus at the septal and left ventricular lateral wall. Scans were performed and analysed by 2 echocardiographers experienced in scanning patients with cardiac amyloidosis. Accepted markers of diastolic dysfunction i.e. isovolumic relaxation time (IVRT), E-deceleration time and E:E' ratio were all measured.¹⁵⁴ Echocardiography was not used to assess left ventricular systolic function for this work, as CMR was seen as the gold standard in this regard.¹⁵¹

7.9 SAP SCINTIGRAPHY:

All AL amyloid patients underwent SAP scintigraphy at the National Amyloidosis Centre as part of their routine workup. A weight adjusted dose of purified human SAP component, radiolabelled with 200MBq of ¹²³I is injected into the patient. Anterior and posterior whole

body, planar images are captured on a General Electric (GE)[®] Infinia gamma camera no less than 6 hours after the injection. Total amyloid load in the liver and spleen were graded by Prof. Philip Hawkins, who has the most experience in reporting these scans in the UK, having co-invented the scan with Prof. Sir Mark Pepys in 1988. Grading criteria were as follows:

- None – No tracer uptake into organs. Normal blood pool signal.
- Small – Tracer uptake into organs with blood pool still clearly visible
- Moderate – Tracer uptake into organs with blood pool only just visible
- Large – Tracer uptake into organs with no blood pool visible

7.10 DPD SCINTIGRAPHY:

Most of the ATTR patients had DPD scans (instead of SAP scans) by the time of their appointment though this was not always possible because of time and scanner limitations on the day. Where performed, patients were scanned using a GE[®] Medical Systems hybrid SPECT-CT gamma camera (Infinia Hawkeye 4) following administration of 700MBq of intravenously injected 99mTc-DPD. Three hour (delayed) whole body planar images were acquired followed by a single photon emission computed tomography (SPECT) of the heart with a low-dose, non-contrast CT scan.

Gated/non-gated cardiac SPECT reconstruction and SPECT-CT image fusion was performed on the GE Xeleris workstation. Cardiac retention of 99mTc-DPD was visually scored according to the classification described by Perugini et al⁸⁴ as follows: Grade 0 - no visible myocardial uptake in both the delayed planar or cardiac SPECT-CT scan; Grade 1 - cardiac uptake on SPECT-CT only or cardiac uptake of less intensity than the accompanying normal bone distribution; Grade 2 – moderate cardiac uptake with some attenuation of bone signal; and Grade 3 – strong cardiac uptake with little or no bone uptake.

7.11 STATISTICAL ANALYSIS:

All statistical analysis was performed by myself using SPSS (IBM Corp. Released 2012. IBM SPSS Statistics for Windows, Version 20.0. Armonk, NY: IBM Corp), except survival analysis which was performed by Aviva Petrie, Head of Biostatistics at the Eastman Dental Institute, UCL, using SPSS (IBM Corp. Released 2012. IBM SPSS Statistics for Windows, Version

21.0. Armonk, NY: IBM Corp) and Stata (StataCorp. 2011. Stata Statistical Software: Release 12. College Station, TX: StataCorp LP) and my colleague Dr. Gabriella Captur using REDCap (Research Electronic Data Capture) electronic data capture tools hosted at the University College London.¹⁵⁵

Normality was tested using the Kolmogorov Smirnov test. All continuous variables were approximately normally distributed except BNP and Troponin T which were log transformed to achieve normality for further analysis. Bivariate analysis compared ECV and pre-contrast T1 with all continuous variables. Pearson's correlation coefficients are presented unless otherwise stated. Means are presented \pm SD. All reproducibility for cardiac ECV is presented in the form of intraclass correlation coefficients (ICC). Agreement was ascertained using the Bland-Altman method where results are presented as mean bias \pm 2SD. For interstudy reproducibility of liver and spleen ECV, only agreement by the Bland Altman and Pearson's correlations are given.

The Chi-squared test was used to compare categorical variables between patients and controls whilst the unpaired t-test was used to compare continuous variables between the patients and controls. A one-way ANOVA with Bonferroni correction was used to test ECV with pre-test clinical probability of cardiac involvement described in section 7.2.

Liver, spleen and muscle ECV measurements in healthy volunteers followed a non-Gaussian distribution and were compared with those in the Amyloidosis population using a Mann-Whitney U test. In order to examine an association between ECV and SAP score in the liver and spleen, a Spearman correlation analysis computing a one tailed P-value was performed.

A goal of this study was to assess the prognostic value of myocardial pre contrast T1 and ECV in Systemic AL Amyloidosis, more specifically the capacity of ECV_i compared to ECV_b and pre contrast T1 for discriminating between surviving and dying patients with AL amyloidosis. ROC curves provide a graphical display for addressing this question by characterizing the distribution of measurements among patients that die by time t, relative to the distribution of the parameter among patients that survive. However, conventional ROC analysis could not be performed because the follow up period was not the same for each patient. Therefore, time-dependent ROC curves¹⁵⁶ were used to assess the capacity of ECV_i

compared to ECV_b and pre contrast myocardial T1 for discriminating between surviving and dying patients with AL amyloidosis. For fixed times ($t = 12$ months, $t = 24$ months) and specificity level, we have compared the sensitivity of ECV_i, ECV_b and pre contrast myocardial T1 measurements for detecting patients that will die by time t . For the ROC curves constructed using the nearest neighbour estimator (NNE), we used a narrow span of λ ($0.25 * \text{nobs}^{-0.20}$) to yield only moderate smoothing. To permit comparison of ROCs by NNE estimator, a set of simple KM estimator ROC curves for this data at $t = 24$ months were also created (see chapter 14 later).

Survival was evaluated using Cox proportional hazards regression analysis, providing estimated hazard ratios (HR) with 95% confidence intervals (CI) and Kaplan Meier curves. Linear regression models measured the association between quantitative ECV and other variables; variance inflation factors (VIF) <3 excluded collinearity. Optimal myocardial T1 and ECV values were explored by Cox regression, using the median and the 1st or 2nd tertiles as cut-off values. The two groups resulting from each cut-off were compared using the Harrell's C statistic (a measure of discrimination between groups) in order to determine the better model and thus biomarker for predicting survival. All variables were first explored with univariate Cox regression. Multivariable models evaluated the independent predictive value of ECV above other clinically and statistically significant covariates.

For the follow up study, the Wilcoxon Signed Rank Test was used to detect statistically significant differences in continuous scale cardiac variables between response groups whilst the McNemar's test detected statistically significant differences in discrete variables between response groups. For each patient, amyloid mass was calculated multiplying the ECV x LV mass whilst cell mass was calculated by multiplying (1-ECV) x LV mass. Difference in amyloid mass and myocyte cell mass was calculated by subtracting follow-up values from the baseline value. As these differences were non-normally distributed, results are presented as median and interquartile range. Comparison between responder groups is assessed using the non-parametric Kruskal Wallis test.

8. RESULTS

8. Myocardial ECV as measured by EQ-CMR in Systemic AL Amyloidosis:

This chapter is based on the publication below:¹⁵⁰

Banypersad SM, Sado DM, Flett AS, Gibbs SD, Pinney JH, Maestrini V, Cox AT, Fontana M, Whelan CJ, Wechalekar AD, Hawkins PN, Moon JC. "Quantification of myocardial extracellular volume fraction in systemic AL amyloidosis: an equilibrium contrast cardiovascular magnetic resonance study." Circ Cardiovasc Imaging. 2013; 6(1):34-9

My contribution was consenting, recruiting and scanning all the patients as well as reporting and analysing all the data. I also wrote the paper.

8.1 Introduction:

As stated earlier in chapter 6, cardiac involvement is the principal driver of prognosis in this condition and can be the presenting feature of the disease.³¹ Whilst a constellation of ECG, echocardiographic and biomarker findings becomes increasingly diagnostic and prognostic as cardiac amyloidosis progresses, evaluation of early stage cardiac involvement can be challenging.

Concentration of the serum biomarkers NT-proBNP and Troponin T form the basis of the Mayo Staging classification³³ but are influenced by renal impairment which is present in a quarter of patients at presentation. ECG criteria, low limb lead voltages²³ or fragmented QRS complexes¹⁵⁷ are also predictive, but are confounded by pericardial effusions and conduction abnormalities. Echocardiographic parameters also predict^{59, 158, 159} but other co-existing causes of LVH or diastolic impairment affect interpretation.

Definitive diagnosis of cardiac amyloidosis, which has critical implications for choice of chemotherapy and management generally, requires cardiac biopsy which is invasive and prone to sampling error. There are currently no non-invasive tests that can quantify cardiac amyloid deposits, the need for this having intensified lately with the development of novel anti-amyloid therapies that will shortly need testing and validation.³

New imaging modalities are showing promise; DPD scintigraphy, discussed earlier in section 6.4.4, appears to be able to image cardiac amyloid, though chiefly transthyretin (ATTR) type,⁸³ whilst imaging with CMR is virtually pathognomonic of amyloid in some patients when the characteristic global, subendocardial late gadolinium enhancement occurs.⁸⁹ However, neither is quantitative.

We therefore tested whether EQ-CMR would accurately measure the degree of interstitial expansion within the heart.

8.2 Hypotheses:

- (1) That EQ-CMR will show a higher ECV in amyloidosis compared to healthy volunteers
- (2) That EQ-CMR will be an effective method for quantifying and tracking cardiac amyloid burden.

8.3 Methods:

Sixty patients from the total AL cohort of 100 mentioned in section 7.2 were recruited. Four patients who were found to have AF/flutter after they had consented were not excluded. Of this cohort, 7 (12%) patients were on treatment for hypertension and 6 (10%) had confirmed coronary artery disease by angiography.

All patients were required to have histological proof of systemic AL amyloidosis by Congo red histology and immunohistochemical staining, which was obtained through specimens of kidney (n=17), endomyocardium (n=4), bone marrow (n=8), upper gastrointestinal tract (n=4), liver (n=1), fat (n=6), spleen (n=1), lung (n=1), rectum (n=8), soft tissues (n=8), lymph node (n=1) and peritoneum (n=1). This is summarised in figure 23 on the next page:

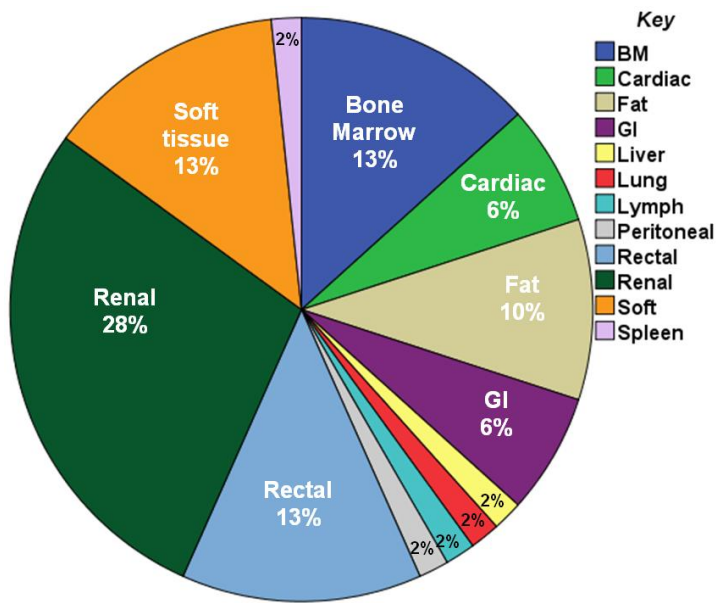


Figure 23: Pie chart showing distribution of tissue biopsies within the patient cohort (n=60).

Healthy subjects (n=82) were the comparator group. As described in sections 7.2 and 7.3, all patients and healthy controls underwent 12 lead ECG. Patients additionally underwent assays of cardiac biomarkers (NT-proBNP and Troponin T), echocardiography, SAP scintigraphy including measurement of total body amyloid load, and a 6-minute walk test, although this was not possible in some patients (n=23, 38%) mainly due to other co-morbid factors (e.g. arthritis, postural hypotension, peripheral neuropathy) and patient choice. NYHA class and ECOG status were also assessed using a standard questionnaire.

All patients underwent EQ-CMR using the FLASH IR method of T1 measurement outlined in section 6.10 and 7.4. A ROI was drawn in the basal septum of the resultant piloted 4-chamber image in all patients as shown in figure 17 on page 46 earlier in this thesis; ROIs were mid myocardial and excluded subendocardial LGE. Where gadolinium was present, it was often extensive and therefore impossible to exclude from the ROI (see figure 24 on the next page). However, where possible, ROIs were also drawn in LGE -ve areas as well as LGE +ve areas to determine ECV in both. Reproducibility testing was performed as described in section 7: intrastudy (n=11), interobserver (n=11) and interstudy (n=6) scans were analysed by myself and Dr. Viviana Maestrini.

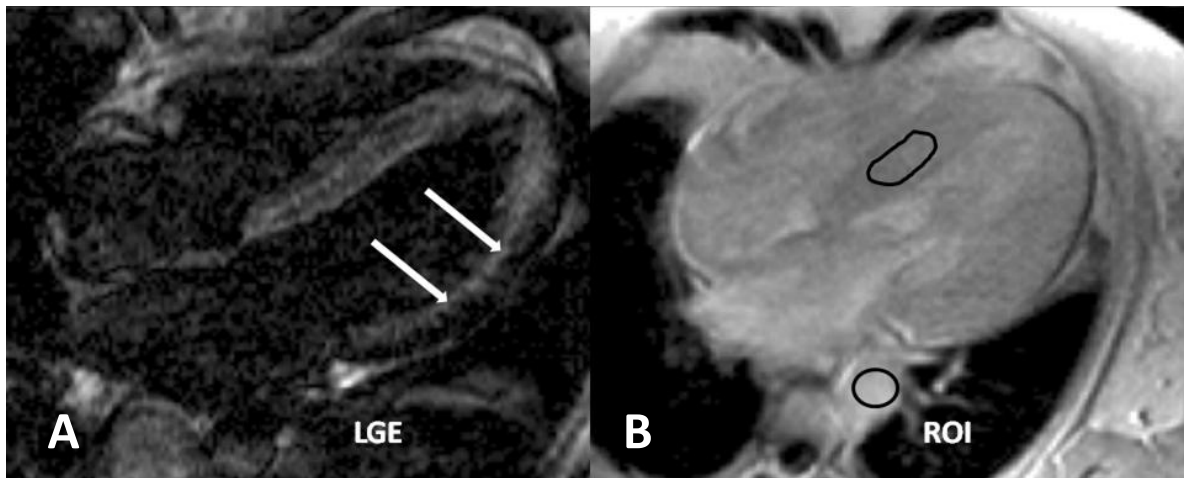


Figure 24: (A) Standard 4-chamber FLASH LGE image; (B) FLASH T1 measurement image at TI of 200ms, demonstrating the difficulty in avoiding areas of LGE when drawing ROIs in cardiac amyloidosis.

Standard CMR parameters of structure (LV mass, left atrial (LA) area with/without indexing, septal thickness), systolic function (EF, MAPSE, TAPSE) were assessed as well as ECV calculations. Diastolic function was assessed by echocardiography as described in section 7.8. Mean ECG QRS voltage in limb and praecordial leads were calculated.¹⁶⁰

All statistical analysis was performed as described earlier in section 7.11.

8.4 Results:

Baseline patient and healthy control characteristics are shown in the table 2 on the next page. Patients were older than healthy volunteers and contained proportionately more males than females. This slightly increases the control group ECV compared to that of a gender matched group (see later in this thesis) but there was no statistically significant increase in ECV with age in the healthy controls.

Patients generally had smaller cavity ventricles and a higher LV mass than healthy volunteers. Renal function was slightly more impaired compared to healthy volunteers but EF was not statistically significantly different.

<u>Characteristic:</u>	<u>Patients:</u>	<u>Healthy volunteers:</u>	<u>P value</u>
Male /female	39/21	41/41	P=0.08
Mean Age ± SD (yrs)	62 ± 10	46 ± 15	P<0.001
Mean Creatinine ± SD (mmol/L)	84 ± 26	74 ± 13	P=0.006
Median NT-pro BNP in pmol/L (IQ range)	121 (20-272)	-	
Organ involvement			
Peripheral/autonomic neuropathy (%)	14 (23)	-	
Renal involvement (%)	30 (50)	-	
<u>Cardiac involvement:</u>			
None (%)	15 (25)	-	
Probable (%)	15 (25)	-	
Definite (%)	30 (50)	-	
Echocardiography/CMR indices			
Mean Indexed LVEDV ± SD (mls)	60 ± 13	72 ± 12	P<0.001
Mean Indexed LVESV ± SD (mls)	19 ± 8	23 ± 7	P<0.001
Mean EF ± SD (%)	67 ± 11	67 ± 5	P=0.44
Mean Indexed LV mass ± SD(g/m ²)	94 ± 34	66 ± 13	P<0.001
AF /atrial flutter (%)	4 (7)	0	

Table 2: Showing patient characteristics and differences between AL amyloidosis patients and healthy volunteers

The mean ECV in patients with systemic amyloidosis was significantly elevated compared to healthy controls (0.400 vs 0.254, P<0.001). Mean ECV increased between groups (P<0.001) from healthy controls to AL with no suspected cardiac involvement (mean ECV 0.276), possible cardiac involvement (mean ECV 0.342) and definite cardiac involvement (mean ECV 0.488) (figure 25 on the next page).

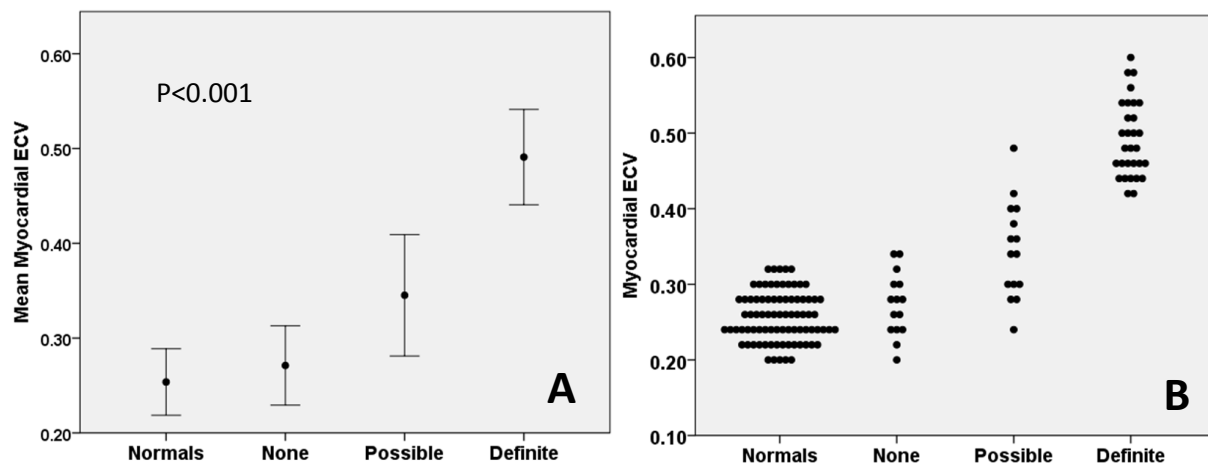


Figure 25: Relationship between myocardial ECV and pre-test probability of cardiac AL amyloidosis demonstrated by (A) Bar graph showing mean +/- SD and (B) Individual plots in bins of 0.02 for ECV on y-axis.

ECV and LGE:

LGE prevalence overall was 35/60 (58%). The pattern of LGE was global, sub-endocardial ($n=21$), patchy ($n=7$) and extensive ($n=7$) (see figure 6 on page 32 for illustrations). There was no significant difference in the mean ECVs between these groups. LGE presence was strongly tied to the pre-CMR likelihood of cardiac involvement: no, possible, definite cardiac involvement LGE prevalences were 0/15 (0%), 6/15 (40%) and 29/30 (99%), respectively ($P<0.001$).

ECV correlated strongly with the presence of LGE ($P<0.001$). All patients with LGE had an elevated ECV. In 4 cases, sufficient LGE negative areas existed to permit additional LGE negative ROIs to be drawn. In these cases, the ECV was lower than that derived from adjacent LGE areas, but still demonstrated substantial elevation. (0.45, 0.44, 0.37 and 0.50 compared with 0.46, 0.50, 0.44 and 0.53 respectively). Of the 25 patients without LGE, 6(24%) had elevated ECV, suggesting earlier detection using ECV measurements.

ECV and LV Structure / Function:

ECV correlated with CMR cardiac parameters of LV mass, septal thickness, size (LVESV and LVESVi) and LAA (see figure 26 on the next page). These findings are summarised in table 3 on page 71.

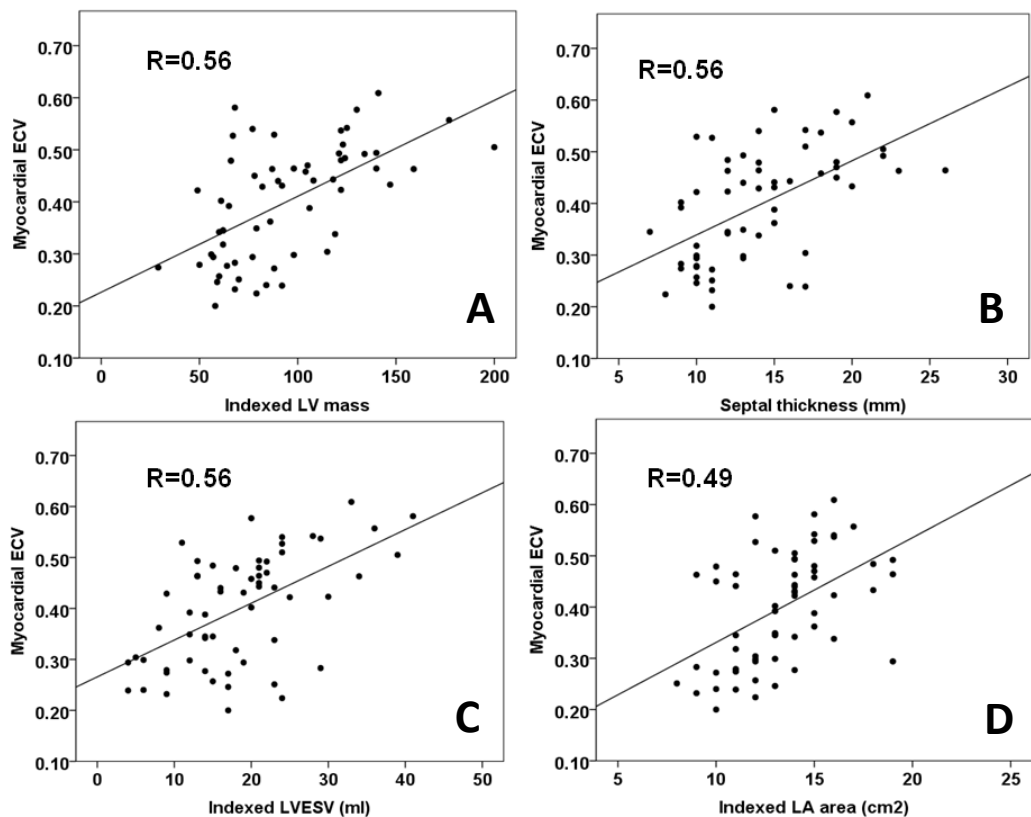


Figure 26: Graphs showing the linear relationship between myocardial ECV and (A) Indexed LV mass; (B) Septal thickness; (C) Indexed LV end-systolic volume; (D) Indexed LA area in systemic AL amyloidosis

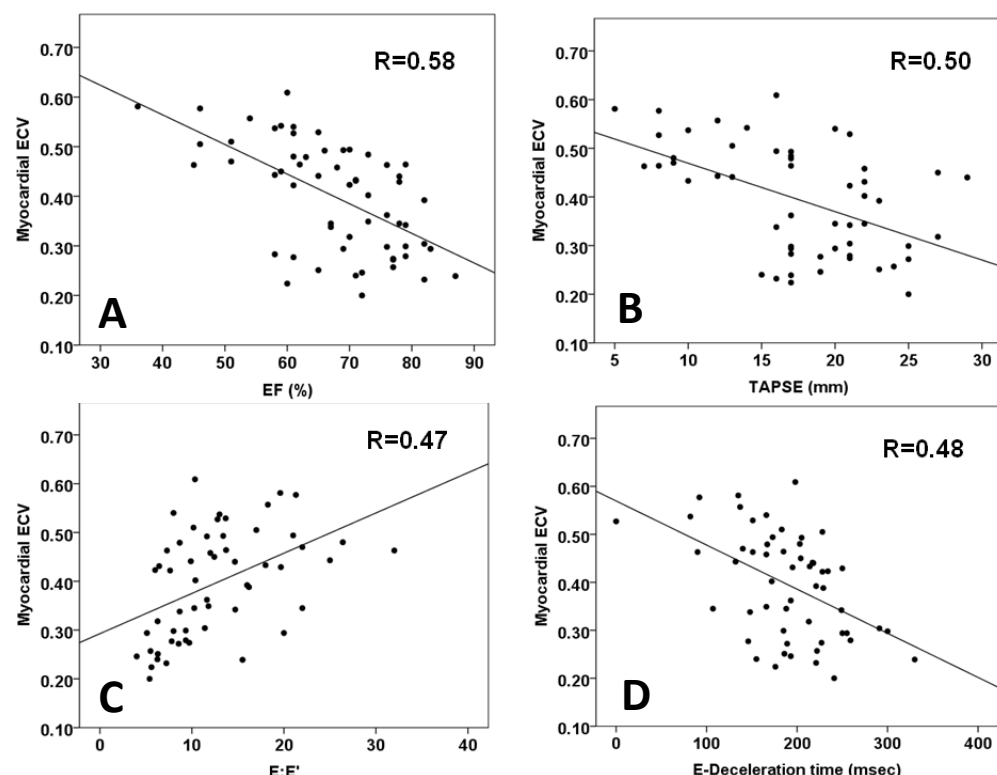


Figure 27: Graphs showing the relationship between myocardial ECV and (A) Ejection fraction; (B) TAPSE; (C) E:E' and (D) Mitral E wave deceleration time in systemic AL amyloidosis.

Measures of cardiac systolic and diastolic function by CMR and echocardiography respectively, including both simple (MAPSE and TAPSE) and advanced (TDI S-wave, E/E') parameters, also showed correlations (see figure 27 on the previous page and table 3 on the next page); interestingly, hypertrophy was not necessary for ECV elevation - 4 patients without hypertrophy (2 of whom had LGE) had raised ECVs (0.34, 0.35, 0.42 and 0.52).

ECV and other parameters:

ECV correlated with the biomarkers NT-proBNP and Troponin T (see table 3). ECV was inversely correlated with mean QRS voltage, particularly in the limb leads (limb leads, $R=0.57$, $P<0.001$; praecordial leads, $R=0.30$, $P=0.02$). (See also figure 28 below and table 3 on page 71).

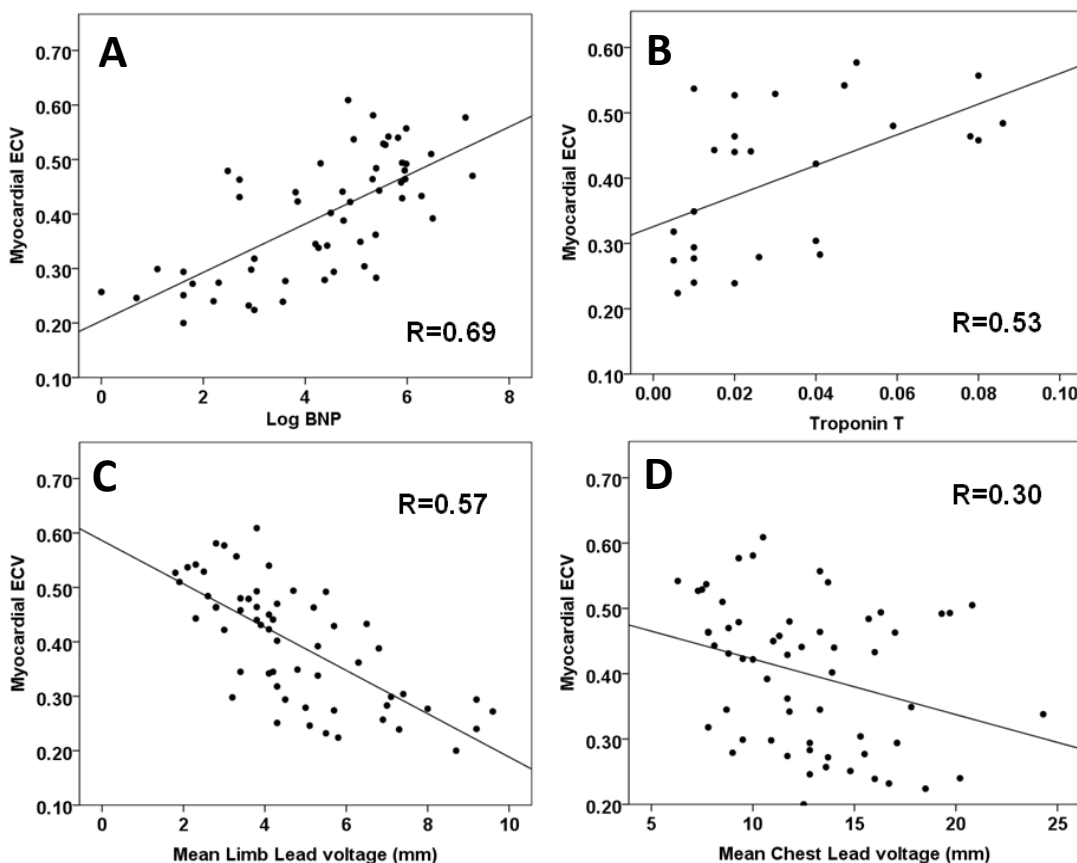


Figure 28: Graphs showing positive, linear relationship between myocardial ECV and (A) Log (base E) BNP; (B) Troponin T and inverse relationship between ECV and ECG (C) Limb lead and (D) Chest lead voltage, in systemic AL amyloidosis. (Note: fewer values for Troponin T as this test was not routinely performed in follow up patients as stated in section 7.6 earlier in this thesis).

Performance in the 6MWT among patients with possible and definite cardiac involvement by conventional assessment was poorer than for those with no suspected cardiac involvement (218 vs 207 vs 265m, both $P=0.01$). ECV weakly correlated with 6-minute walk

test ($R=0.36$, $P=0.03$). There were no differences of ECV with NYHA class or ECOG class. These results are summarised in table 3 below.

ECV compared against:	R	P-value
LV Structure by CMR		
LV mass	0.52	$P<0.001$
Indexed LV mass	0.56	$P<0.001$
Septal thickness	0.56	$P<0.001$
LA area	0.40	$P=0.002$
Indexed LA area	0.49	$P<0.001$
LV Systolic Function by CMR		
Ejection Fraction	0.58	$P<0.001$
MAPSE	0.58	$P<0.001$
LV end-systolic volume	0.52	$P<0.001$
Indexed LV end-systolic volume	0.56	$P<0.001$
TDI-S wave	0.52	$P<0.001$
LV Diastolic Function by Echo		
E:E'	0.47	$P<0.001$
IVRT	0.36	$P=0.03$
E-Deceleration time	0.48	$P<0.001$
RV Structure & Function by CMR		
RV end-systolic thickness	0.40	$P=0.005$
TAPSE	0.50	$P<0.001$
Functional Assessment		
6-minute walk test	0.36	$P=0.03$
Biomarkers		
Serum NT-pro BNP (logBNP)	0.69	$P<0.001$
Troponin T	0.53	$P=0.006$
ECG		
ECG Limb Lead mean voltage	0.57	$P<0.001$
ECG chest lead mean voltage	0.30	$P=0.02$

Table 3: Showing Pearson's R correlation coefficients and P-values for relationship between myocardial ECV and standard cardiac parameters in systemic AL amyloidosis

Reproducibility:

The ICC for **intrastudy** reproducibility of cardiac ECV measurement was 0.99 (0.96-0.99) with a bias of 0.002 (-0.009 to +0.014). The ICC for **interobserver** reproducibility was 0.92 (0.76-0.98) with a bias of 0.01 (-0.01 to +0.04). For **interstudy** reproducibility, the ICC for myocardial ECVs was 0.96 (0.90-0.99) with a bias of 0.02 (-0.03 to +0.07).

8.5 Discussion:

Amyloidosis is the exemplar of an interstitial disease, the quantity of amyloid in the extracellular space amounting to kilograms in some patients. Cardiac involvement is a major cause of morbidity and mortality, particularly in AL type, but there are currently no non-invasive methods to quantify it.

Here, the ECV was measured using EQ-CMR in systemic AL amyloidosis. ECV was massively elevated in the patients with definite cardiac involvement but also significantly higher in patients where conventional clinical testing suggested no cardiac involvement, and was significantly elevated in a quarter of patients with no LGE.

Expansion of the myocardial ECV represents a non-specific increase in free water between myocytes, and occurs in a variety of pathologies including focal and diffuse fibrosis, oedema and amyloidosis. However, the ECV in amyloidosis is higher than in any other disease generating diagnostic specificity above a certain threshold – for example, in our previous work (n=238) the highest ECV we have found to date in severe AS, DCM or HCM was 0.37 in a severe AS patient with previous coarctation repair and a poor LV.¹⁶¹ Here, the average value for definite cardiac AL amyloid was 0.488 with the lowest value being 0.423. We note however that the amyloid ROIs frequently included a proportion of areas of LGE, which was excluded in the previous study. Nevertheless, this data suggests that ECV can detect disease earlier than conventional testing.

In this study, strong correlations of ECV were also seen with indexed LV mass, LA area, septal thickness and CMR markers of LV systolic function, and more modest correlations with measurements of diastolic function. The correlations appear to support many conventional clinical strategies – for example, that indexed LA area as an excellent indicator of ventricular disease, the use of limb lead QRS voltages and the use of NT-proBNP and Troponin T in the Mayo clinical staging system.³³ However, biomarker experience shows that single timepoint ECV measurement is not the whole picture - post chemotherapy, suppression of light chain

production may trigger a swift change in NT-proBNP levels (usually falls, sometimes elevation)^{78, 80} with no ECG or echo changes, suggesting that simple amyloid burden quantification incompletely reflects myocardial pathology in amyloid.

Mean limb, rather than praecordial, lead QRS voltage on ECG showed an inverse correlation with ECV. Approximately 50% of patients with cardiac AL amyloidosis have low QRS voltage (<6mm)⁵² which has been attributed to “insulation” of the electrical impulse on the surface ECG due to infiltration. However, it is not seen in all patients and increased QRS voltages sometimes occur.⁵³ Cardiac ATTR amyloidosis may have far more wall thickening than AL amyloid, yet low voltages may not occur. Wall thickening in amyloid is the composite of myocyte volume and amyloid burden, with myocyte volume being a net balance of myocyte death^{74, 77} and hypertrophy.¹⁶² Conventional testing (such as LV mass) measures the composite of infiltration and cell volume. Further study with EQ-CMR histological calibration to derive myocyte volume as well as ECV will be able to answer important questions about the biology of cardiac amyloid.

A significant correlation with ECV was seen with performance in the 6-minute walk test but not with NYHA and ECOG performance status, although walking ability in patients with systemic amyloidosis can be influenced by many non-cardiac factors including peripheral and autonomic neuropathy, peripheral oedema, pleural effusions due to nephrotic syndrome, bone pain due to myeloma, and skeletal muscle loss associated with malnutrition.

In summary, ECV is reproducible and tracked a wide variety of markers of disease activity such as cardiac function and blood biomarkers, linked to patient’s functional performance, and strongly correlated with limb lead ECG complex sizes. These data suggest that ECV measurement is picking up infiltration earlier than conventional testing and is a direct measure of the amyloid burden with potential utility in early diagnosis, disease monitoring, and potentially as a much needed cardiac surrogate endpoint for the various promising new therapies for amyloidosis currently in preclinical development and early phase clinical trials.^{3, 163}

This has recently become particularly relevant with the first-into-man study of the dual CPHPC-monoclonal antibody trial being run by GSK as described back in section 6.8.2.3 where the baseline study demonstrated a dramatic reduction in amyloid load measured histologically in the liver and spleen of mice after treatment. The first-into-man study is currently underway

and ECV as measured by EQ-MRI is now a surrogate endpoint in determining response to treatment, based on this work, because SAP scintigraphy is no longer useful once circulating SAP has been depleted by CPHPC administration. ECV is therefore the only non-invasive measure of extracellular compartment (and by inference, amyloid load).

As stated already, a limitation of this study is the lack of histological correlations. In previous work, we have correlated diffuse fibrosis with ECV, but only 4 patients in our present cohort had undergone cardiac biopsy, and only one of these was contemporaneous, being performed within 4 months of the CMR study. Precise calibration of ECV with histological estimation of amyloid burden is desirable but challenging, as often in this multisystem disease other organs are biopsied before cardiac involvement is recognised and other organs are easier to sample. Furthermore, amyloid is patchy, predisposing to biopsy sampling error. Another limitation is that the patient and control populations were not age and sex matched; ECV is generally higher in women than men although no significant change with age has been observed.¹⁴⁸

As well as histological calibration, populations with ATTR amyloidosis merit study, as do the prognostic implications of ECV measurements and their reproducibility (all addressed later in this thesis). Newer, single breath-hold, T1 measurement techniques permit multislice mapping and have potential for whole heart quantification,^{145, 164, 165} holding the promise that it may be possible to avoid the gadolinium infusion in favour of a dynamic/pseudo equilibrium method, which would have substantial clinical advantages in terms of simplicity (also addressed later in this thesis).

8.6 Conclusion:

EQ-CMR using the FLASH IR method in systemic AL Amyloidosis has potential to become the first, non-invasive quantifier of cardiac amyloid burden.

9. Extracardiac ECV as measured by EQ-CMR in Systemic AL Amyloidosis:

This chapter is based on the following publication:¹⁶⁶

Bandula S, Banypersad SM, Sado D, Flett AS, Punwani S, Taylor SA, Hawkins PN, Moon JC. Measurement of Tissue Interstitial Volume in Healthy Patients and Those with Amyloidosis with Equilibrium Contrast-enhanced MR Imaging. Radiology 2013; 268(3): 858-64

My contribution was consenting, recruiting and scanning all the patients as well as reporting and analysing all the data. I also co-wrote the paper. Authorship reflects a departmental level agreement between Radiology at UCLH and MRI at the Heart Hospital.

9.1 Introduction:

All organs, not just the heart, are composed of metabolically active cells supported by an extracellular framework. In health, this architecture provides the medium through which cells exchange components necessary for intracellular metabolism, and can contribute, physically and metabolically, to the function of their constituent tissue. In disease, this alters such that amyloid infiltration causes expansion of the interstitium and thus organ dysfunction.

The liver and spleen are frequently affected in systemic AL amyloidosis. The only conventional non-invasive quantitative test being SAP scintigraphy, as mentioned previously in section 6.5. Interstitial expansion in the liver and spleen can be massive but difficult to measure; one reason for this has been an inability thus far to reliably and accurately quantify the interstitium. The reference standard of invasive tissue biopsy is limited by its technical difficulty, complication rate, and sampling error.¹⁶⁷ There are alternative non-invasive tests,¹⁶⁸ including biomarkers and tissue elastography,¹⁶⁹⁻¹⁷¹ however these are frequently organ specific or suffer from similar sampling error.

In the previous chapter, we demonstrated how EQ-CMR could be used to calculate the interstitial expansion in cardiac amyloidosis. We described how this technique creates equilibrium in gadolinium concentrations between myocardium and blood by use of a primed gadolinium infusion. However when the heart is at contrast equilibrium, so too are other tissues, excluding privileged sites such as structures behind the blood:brain barrier. This raises the possibility of extending the technique from EQ-CMR to EQ-MRI in order to assess the extracardiac organs and tissues.

The purpose of this study therefore was to assess liver, spleen and skeletal muscle ECV in patients with systemic AL Amyloidosis and healthy volunteers.

9.2 Hypotheses:

- (1) Liver, spleen and skeletal muscle ECV as calculated by EQ-MRI will be greater in systemic AL Amyloidosis than in health
- (2) Liver, spleen and skeletal muscle ECV as calculated by EQ-MRI will track abdominal organ amyloid burden.

9.3 Methods:

Sixty-seven patients from the AL cohort described in section 7.2 and 40 healthy volunteers were recruited. We attempted EQ-MRI using the FLASH IR method described in section 7.4.3.2 in all 40 volunteers and 67 amyloidosis patients, but, because of time limitations, patient discomfort, breathing and wrap-around artefacts and previous surgical resections, complete imaging was available as follows:

- Liver - 35 healthy volunteers and 56 amyloidosis patients
- Spleen - 32 healthy volunteers and 48 amyloidosis patients
- Paravertebral muscle - 34 healthy volunteers and 53 amyloidosis patients.

Imaging of all 3 tissues was available in 30 healthy volunteers and 46 amyloidosis patients. All amyloidosis patients underwent SAP scanning of the liver and spleen as described earlier in section 7.9. All SAP scans were graded on a scale of 0 (none) to 3 (large load) as described earlier in section 7.9. ECV calculated as previously and all statistical analysis performed as described earlier in section 7.11. Interstudy variability for ECV calculations of the liver and spleen were tested for 6 patients as described in section 7.

9.4 Results:

Baseline characteristics:

As in the last chapter, median age was higher in the patient group at 62 years (range 40-81) for patients and 45 years (range 24-88) for healthy volunteers ($P<0.001$). There were

also proportionately more males in the patient group than the healthy volunteers (n=43 vs n=18, P<0.001).

Liver, spleen and muscle ECV were non-normally distributed and ECVs are presented as median and interquartile (IQ) range.

Organ ECV in Health and Amyloidosis:

Within the healthy volunteer cohort, there was a statistically significant difference in individual organ median ECVs: liver ECV was 0.29 (IQ range: 0.27–0.33), spleen ECV was 0.34 (IQ range: 0.32–0.35) and paravertebral muscle ECV was 0.09 (IQ range: 0.08–0.14), P<0.001 (see figure 29A).

In amyloidosis, the median ECVs for each organ also varied significantly: liver ECV was 0.32 (IQ range: 0.28–0.37), spleen ECV was 0.39 (IQ range: 0.35–0.51) and paravertebral muscle ECV was 0.16 (IQ range: 0.13–0.22), P<0.001. We found a statistically significant increase in the ECV in amyloidosis patients compared with healthy volunteers for all organs (see figure 29B).

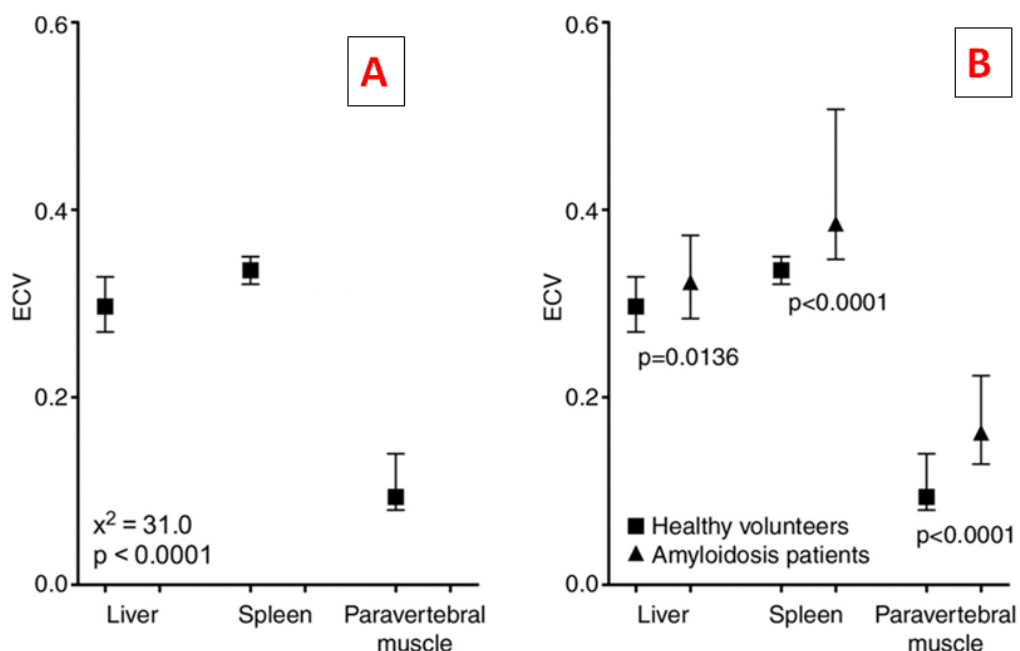


Figure 29: (A) Graph showing Median ECV values in the liver, spleen and paravertebral muscle in healthy volunteers and (B) Graph comparing median ECVs of healthy volunteers to AL amyloidosis patients for liver, spleen and paravertebral muscle.

Interstudy correlation for the spleen revealed an r^2 was 0.98 with a mean bias of -0.005 (-0.04 to +0.04) although most of these results were clustered around the normal range with only 1 outlier result. For the liver, r^2 was 0.51 with a mean bias of 0.02 (-0.02 to +0.08).

ECV vs SAP grade:

Matched liver ECV measurement and SAP scintigraphy was available in 56 patients. In 15 cases, SAP imaging demonstrated a congested liver pattern with an increased blood-pool signal associated with cardiac failure, and in one case, localization of the tracer was equivocal; this left 40 patients who could be assigned a liver SAP grade - 29 patients received a score of 0, five patients received a score of 2, and six patients received a score of 3. Liver ECV showed a positive correlation with SAP score (r_s 0.54, $P<0.001$) (see figure 30A).

We performed matched splenic ECV measurement and SAP scintigraphy in 48 patients. Six cases were excluded because SAP activity was scored as equivocal leaving: 22 patients scored 0, eight patients scored 1, seven patients scored 2, and five patients scored 3. As with the liver, spleen ECV showed a positive (stronger) correlation with SAP score (r_s 0.57, $P<0.001$) (see figure 30B below).

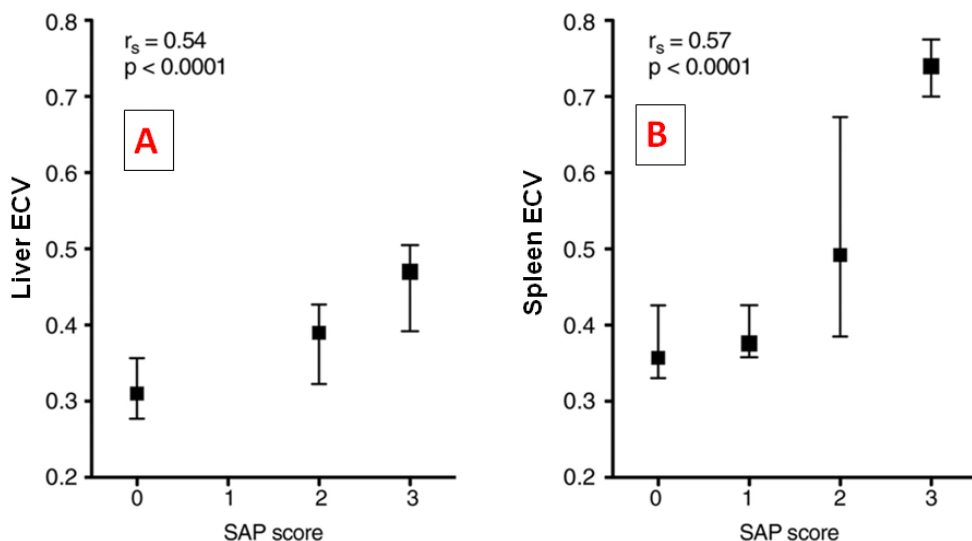


Figure 30: Graphs showing relationship of median ECV plotted against SAP grade for (A) Liver and (B) Spleen in systemic AL amyloidosis.

9.5 Discussion:

In this study, we used equilibrium MR imaging to define ECV in healthy tissues and to document variation in ECV between tissues. Such data are vital if ECV is to be used to detect pathologic processes. We showed significant differences in a disease process that exemplifies

expansion of the extracellular space (systemic AL amyloidosis), which provides strong proof that the equilibrium techniques can be successfully applied outside the heart.

Some pharmacokinetic model based ECV estimates exist. Levitt collected data from earlier experiments to produce a physiologic-based pharmacokinetic model by allowing estimation of the ECV in organs of a hypothetical standard human. He estimated the extracellular fluid fraction of the liver and muscle to be 0.23 and 0.15, respectively.¹⁷²

More recent studies used dynamic contrast-enhanced MR imaging to quantify the extracellular space and evaluate changes in response to treatment with a tumour disease model.¹⁷³ Dynamic contrast-enhanced MR imaging is a complex technique that is prone to substantial measurement error, and application is limited to only one tissue site.¹⁷⁴ A direct comparison of equilibrium MR imaging and dynamic contrast-enhanced MR imaging ECV has not yet been made; however, other authors who used dynamic contrast-enhanced MR imaging reported ECVs of 0.2–0.3 in healthy liver¹⁷⁵ and ECVs of 0.106–0.115 in skeletal muscle.¹⁷⁶ The estimates of ECV from pharmacokinetic modelling and dynamic contrast-enhanced MR imaging are consistent with each other and with our equilibrium MR imaging results.

In this study, we compared a disease-specific, in-vivo probe for extracellular amyloid deposition. SAP scintigraphy is the current reference standard for evaluation of systemic amyloidosis and has enabled wider assessment of organ amyloid involvement. Unlike histological analysis, SAP scintigraphy can be used to monitor changes in whole organs over time. These results demonstrated that an increase in tissue amyloid burden, assessed by SAP scintigraphy, was associated with an increase in tissue ECV. Therefore, equilibrium MRI imaging may be a useful non-invasive tool for amyloid assessment and potentially therapeutic monitoring with the added advantage of not exposing the patient to radiation.

Disease evaluation and quantification with SAP scintigraphy requires specific expertise, and it is only available in highly specialized centres. As described in sections 6.4.4 and 6.5 earlier, the high atomic mass of the SAP molecule (125 kDa) also favours evaluation in tissues with a fenestrated endothelium, such as the liver and spleen, where the large molecule is able to pass into the interstitium. Hence, SAP scintigraphy provides little information about amyloid deposition in skeletal muscle and myocardium.

This study had several limitations. The FLASH-based T1 mapping technique is complicated and time-consuming. Although the bolus-with-infusion protocol used in this study provided steady-state equilibrium in all tissues of interest, prolonged contrast infusions are not practical for clinical imaging. Our preliminary experimental findings concur with other authors' findings by showing that steady-state equilibration is reached approximately 15 to 20 minutes after administration of contrast bolus with infusion.¹⁴⁷ Future protocols may incorporate equilibrium-phase imaging after a shorter delay.

The ideal comparator for this study would have been histological assessment of the liver extracellular space. Histological techniques to quantify extracellular collagen matrix do exist; automated collagen proportionate area measurement showed good association with other indices of diffuse liver fibrosis when applied to the liver.¹⁷⁷ However, collagen-proportionate area measurements in the healthy liver are around 2%–3%,¹⁷⁸ which is much lower than our ECV estimate. This difference is most likely because the extracellular collagen matrix occupies only part of the extracellular space within the liver. Current histological techniques are unable to directly measure the ECV because the process of tissue sampling and preparation almost certainly alters tissue ECV.

Equilibrium MRI evaluation of ECV is not specific to an aetiological class of disease. In addition to amyloid deposition and diffuse fibrosis, tissue ECV may be elevated by interstitial oedema or an inflammatory infiltrate. Although these potential confounders could not be specifically excluded in this study, cases that demonstrated a congested pattern of activity on SAP scintigraphy were excluded from the SAP and ECV correlation.

It should be noted that healthy volunteer and amyloidosis patient groups were not matched for age or sex. As mentioned in the previous chapter, mean myocardial ECV in healthy women is around 4% higher than in healthy men but there is no change with age.¹⁴⁸ This has not been assessed in other organs. In this study, the higher ratio of women in the healthy group (18 men, 22 women) compared with the amyloidosis group (43 men, 24 women) may have reduced the difference in mean ECV measured between these groups. To minimize such bias, future studies should ensure that groups are matched for sex.

Although we assessed equilibrium MR imaging in one disease, it is worth noting that amyloidosis forms part of a larger set of conditions where extracellular disruption and

expansion leads to organ dysfunction e.g. liver cirrhosis. The application of equilibrium imaging in these organs could potentially provide a new biomarker for disease evaluation

9.6 Conclusion:

EQ MRI allows ECV of abdominal organs to be calculated; ECV is higher in systemic AL amyloidosis compared to healthy volunteers and tracks organ amyloid burden.

10. Technical Development – Refining Clinical Applicability:

My contribution was consenting, recruiting and scanning all the patients as well as reporting and analysing all the data as first operator. I supplied the entire amyloid component of the 2 technical development papers which I co-wrote with other colleagues within the department during the time of my MD.^{179, 180}

10.1 Introduction:

In the previous two chapters 8 and 9 in this thesis, we have shown how the EQ-CMR method uses high resolution FLASH-IR sequences at increasing inversion times to produce a T1 measurement for heart, blood, liver, spleen and skeletal muscle. The ECV is then calculated as previously described in section 6.10. This technique has advantages in that it is not vendor specific and is used in everyday clinical practice to obtain high resolution late gadolinium enhancement images.

However, there are a number of factors which limit its clinical utility in the current format. Firstly, there exist a number of ways where error may be introduced; patients are frequently short of breath, not only from the cardiac dysfunction due to amyloidosis, but also as a result of pleural and pericardial effusions. The FLASH method of T1 measurement, although high resolution, can be a problem for many patients because of the length of time required to breath-hold for one sequence; add to this that there are 9 sequences for the heart with a further 9 sequences repeated for the liver and spleen. This leads to image degradation because of breathing artefact as well as “ghosting” from the effusions. Indeed, the worst case scenario is patients being unable to undergo the research sequences at all.

Secondly, because it is a multi breath hold technique, patients may take a slightly different breath-hold with each sequence, altering not only position of the resultant image, but also affecting the R-R interval during the breath-hold (NB: a relatively stable R-R interval is necessary to accurately apply the heart rate correction). Furthermore, once the images have been obtained, the post processing is laborious, involving drawing a ROI on multiple images and a manual curve fit to the data points to calculate the TI of interest, plus correction, as extensively described in section 6.10. It is also ideal to try and avoid areas of LGE where possible and it is likely that this would vary between different operators using this technique.

Finally, there is the issue of the cumbersome gadolinium infusion. We calculate the ECV using the formula outlined in section 6.10. This formula holds true as long as a steady-state equilibrium of gadolinium concentration exists between the plasma and the tissue extracellular space i.e. elimination of the normal gadolinium kinetics (see figure 18 in section 6.10). We achieve this with EQ-CMR using a primed infusion of gadolinium commenced at 15mins post bolus. Recent work however, suggests that a “window of opportunity” may arise at 15mins post bolus, where a dynamic equilibrium or “pseudoequilibrium” may exist because renal excretion of gadolinium is slower than the free movement of gadolinium between blood and tissue extracellular compartments.^{165, 181} Imaging (T1 mapping) at this time may allow an accurate ECV to be calculated, saving approximately 45 minutes per scan, and sparing the patient from 30 minutes of a 0.0011 mmol/kg/min infusion of gadolinium; such a technique would clearly greatly enhance the applicability of ECV assessment further in the clinical setting.

However, there are concerns that if the timing of the image acquisition is not consistently accurate, that this would adversely affect the resultant ECV; the ECV does gradually rise linearly with time as a result of normal gadolinium kinetics.¹⁸² Moreover, this bolus only technique has only been tested in healthy volunteers¹⁸¹ and only very recently in some cardiac disease states.¹⁸³ It has crucially **not** been tested in patients with systemic amyloidosis which adds its own, almost unique, set of problems because of how amyloid affects normal gadolinium kinetics; normally and in most disease states, it is the blood and not the myocardium which has the highest concentration of gadolinium in the first few minutes after the bolus injection - in cardiac amyloidosis however, the opposite is observed. Whilst the mechanism for the observation is unclear, it is thought that a high free water content within the amyloid matrix in the heart, rapidly extracts gadolinium from the plasma into the myocardial interstitium – this produces the pathognomonic reversed nulling seen on TI scouts as described in section 6.4.5.

This chapter therefore first evaluates how the FLASH T1 measurement technique was made more clinically applicable by reducing breath-hold times for the patients by using the ShMOLLI T1 mapping sequence recently devised by Oxford. Finally, I describe how the technique was further refined by removal of the gadolinium infusion whilst still maintaining accuracy.

10.2 Hypotheses:

1. ECV derived using the ShMOLLI technique will closely match ECV derived from the FLASH technique.
2. ECV derived without a gadolinium infusion (ECV_b) would correlate with ECV calculated using the infusion (ECV_i)

10.3 Methods:

10.3.1 Comparison of FLASH ECV vs ShMOLLI ECV:

Our group acquired the ShMOLLI sequence in 2011, therefore only 50 of the 100 AL Amyloid patients outlined in section 7.2 underwent EQ-CMR of the heart using both FLASH IR and ShMOLLI T1 mapping methods and 13 of these also had liver and spleen ECV by both methods (n=12 for spleen as 1 patient had a splenectomy). All scans were analysed as described previously and ECV results at equilibrium calculated by myself.

ShMOLLI ECV results were compared for correlation (Pearson's) and agreement (Bland Altman) with ECVs derived using the histologically validated FLASH technique.

10.3.2 Comparison of Equilibrium vs Pseudoequilibrium ECV:

Fifty-one patients from the AL Amyloid cohort described in section 7.2 underwent full EQ-CMR with ShMOLLI T1 mapping and all patients additionally had a ShMOLLI T1 map at 15 minutes post bolus. The T1 was measured in the basal septum in the 4-chamber slice and in aortic blood and the mean cardiac ECV_b and ECV_i calculated. Bland Altman analysis was used to assess agreement between the 2 methods and Pearson's correlation coefficient used to assess correlation.

10.4 Results:

10.4.1 Comparison of FLASH ECV vs ShMOLLI ECV:

There was a correlation between FLASH and ShMOLLI ECV for the heart with an R^2 of 0.86. Tests for agreement showed a bias of -0.03 (-0.13 to +0.05) for FLASH. All values except 1 fell within the 2 SDs (see figure 31 below):

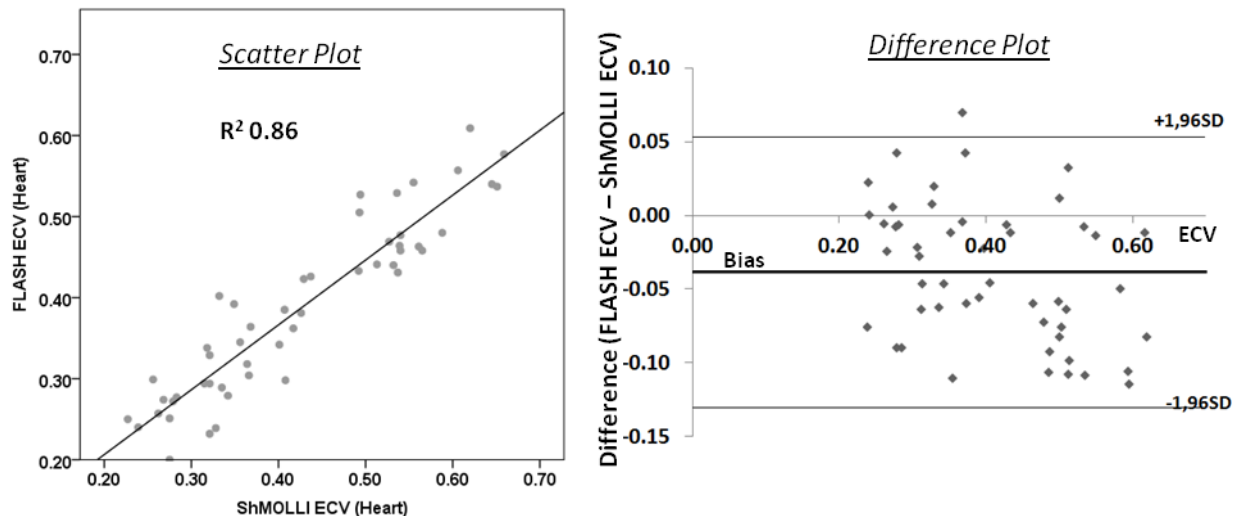


Figure 31: FLASH vs ShMOLLI reproducibility (Left) Scatterplot showing the correlation of the 2 myocardial ECVs; (right) Bland Altman graph showing agreement of the 2 myocardial ECVs.

Liver ECV by FLASH also correlated well with ShMOLLI values with an R^2 of 0.80. There was good agreement between the 2 methods with a bias of -0.04 (0.12 – 0.03) for FLASH. As above, all values except 1 fell within the 2 SDs (see figure 32 below).

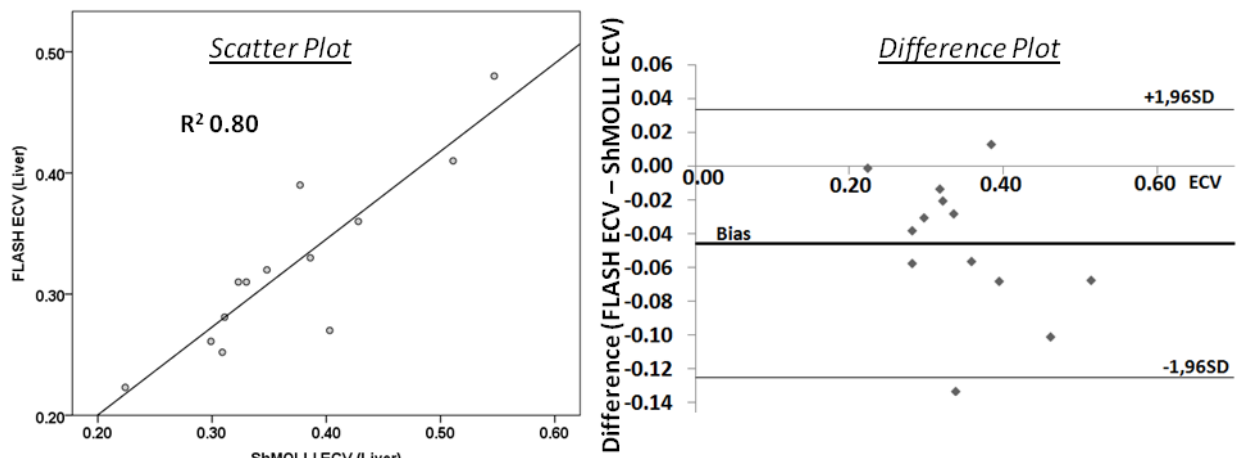


Figure 32: FLASH vs ShMOLLI reproducibility (Left) Scatterplot showing the correlation of the 2 Liver ECVs; (right) Bland Altman graph showing agreement of the 2 Liver ECVs.

There was good correlation and agreement between FLASH and ShMOLLI methods for ECV of the spleen with an R^2 of 0.95 and a bias of -0.007 (-0.07 – 0.05) for FLASH. Once again, I acknowledge that the majority of data points lie at the lower end of the ECV spectrum. All values fell within the 2 SD limits (see figure 33 on the next page):

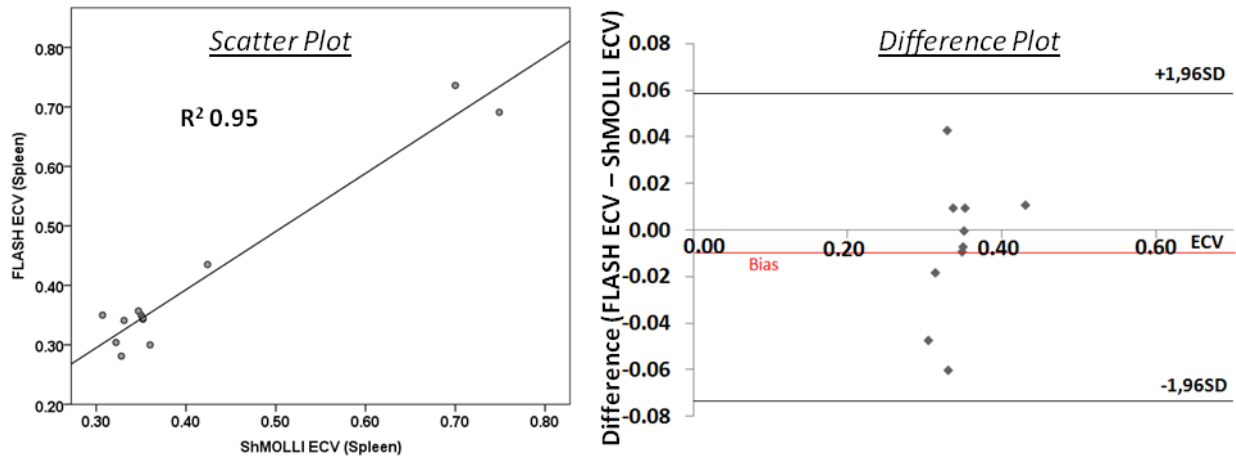


Figure 33: FLASH vs ShMOLLI reproducibility (Left) Scatterplot showing the correlation of the 2 Spleen ECVs; (right) Bland Altman graph showing agreement of the 2 Spleen ECVs.

10.4.3 Comparison of Equilibrium ECV_i vs Pseudoequilibrium ECV_b:

Mean ECV_b and ECV_i were both 0.45 (SD 0.12). Both correlation and agreement were good with a R² correlation coefficient of 0.88 and a minimal bias of -0.008 (-0.08 to +0.07) (see figure 34 below). The scatter plot shows little spread at ECVs of less than 0.45 and slightly wider spread with higher ECVs.

Bland Altman analysis revealed an equal spread of results above and below the identity line with the vast majority of values falling within the 2 SD limits:

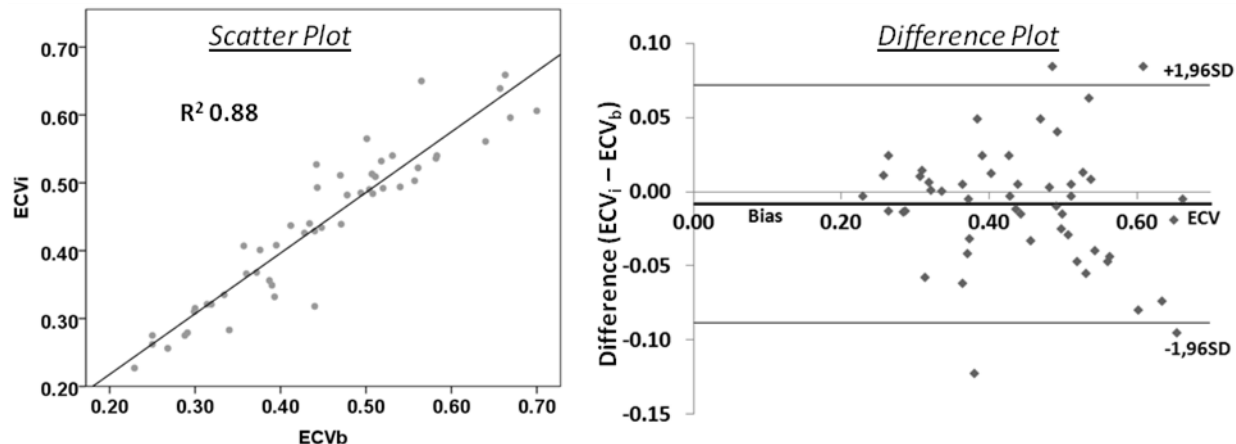


Figure 34: ECV_i vs ECV_b (Left) Scatterplot showing the correlation of myocardial ECV_i and myocardial ECV_b; (right) Bland Altman graph showing agreement of myocardial ECV_i and myocardial ECV_b.

10.5 Discussion:

Correlation and agreement were assessed between FLASH EQ-CMR and ShMOLLI EQ-CMR methods of ECV calculations for heart (n=50), liver (n=13) and spleen (n=12) ECV. FLASH and ShMOLLI ECV values showed excellent correlation with each other for heart, liver and spleen ECV, all yielding an R^2 of ≥ 0.8 . Agreement was also very good across heart, liver and spleen ECVs with the largest mean difference being 0.04 for liver ECV. This suggests that the EQ-CMR using ShMOLLI is an equally accurate method for ECV quantification when compared to the histologically validated and current gold standard FLASH method, with the significant advantage however of being more patient friendly, having better clinical applicability and having a much less laborious off-line analysis. Additionally, interstudy reproducibility has since been performed, demonstrating that ShMOLLI ECV carries better reproducibility than FLASH ECV (see figure 35 below).¹⁷⁹

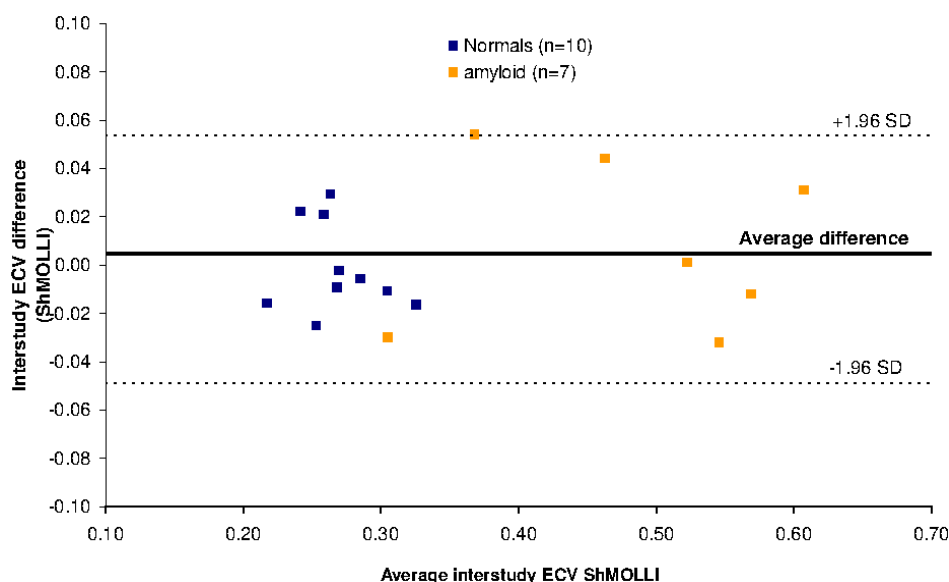


Figure 35: Bland Altman graph showing agreement for interstudy reproducibility of myocardial ECVs using the ShMOLLI method. Adapted from Fontana M et al¹⁷⁹

We assessed ECV_b and ECV_i in 51 patients with systemic AL Amyloidosis and compared the results for agreement and correlation. There is a strong, linear correlation and strong agreement between the 2 values suggesting that ECV_b is a comparable marker to ECV_i but carries the significant advantage that it does not require the infusion of gadolinium, rendering it a much shorter technique, easier for patients to perform and less cumbersome for the operator. It also opens up the practical possibility of whole heart mapping, which

would require only 3 sequences in either long axis or short axis to acquire all 17 segments of the heart.

These findings are contrary to other published work. A study of n=20 per various cardiac diseases concluded that in high ECV diseases i.e. > 0.40 (e.g. cardiac amyloid, MI), ECV_b consistently overestimates compared to ECV_i. The bias for ECV_b > 0.40 was +0.04, compared to -0.004 here for ECV_b > 0.40.¹⁸⁰ The study concluded, perhaps because of the large amount of amyloid predominating in the subendocardium, that gadolinium was still diffusing into the myocardium at 15 minutes rather than being at true equilibrium – hence, a longer wait may be necessary to obtain a more accurate ECV. This observation appears now less marked but still present as evidenced by the scatter at high ECVs. Ultimately, as a diagnostic tool, ECV_b is likely to be adequate, but for follow up or research purposes where the most accurate result is needed, an infusion may be necessary.

For the FLASH vs ShMOLLI comparison, there were smaller numbers for liver and spleen ECV compared with cardiac ECV. This was because there was initially no expertise regarding how to image the liver using the ShMOLLI, as this had only been validated in the heart. Secondly, there was a brief period when our department experienced a generic problem with imaging the liver due to several artefact problems and ShMOLLI liver maps were not performed therefore during this period. This was eventually tracked down to be a broken coil element that was causing error despite passing Siemens quality control.

Finally, ECV_b and ECV_i have not been validated against histology in amyloidosis. Both have been validated against collagen volume fraction in aortic stenosis though. Histological validation for systemic amyloidosis remains work in progress. There has been recent evidence to support the role of ECV_b in prognosis¹⁸⁴ but this will be explored later in this thesis.

10.6 Conclusions:

1. EQ-CMR using ShMOLLI to calculate cardiac and extracardiac ECV is as accurate in systemic AL amyloidosis as the FLASH method, but is much more clinically applicable, reproducible and easier to use for patients and operators. Histological validation is required.
2. ECV_b can be used instead of ECV_i when assessing systemic AL amyloidosis. Again, histological validation is required.

11. Pre Contrast T1 mapping in Systemic AL Amyloidosis:

This chapter is based on the publication below:¹⁸⁵

Karamitsos TD, Piechnik SK, Banypersad SM, Fontana M, Ntusi NB, Ferreira VM, Whelan CJ, Myerson SG, Robson MD, Hawkins PN, Neubauer S, Moon JC. "Non-Contrast T1 mapping for the diagnosis of cardiac amyloidosis." JACC Cardiovasc Imaging. 2013 Apr;6(4):488-97

All amyloid patients in this study were AL type and were recruited by myself. All scanning, reporting and analysis was done by myself – authorship reflects the aortic stenosis contribution to the paper (not included in this thesis) and also a reciprocal department level agreement between the Heart Hospital and Oxford for early access to ShMOLLI.

11.1 Introduction:

We have so far demonstrated how ECV can be used to quantify organ amyloid burden in systemic AL amyloidosis. We have also shown in chapter 10 that the ShMOLLI method of acquiring ECV measurements is superior to the original FLASH IR method. But this is not always possible in all patients with systemic AL amyloidosis e.g. severe renal impairment.

The main advantage of CMR compared to echocardiography is in myocardial tissue characterisation, whether that be through the appearance of global subendocardial LGE, the hallmark for making the diagnosis of cardiac amyloidosis^{90, 93} or with ECV measurements.

However, many of these patients have significant renal impairment and so the administration of a gadolinium-based contrast is problematic. Furthermore, the pattern of LGE may be atypical and patchy as described in section 6.4.5, particularly in early stages of the disease.^{90, 91, 186} Therefore, a non-contrast CMR technique that could provide quantitative assessment of myocardial amyloid load would prove particularly useful in these patients.

Measurement of myocardial T1 relaxation times using non-contrast T1 mapping has been shown to be useful in the detection of interstitial expansion due to myocardial oedema and fibrosis.¹⁸⁷⁻¹⁹⁰ Furthermore, alterations of T1 times in the liver, spleen, and fat in patients with systemic AL amyloidosis have been described using low field MRI.¹⁹¹

We explored therefore whether non-contrast T1 mapping using the single breath-hold ShMOLLI technique would provide diagnostic information in patients with suspected cardiac AL amyloidosis.

11.2 Hypothesis:

That pre contrast T1 mapping with the ShMOLLI technique will provide adequate diagnostic information of the cardiac status in patients with systemic AL amyloidosis.

11.3 Methods:

Fifty-three patients with systemic AL amyloidosis and no contraindications for CMR were recruited from the cohort described in section 7.2. Histological proof of AL amyloid was obtained through specimens of: kidney (n=15), bone marrow (n=8), soft tissues (n=8), fat (n=5), rectum (n=5), endomyocardium (n=4), liver (n=2), lymph node (n=2), upper GI tract (n=1), lung (n=1), and peritoneum (n=1). See figure 36 below:

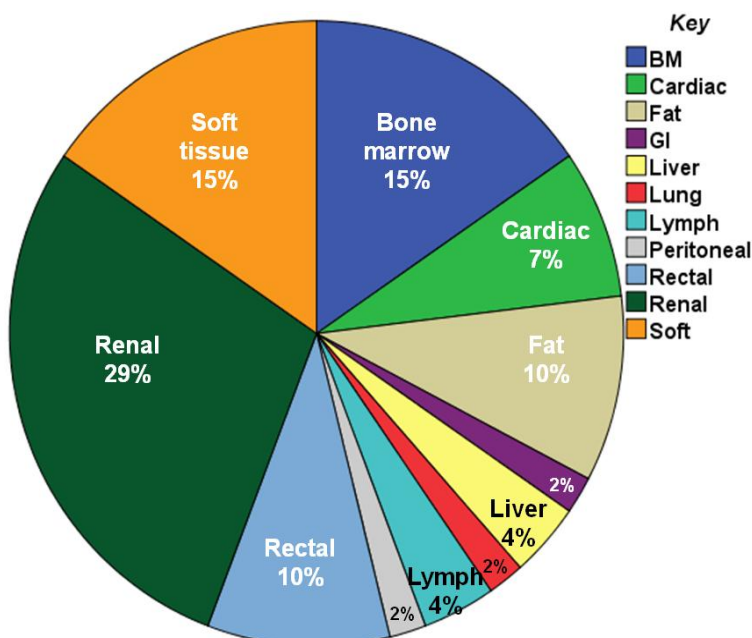


Figure 36: Pie chart showing distribution of tissue biopsies within the AL amyloidosis patient cohort (n=53).

Four patients who were found to have AF/flutter after they had consented were not excluded. Based on the classifying criteria detailed in section 7.2, the amyloid patients were characterized as having no (n=14), possible (n=11) and definite (n=28) cardiac involvement. Thirty-six normal volunteers from the cohort in section 7.3 were also recruited.

All subjects underwent pre contrast myocardial T1 mapping with ShMOLLI as part of their EQ-CMR where a bolus of 0.1mmol/kg of Dotarem™ was ultimately given as described in

previous chapters. All patients underwent echocardiography for diastolic measures as described in section 7.8 and all statistical analysis performed as described in section 7.11.

11.4 Results:

Patient characteristics are described in table 4. There were no differences in age, sex and body surface area between the groups of patients and healthy volunteers. Patients with definite cardiac amyloid had significantly increased LV mass index ($P<0.001$) and smaller LV end-diastolic volume ($P=0.001$) compared to healthy controls. EF was mildly reduced in patients with definite cardiac involvement compared to the other groups ($P<0.01$ for all comparisons) although values remained within normal limits. There were no differences in renal function between the 3 groups of systemic AL amyloidosis patients.

	Normals N=36	Amyloid: No cardiac N=14	Amyloid: possible cardiac N=11	Amyloid: definite cardiac N=28	P-value
Age	59 ± 4	58 ± 12	65 ± 10	63 ± 10	0.07
Gender (M/F)	22/14	8/6	7/4	20/8	0.85
NYHA class > III (n)	-	0	1	2	-
eGFR (ml/min/1.73m²)	NA	85 ± 10	74 ± 32	77 ± 20	0.42
LVEDV index (ml/m²)	77 ± 13	59 ± 11	58 ± 9	65 ± 11	<0.001
LVESV index (ml/m²)	20 ± 5	16 ± 5	13 ± 5	25 ± 8	<0.001
EF (%)	74 ± 5	73 ± 6	77 ± 6	62 ± 12	<0.001
LV mass index (g/m²)	58 ± 11	69 ± 20	77 ± 20	118 ± 32	<0.001

Table 4: Showing patient characteristics and differences between patients with differing pre-test probabilities of cardiac amyloidosis in systemic AL amyloidosis and healthy volunteers.

Mean pre contrast myocardial T1 as measured by ShMOLLI was higher in patients at 1086 ± 90 msec, compared to healthy volunteers of 958 ± 20 msec ($P<0.001$). Myocardial T1 times showed a stepwise elevation as the probability for cardiac involvement increased: 1009 ± 31 msec without cardiac involvement, 1048 ± 48 msec with possible cardiac involvement, 1140 ± 61 msec with definite cardiac involvement (see figure 37 on the next page).

Between group comparisons are summarized in the list below:

- Normals vs amyloid without cardiac involvement, $P=0.003$
- Normals vs possible cardiac amyloid, $P<0.001$
- Normals vs definite cardiac amyloid, $P<0.001$
- Amyloid without cardiac involvement vs possible cardiac amyloid, $P=0.265$
- Amyloid without cardiac involvement vs definite cardiac amyloid, $P<0.001$
- Possible cardiac amyloid vs definite cardiac amyloid, $P<0.001$

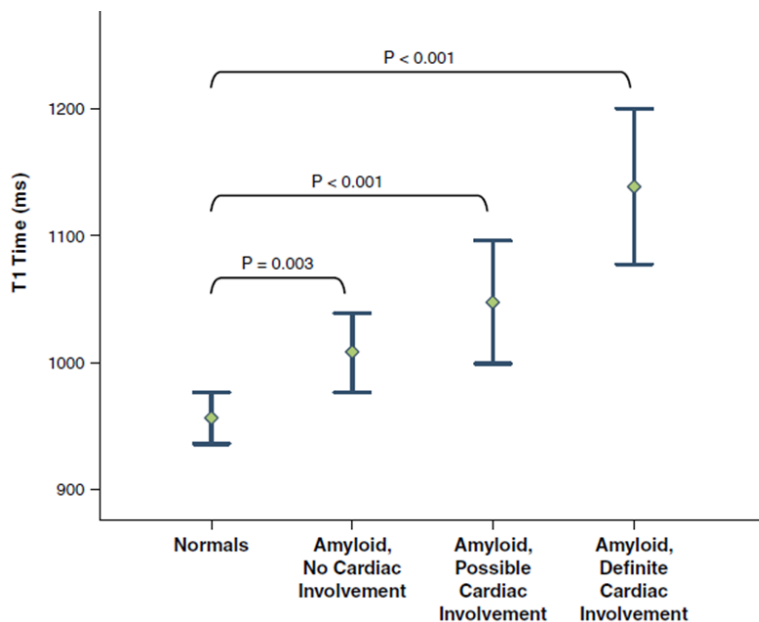


Figure 37: Graph showing the relationship between mean pre contrast myocardial T1 time and pre-test probability of cardiac involvement in systemic AL amyloidosis, compared to healthy volunteers.

ROC analysis (see figure 38 on the next page) showed that a pre contrast myocardial T1 cut-off value of 1020msec using ShMOLLI T1 mapping yielded a 92% accuracy for identifying cardiac involvement (area under the ROC curve 0.969 ± 0.01 , $P<0.0001$). Based on this cut-off, 3 patients with possible cardiac amyloid would have been wrongly classified as having no cardiac involvement (sensitivity 92%). In contrast, there are 3 false positive cases: 3 amyloid patients with no cardiac involvement clinically who have myocardial T1 above the threshold (specificity 91%).

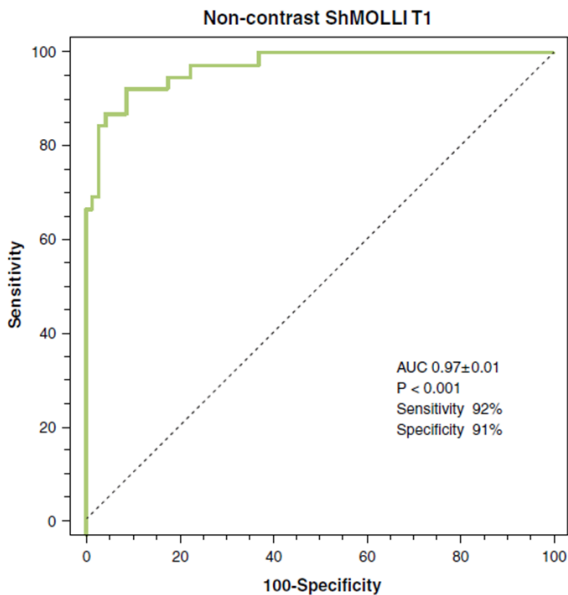


Figure 38: ROC curve analysis for pre-contrast myocardial T1 times in Systemic AL amyloidosis.

LGE findings and T1 in cardiac amyloid:

There was no evidence of LGE in the group of AL systemic amyloidosis patients without cardiac involvement.

In the group of patients with possible cardiac involvement, 3 patients had typical circumferential subendocardial LGE, 1 patient had patchy enhancement, 2 patients had reversed nulling on T1 scout and 5 patients had no evidence of LGE.

In the definite cardiac involvement group, 1 patient had no evidence of LGE, and another one had only abnormal kinetics on T1 scout. All other patients in this group had evidence of LGE (9 circumferential subendocardial, 6 patchy, 11 extensive LGE - involving not only the subendocardium but also the subepicardial layer).

All patients with patchy enhancement had increased T1 times (above the threshold of 1020ms determined by ROC analysis), irrespective of the clinical classification as possible or definite cardiac involvement. Furthermore, 2 out of 3 patients with abnormal kinetics on T1 scout also had elevated T1 times. Interestingly, 3 out of 5 patients with possible cardiac involvement but no discernible LGE, had significantly elevated T1 times and this also applies to the patients with definite cardiac involvement who had no LGE. Representative examples of the CMR scans are shown in figure 39 on the next page:

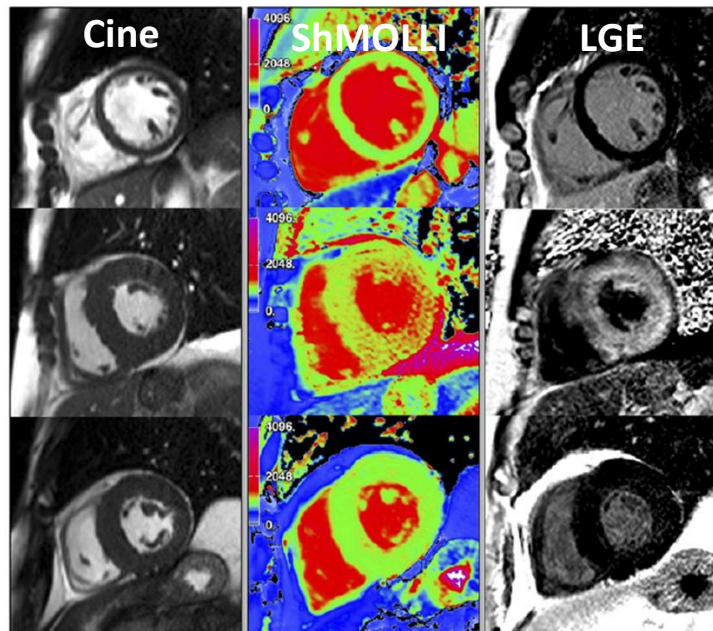
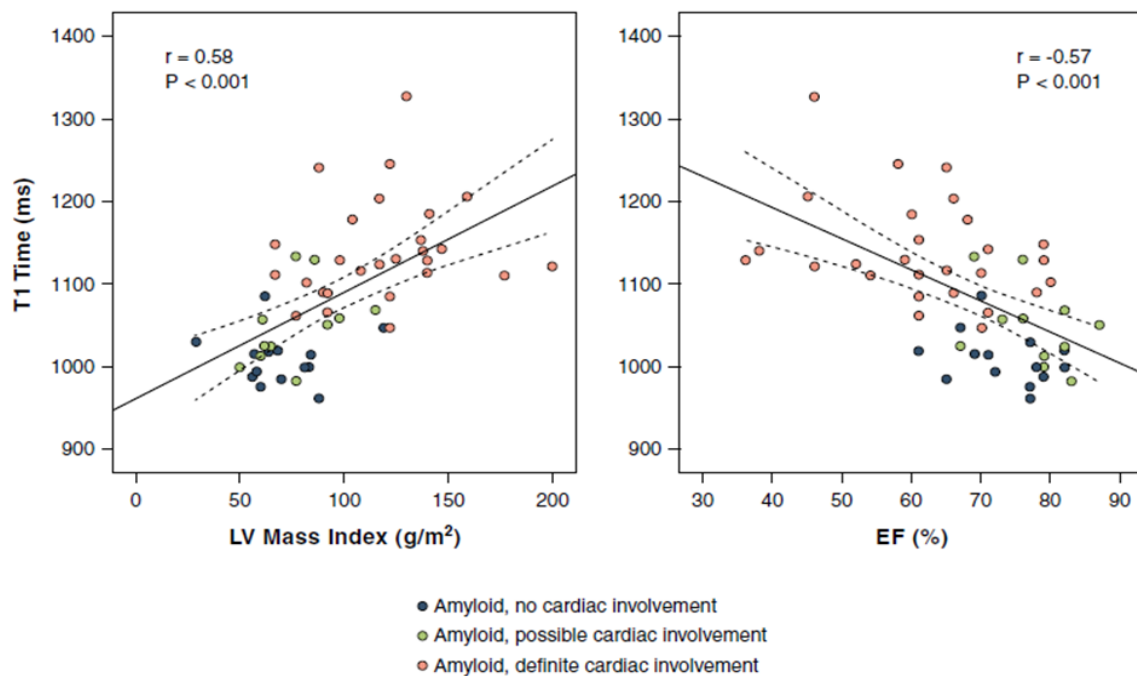


Figure 39: Cine still, ShMOLLI and LGE images from (Top 3) Healthy volunteer; (middle 3) AL Amyloidosis patient with extensive LGE; (bottom 3) AL Amyloidosis patient with little LGE
This image became the front cover of JACC Cardiovascular Imaging, April 2013.

T1 and cardiac function in cardiac amyloid:

There were significant correlations between pre contrast T1 relaxation times and indices of systolic and diastolic function in the AL amyloidosis cohort. EF decreased ($R=-0.57$, $P<0.001$) and indexed LV mass increased ($R=0.58$, $P<0.001$) as T1 times increased, indicating that the changes in myocardial T1 times reflect to some extent the severity of cardiac involvement (see figure 40 on the next page). In addition, T1 times increased significantly as diastolic function worsened, evidenced by the positive correlation between T1 times and E/E' ratio ($R=0.45$, $P=0.001$) and the negative correlation between T1 times and E deceleration time ($R=-0.44$, $P= 0.002$). See also table 5 on the next page:



	Normals N=36	Amyloid: No cardiac N=14	Amyloid: possible cardiac N=11	Amyloid: definite cardiac N=28	P-value
ShMOLLI T1 (msec)	958±20	1009±31	1048±48	1140±61	<0.001
E:A ratio	NA	0.88±0.15	0.97±0.38	1.72±0.81	<0.001
E:E' ratio	NA	7.6±2.3	14.2±4.5	15.4±6.4	<0.001
E dec time (msec)	NA	204±42	231±66	174±62	0.03

Table 5: Showing pre contrast myocardial T1 values and echocardiographic markers of diastolic function for patients according to their pre-test probability of cardiac disease in systemic AL amyloidosis and healthy volunteers.

11.5 Discussion:

This study finds that patients with systemic AL amyloidosis show significantly increased pre contrast myocardial T1 values compared to healthy controls. This increase is tied to the extent of cardiac involvement and there is increase in T1 times even when involvement is uncertain or thought not present. Furthermore, pre contrast T1 correlates well with markers of systolic and diastolic dysfunction, indicating that the changes in myocardial T1 reflect to

some extent the severity of cardiac involvement. T1 mapping appears to be a useful test to diagnose cardiac involvement in systemic AL amyloidosis.

As mentioned already in this thesis in section 6.7, cardiac involvement portends a poor prognosis in AL amyloidosis patients. Its detection informs the intensity of therapy in many cases. The gold standard for diagnosis of cardiac involvement is cardiac biopsy but sampling error prevents quantification and there can be false negatives. As mentioned in chapter 6, ECG abnormalities such as low QRS voltages in limb leads (<0.6mV) and poor R-wave progression in chest leads occur in up to $\frac{2}{3}$ of cardiac AL amyloid patients.^{23, 53} Echocardiography may demonstrate wall thickening, poor longitudinal function, biatrial dilatation, early diastolic and late systolic dysfunction,^{63, 192} but only in the advanced stage do these features become discriminatory over other diseases such as the hypertensive heart.

CMR provides additive information in cardiac amyloid via myocardial tissue characterization with contrast. The appearance of global, subendocardial LGE and associated dark blood-pool is characteristic and correlates with prognosis.^{88-91, 93} Other LGE patterns do exist as described in section 6.4.5, and LGE may occur even without overt hypertrophy. However, LGE patterns may be non-specific or only occur in later disease, and require contrast which may be contraindicated in patients with renal failure which is common in amyloid.¹⁹³

With the degree of myocardial infiltration present in amyloid, pre contrast T1 mapping has the potential to detect cardiac involvement and be clinically useful. Changes in T1 times had previously been demonstrated in the liver, spleen, and fat in amyloidosis using low field MRI¹⁹¹ and early results supported myocardial changes.^{86, 194, 195} Here, we build on these results using the latest, robust and more accurate advanced short breath-hold T1 mapping technology incorporating a single output colour T1 map¹⁹⁶ in a large cohort with robust controls and demonstrate functional consequences and early disease detection. Although there are technical differences between the MR sequences used to measure T1 relaxation times, our results are in agreement with previous work from Hosch and colleagues who found a 19% increase in T1 times in cardiac amyloid patients compared to normal controls.⁸⁶

Measurement of T1 times using ShMOLLI T1 mapping has shown very good accuracy for the detection of cardiac involvement in AL amyloidosis and correlate well with the extent of systolic and diastolic dysfunction. It is tempting to speculate that pre contrast T1 mapping is

more sensitive than the LGE technique for the detection of cardiac involvement, as all amyloid patients with non-typical patchy enhancement had increased T1 values.

This study has similar limitations to previous chapters in this thesis, chiefly that patients had histologically proven amyloid but not routine endomyocardial biopsies. No histological correlation with T1 is therefore available. T1 mapping is also of course a composite value of myocytes and interstitium and does not therefore represent the interstitium alone; ECV is the better marker for this. Finally, the prognostic value of T1 values in amyloid was not explored here, but this is assessed in the next chapter.

11.6 Conclusion:

Pre contrast myocardial T1 appears to be a useful test to diagnose the presence and extent of cardiac involvement in systemic AL amyloidosis.

12. T1 mapping and Survival in Systemic AL Amyloidosis:

This chapter is based on the publication below:

Banypersad SM, Fontana M, Maestrini V, Sado DM, Captur G, Petrie A, Whelan CJ, Herrey AS, Gillmore JD, Lachmann HL, Wechalekar AD, Hawkins PN, Moon JC. “T1 Mapping and Survival in Systemic Light Chain Amyloidosis.” European Heart Journal (2015); 36(4): 244-51.¹⁹⁷

An abstract of this work also won \$500 at the Young Investigator Awards finals at the American Heart Association in Dallas when presented on 17th November 2013 and was also presented at the Young Investigator Awards at SCMR in New Orleans earlier this year on 17th January 2014. My contribution was recruiting all the patients, reporting and analysing all scans and writing the paper.

12.1 Introduction:

As mentioned earlier in chapter 6, cardiac involvement in systemic AL amyloidosis is present in around 50% of patients at presentation and is the principal driver of prognosis.¹⁹⁸ Current predictors of survival rely on measuring surrogate rather than direct markers of interstitial expansion (e.g. serum cardiac biomarkers). ECG criteria such as low limb lead voltages²³ or fragmented QRS complexes¹⁵⁷ are also predictive, but are confounded by pericardial effusions and conduction abnormalities. Echocardiographic parameters also predict outcome^{59, 158, 159} but coexisting causes of LVH or diastolic impairment may affect interpretation.

CMR with LGE imaging adds value in the diagnosis of cardiac involvement in AL amyloidosis. Altered gadolinium kinetics also shows some correlation with survival.⁹³ In this chapter therefore, we now consider the predictive power of ECV after primed infusion (ECV_i) with survival. In addition, we also tested the predictive power of ECV_b, pre contrast T1 and post contrast T1.

12.2 Hypotheses:

1. That ECV will correlate with survival
2. That ECV correlates better with survival than pre contrast and post contrast myocardial T1.

12.3 Methods:

The 100 consecutive patients with systemic AL amyloidosis stated in section 7.2 were recruited (this includes all 60 patients in chapter 8 and all 53 patients in chapter 11). Six patients, who were found to have AF/flutter once in the scanner after they had consented, were not excluded.

All patients had histological proof of systemic AL amyloidosis except 2 (2%), who died before biopsy could be undertaken, but in whom monoclonal gammopathies were present and the organ distribution of amyloid on SAP scintigraphy was characteristic of AL type. Histology was performed with Congo red followed by immunohistochemical staining; tissues examined were: kidney (n=26, 26%), endomyocardium (n=7, 7%), bone marrow (n=13, 13%), upper gastrointestinal tract (n=7, 7%), liver (n=3, 3%), fat (n=15, 15%), spleen (n=1, 1%), lung (n=1, 1%), rectum (n=9, 9%), soft tissues (n=12, 12% - included skin, tongue, buccal mucosa, labia), lymph node (n=3, 3%) and peritoneum (n=1, 1%). See figure 41 below:

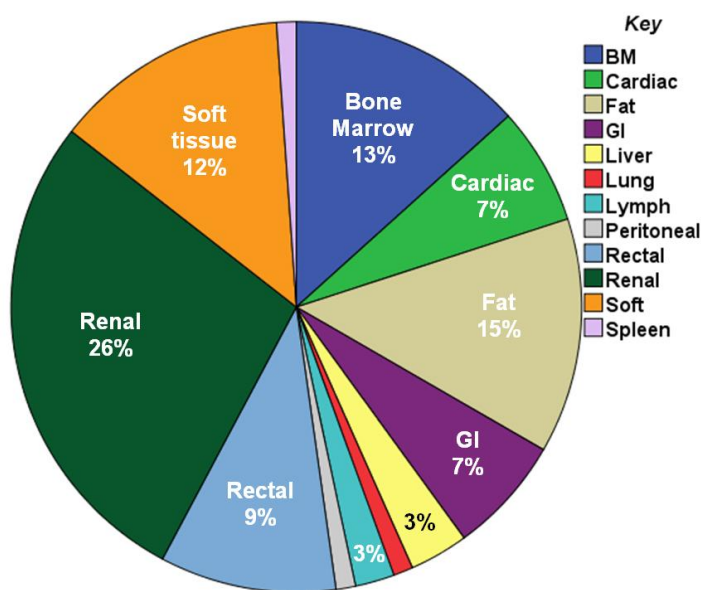


Figure 41: Pie chart showing distribution of tissue biopsies within the AL amyloidosis patient cohort (n=100).

As described in chapter 7, all patients underwent 12 lead ECG, assays of the cardiac biomarkers NT-proBNP and Troponin T, and echocardiography at baseline. Mean ECG QRS voltage in limb and praecordial leads were calculated.¹⁶⁰ Echocardiographic assessment of diastolic function was performed as described in section 7.8. All patients underwent conventional CMR and EQ-CMR as previously described in sections 6.10 and 7.4. Standard

CMR parameters of structure (LV mass, LAA, maximal septal thickness) and systolic function (EF, MAPSE, TAPSE) were assessed. Pre contrast myocardial values were calculated and the post contrast T1 map was performed at 15 minutes post bolus and after equilibration so that the ECV_b and ECV_i could be calculated.

Some ECV data (n=19 of the 100) pre-dated the availability of ShMOLLI T1 mapping and had thus utilised multibreath-hold FLASH T1 measurement described in chapter 6.10. But as we have demonstrated equivalence of these ECVs in chapter 10, these patients are not excluded from the ECV_i data.

That said, these patients did not have an ECV_b value or the subsidiary component of the ECV equation, pre contrast T1; multibreath-hold measurement has been shown to be inferior to T1 mapping, so accordingly, these were excluded from the sub-analysis comparing techniques - this particular analysis therefore consists of 81 rather than 100 patients.

ECV and Myocardial T1 results were compared to 54 healthy volunteers who underwent pre contrast T1 mapping and ECV measurement (bolus and infusion). The number of patients dead and alive was assessed after a median duration of 23 (Interquartile range: 6-25) months. Some analysis involved sub-grouping patients into pre-test probability of cardiac involvement as previously described in section 7.2. All statistical analysis was performed as stated in section 7.11.

12.4 Results:

Table 6 on the next page summarises baseline characteristics for patients and healthy volunteers. Within the patient cohort, 14 (14%) patients were on treatment for hypertension; 10 (10%) had confirmed coronary artery disease by angiography, 1 (1%) had had a stroke and 2 (2%) had diabetes.

<u>Characteristic:</u>	<u>Patients:</u>	<u>Healthy Controls:</u>	<u>P value</u>
Male /female	62/30	25/29	P=0.02
Mean Age ± SD (yrs)	62 ± 10	46 ± 15	P<0.001
Mean Creatinine ± SD (mmol/L)	89 ± 33	74 ± 13	P<0.001
Median NT-proBNP in pmol/L (IQ range)	146 (27-359)	-	
Median Troponin T in ng/L (IQ range)	0.03 (0.01-0.06)	-	
ECG/CMR indices			
Mean Indexed end-diastolic LV volume ± SD (mls)	60 ± 13	73 ± 12	P<0.001
Mean Indexed end-systolic LV volume ± SD (mls)	19 ± 10	25 ± 7	P<0.001
Mean EF ± SD (%)	67 ± 11	67 ± 6	P=0.42
Mean Indexed LV mass ± SD(g/m ²)	97 ± 35	65 ± 15	P<0.001
AF /atrial flutter (%)	6 (7)	0	

Table 6: Showing patient characteristics and differences between AL amyloidosis patients and healthy volunteers

Fifty patients were treated with chemotherapy for the first time which comprised triple therapy with either Cyclophosphamide, Thalidomide and Dexamethasone (CTD) or Cyclophosphamide, Velcade and Dexamethasone (CVD), depending on local guidelines of regional NHS Trusts within the UK. Seventeen patients were treated for a 2nd or 3rd time having relapsed – treatment was either with CVD or a Lenalidomide-containing regimen in these instances. Nine patients had not received any chemotherapy as there was no clinical indication (e.g. renal amyloid with established renal failure, isolated neuropathic presentations) and 24 patients were under stable follow up with no indication for further chemotherapy at the time of scan.

Twenty-one patients had a pre-test probability of no cardiac involvement, 26 had possible cardiac involvement and 53 had definite cardiac involvement.

All ECV values are the ECV_i from infusion measurement unless otherwise stated. Healthy controls were younger on average, but our work and others suggests any ECV changes with age are small compared to amyloid changes.^{148, 165} There were proportionately more females in the control vs patient group. This slightly increases the control group ECV and pre

contrast T1 compared to that of a gender matched group (male vs female: ECV 0.24 vs 0.27, P<0.001; T1 940 vs 966ms, P=0.006).

	ECV	Myocardial T1				
		Pre contrast		Post contrast		
LV Structure by CMR	R	P-value	R	P-value	R	P-value
LV mass	0.48	P<0.001	0.43	P<0.001	0.40	P=0.004
Indexed LV mass	0.50	P<0.001	0.43	P<0.001	0.36	P=0.01
Septal thickness	0.61	P<0.001	0.53	P<0.001	0.34	P=0.01
LA area	0.32	P=0.002	0.13	P=0.28	0.29	P=0.043
Indexed LA area	0.30	P=0.005	0.09	P=0.45	0.14	P=0.31
LV Systolic Function by CMR						
Ejection Fraction	0.48	P<0.001	0.32	P=0.005	0.20	P=0.17
MAPSE	0.58	P<0.001	0.50	P<0.001	0.23	P=0.10
LV end diastolic volume	0.06	P=0.58	0.12	P=0.30	0.09	P=0.51
LV end-systolic volume	0.31	P=0.002	0.15	P=0.19	0.07	P=0.63
Indexed LV end diastolic volume	0.10	P=0.32	0.17	P=0.14	0.25	P=0.07
Indexed LV end systolic volume	0.32	P=0.002	0.14	P=0.24	0.01	P=0.93
LV Diastolic Function by Echo						
E:E'	0.37	P<0.001	0.25	P=0.03	0.28	P=0.052
IVRT	0.34	P=0.007	0.27	P=0.05	0.19	P=0.28
E-Deceleration time	0.23	P=0.03	0.40	P<0.001	0.05	0.71
RV Systolic Function by CMR						
TAPSE	0.57	P<0.001	0.52	P<0.001	0.41	P=0.003
Biomarkers						
Serum NT-pro BNP (LnBNP)	0.65	P<0.001	0.58	P<0.001	0.25	P=0.07
Troponin T (LnTropT)	0.52	P<0.001	0.36	P=0.02	0.62	P=0.001
ECG						
ECG Limb Lead mean voltage	0.42	P<0.001	0.35	P=0.002	0.03	P=0.98
ECG chest lead mean voltage	0.23	P=0.03	0.12	P=0.28	0.15	P=0.28

Table 7: Showing the Pearson's correlation coefficients and P values for the correlations of myocardial ECV, pre contrast T1 and post contrast T1 with standard cardiac parameters in patients with systemic AL amyloidosis.

As in chapter 8, mean cardiac ECV was greater in patients compared to healthy volunteers with a wider range (0.44 ± 0.12 vs 0.25 ± 0.02 , $P<0.001$) and tracked pre-test probability of cardiac involvement by conventional parameters ($P<0.001$).¹⁵⁰ Mean pre contrast myocardial T1 values were raised in patients compared to healthy volunteers (1080 ± 87 ms vs 954 ± 34 ms, $P<0.001$) and also tracked pre-test probability of cardiac involvement ($P<0.001$).¹⁸⁵ Table 7 on the previous page provides the Pearson correlation coefficients of ECV, pre contrast and post contrast myocardial T1 compared to other cardiac parameters, many of which typically change in cardiac amyloid. ECV correlated significantly with 17 of 19; pre contrast T1 with 12, and post contrast T1 with 10.

With regards late gadolinium enhancement, 25 patients had no LGE, 50 had global subendocardial enhancement and 10 had extensive enhancement. Eight had patchy enhancement and 7 had evidence of only altered gadolinium kinetics. ECV correlated significantly with increasing degrees of late gadolinium enhancement ($P<0.001$) as shown in figure 42 below.

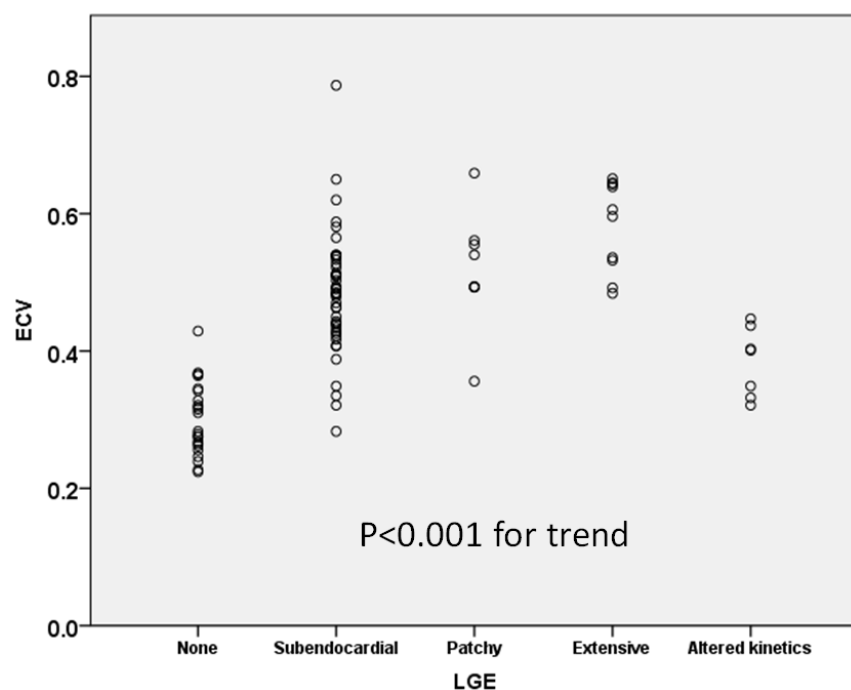


Figure 42: Dot plot showing correlation between ECV and late gadolinium enhancement

ECV correlates with survival:

At follow up (median 23 months), 25 of 100 patients had died. For each potential predictor, median and tertile cut-points were assessed for predictive power using the Harrell's C statistic and the best result presented (see table 8).

	Tertile	Cut point	HR (95% CI)	P-value	Harrell's C
ECV _i	Tertile 1	0.40	4.67 (1.39 - 15.5)	0.013	0.63
	Median	0.45	3.83 (1.53 - 9.61)	0.004	0.66
	Tertile 2	0.49	3.61 (1.56 - 8.38)	0.003	0.65
Pre contrast Myocardial T1	Tertile 1	1044ms	5.39 (1.24 - 23.4)	0.02	0.64
	Median	1080ms	3.01 (1.08 - 8.44)	0.035	0.62
	Tertile 2	1116ms	3.22 (1.30 – 8.04)	0.01	0.63
ECV _b	Median	0.44	5.09 (1.09 – 23.7)	0.03	0.68
Post contrast T1	Median	565ms	0.45 (0.17 – 1.20)	0.11	0.41

Table 8: Showing the hazard ratios and P-values for the median / tertiles of ECV_i, ECV_b (median only), pre contrast T1 and post contrast T1 (median only). The Harrell's C statistic is also shown (a value higher than 0.6 indicates a stronger discriminator).

For ECV_i, a median ECV of 0.45 was the best model for assessing survival: HR 3.84 (1.53 – 9.61), P=0.004 (figure 43 on the next page). The survival curve indicates that there is an approximately 40% chance of death at 23 months in patients with an ECV > 0.45 compared to 15% for ECV < 0.45.

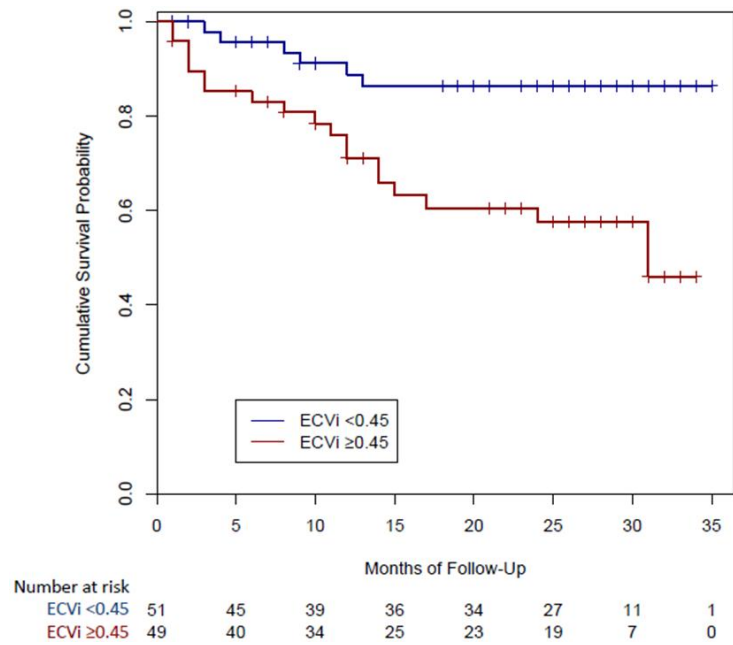


Figure 43: Kaplan Meier survival curve showing worse survival for patients with an $ECV_i > 0.45$ compared to patients with an $ECV_i < 0.45$ in systemic AL amyloidosis.

For pre contrast myocardial T1, the 1st tertile (cut point 1044ms) was the best model: HR 5.39 (1.24 – 23.4), P=0.02 (figure 44A). ECV_b with median of 0.44 also correlated with survival, with a HR of 5.09 (1.09-23.7), P=0.04 (figure 44B). Post contrast T1 did not correlate with survival (HR=0.5, P=0.11).

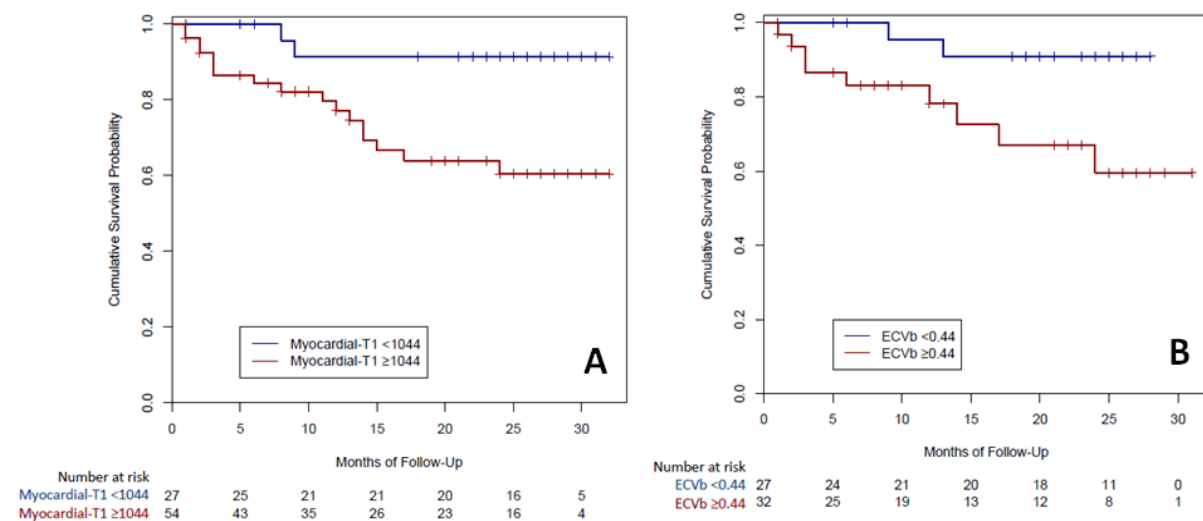


Figure 44: Kaplan Meier survival curve showing worse survival for patients with (A) a pre contrast myocardial T1 of > 1044 msec compared to patients with a T1 of < 1044 msec and (B) an $ECV_b > 0.44$ compared to patients with an $ECV_b < 0.44$ in systemic AL amyloidosis.

When the 3 models (ECV_i , ECV_b and pre contrast T1) were compared to determine the best correlator with survival using the Harrell's C statistic, all 3 performed similarly, although there was a trend to suggest ECV_b was the best model then ECV_i , then pre contrast T1 (Harrell's C statistics: 0.68, 0.65, 0.64 respectively, see also table 8 on page 104).

The time-dependent ROC curves for $t=12$ months and $t=24$ months using the NNE method are shown in figure 45. For comparison, time-dependent ROC curves by Kaplan Meier analysis for $t=24$ months are also shown in figure 46. At earlier follow-up times ($t=12$ months), the three ROC curves are not dissimilar and ECV_i does not provide improved discrimination for cumulative mortality when compared to ECV_b and pre contrast T1. At 24 months, they remain similar, although the NNE ROC curve for ECV_i appears to dominate the ROC curves for both ECV_b and pre contrast T1. This implies that, for any fixed specificity, the ECV_i measurement at later follow up ($t = 24$ months) is a more sensitive marker. In contrast, the Kaplan Meier based ROC curves exhibit monotonicity violations.

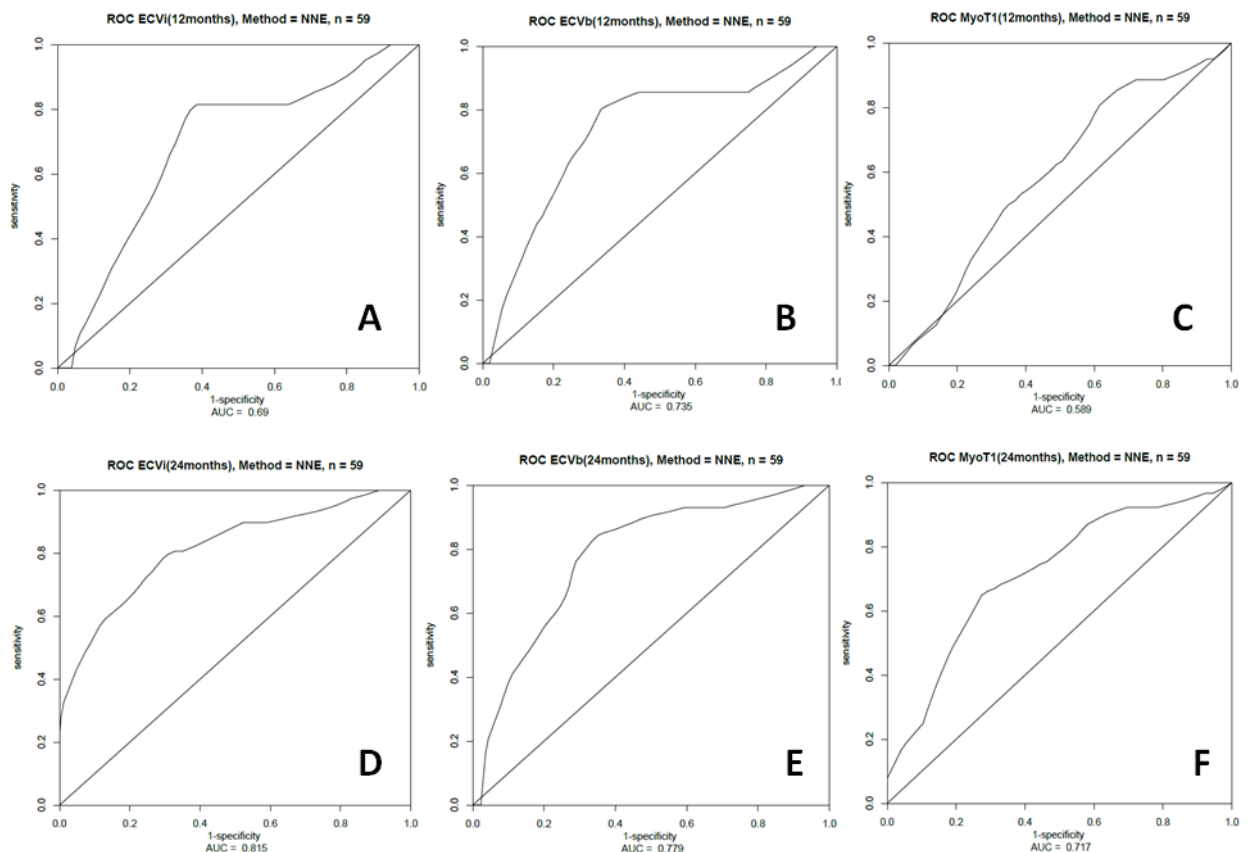


Figure 45: ROC curves for ECV and pre contrast myocardial T1 measurements against survival in AL amyloidosis at $t=12$ months and $t=24$ months. Panels A-C show the ROC curves for $t=12$ months using the nearest neighbour estimator (NNE) and panels D-F show these for $t=24$ months.

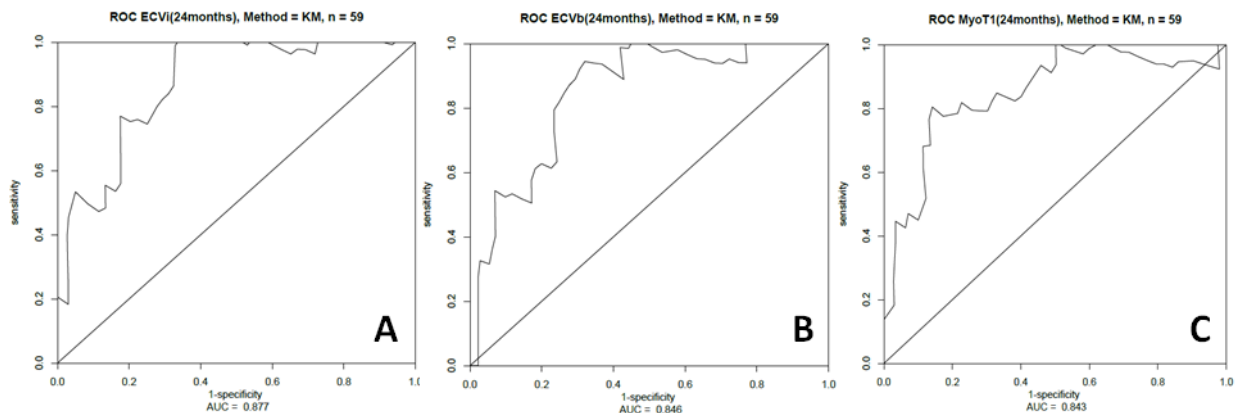


Figure 46: Panels A-C show the ROC curves for t=24 months based on direct use of the simple Kaplan-Meier estimator. Comparison to the NNE-based ROC curves in figure 45 shows how KM-based ROC curves exhibit monotonicity violations.

ECV independently predicts survival:

Table 9 below shows the univariate data for ECV with measures of systolic and diastolic function and serum biomarkers.

Measure	HR (95% CI)	P-value
ECV	3.84 (1.51-9.60)	P<0.001
EF	0.95 (0.92-0.98)	P=0.001
MAPSE	0.80 (0.71-0.90)	P=0.001
TAPSE	0.81 (0.75-0.88)	P<0.001
Indexed LVEDV	0.95 (0.92-0.99)	P=0.005
Indexed LVESV	1.02 (0.98-1.06)	P=0.32
NT-proBNP	5.80 (2.75-12.2)	P<0.001
E:E'	1.09 (1.05-1.14)	P<0.001
E-deceleration time	1.00 (0.99-1.01)	P=0.29
LGE	10.3 (1.39-76.5)	P=0.02
ECG (limb)	0.92 (0.77-1.08)	P=0.35
ECG (chest)	0.99 (0.97-1.02)	P=0.83

Table 9: Showing hazard ratios and 95% confidence intervals for the univariate analyses of all measures against mortality.

After excluding collinearity (VIF < 3), $ECVi > 0.45$ remained significantly associated with mortality (HR=4.41, 95% CI 1.35-14.4; P=0.01) in multivariate Cox models that included

measures of systolic and diastolic function and serum biomarkers: E:E', diastolic dysfunction grade (≥ 2), EF and LnNT-proBNP (Troponin was not available in all patients). E:E' and NT-ProBNP also remained independently predictive (see table 10 below).

Measure	HR (95% CI)	P-value
ECV	4.41 (1.35-14.4)	P=0.01
EF	1.02 (0.98-1.07)	P=0.37
E:E'	1.08 (1.02-1.15)	P=0.009
NT-proBNP	4.41 (1.66-11.8)	P=0.003
Diastolic dysfunction grade	0.31 (0.10-0.92)	P=0.03

Table 10: Showing hazard ratios and 95% confidence intervals for the multivariate analysis for ECV, EF, E:E', NT-proBNP and diastolic dysfunction grade against mortality.

12.5 Discussion:

Myocardial ECV in cardiac AL amyloid correlates with mortality. When dichotomised, a higher than mean ECV associates with roughly a 35-40% increased chance of death at 23 months compared to lower ECV patients, despite therapy. Pre contrast T1 also correlated with survival. Both correlated with baseline clinical parameters. In practice, since the two parameters are typically measured together, their combination may confer diagnostic confidence.

In chapters 8 and 11, I have previously described both ECV measurement and pre contrast T1 mapping as potential, non-invasive techniques for directly measuring the cardiac disease burden in AL amyloid.¹⁵⁰ Here, those earlier results are now strengthened by higher numbers and additionally, prognostic significance of the biomarkers is demonstrated even with therapy.

The marked survival prediction power of ECV lends support to ECV as a key amyloid biomarker. Prior work in non-amyloid patients, where ECV likely measures diffuse fibrosis, has also showed predictive power – in 1176 consecutive CMR referral patients over a median of 1.3 years follow up, 24 deaths occurred with ECV carrying a hazard ratio of 1.52 (1.21 – 1.89) for admissions with heart failure and all cause mortality.¹⁹⁹ Here, we have demonstrated that ECV adds incremental value over and above existing clinical markers when risk-stratifying patients. Unfortunately, it was not possible to include NYHA class in the multivariable model

because this information was not available in all patients due to other factors limiting exertion such as peripheral and autonomic neuropathy due to systemic amyloidosis. Additionally, the limited number of deaths limits very extensive multivariable analysis so this may not represent the optimal multivariable model.

We used an arbitrary categorization for the presence or otherwise of cardiac amyloid. The Mayo staging system is the most recognized predictor of survival in systemic AL Amyloidosis.³³ In new presentations, median survival was reduced from 26 months to 10 months when either NT-proBNP or Troponin T was raised and reduced further still to only 3 months if both biomarkers were raised, although the authors are in the process of further refining this model with inclusion of values for serum free light chain concentration.²⁰⁰ Our survival data in the 45 patients scanned at presentation would support these findings but is currently underpowered (only 17 deaths) to determine incremental benefit of ECV; this remains work in progress.

ECV is predictive regardless of treatment status and indeed irrespective of whether patients are presenting at diagnosis or years into the disease process. Some patients in the cohort had modest ECV increases (ECV 0.30-0.40) without any other evidence of cardiac involvement (no LGE, no wall thickness increase and no biomarker elevation) reinforcing our original findings that even patients classified as having no cardiac amyloid do have raised ECVs suggestive of low grade cardiac disease. A plausible role for aggressive therapy in such patients to prevent progression to overt cardiac disease can be entertained.¹⁵⁰

The simpler, pre contrast myocardial T1 technique does not require a contrast agent and shows promise,¹⁸⁵ particularly as 20-30% of patients with systemic AL amyloidosis have an eGFR < 30ml/min at presentation. In these patients, the Mayo staging system is in part confounded by elevation of serum biomarkers due to renal dysfunction. Here, pre contrast myocardial T1 by ShMOLLI is an alternative to ECV. It is an equally strong correlator with survival but as mentioned earlier, it represents a composite signal from cells and interstitium, not just the interstitium alone like ECV. Some work may be needed to derive normal pre contrast T1 values in patients with renal impairment due to non-amyloid related pathologies. An additional issue is that ECV measurement appears more independent of measurement approaches (magnet field strength, manufacturer, precise sequence details) and is likely to be easier to standardize as a clinical test than pre contrast T1.

From a practical perspective, the bolus only approach to ECV (ECV_b) was as good, if not better, a predictor of survival as the more cumbersome infusion ECV_i . We showed in chapter 10 (and indeed our group has shown that in most disease states) that ECV_b carried excellent agreement with ECV at true equilibrium.¹⁸⁰ This study suggests that the ECV_b passes a key clinical utility test of being prognostic. Post contrast T1 however, was not useful either at baseline or to predict outcome.

Limitations of the study are that patients were followed up for different time periods and are at different disease and treatment stages, with treatment here reflecting current UK practice. Unfortunately, the cause of death is not always known in these patients as the National Amyloidosis Centre only generally receives notification of death rather than information on the formal cause of death. However, it is widely accepted that most death due to AL amyloidosis are cardiac in nature. Studies looking to correlate ECV change with haematological and clinical response as well as histology in AL amyloidosis, have yet to be performed. Whole heart ECV calculations were not possible in this study because of through-planing of blood pool in areas of thinner myocardium towards the apex but as technology advances with motion correction T1 mapping sequences, this will become possible. The advent of PSIR imaging is of growing importance in LGE imaging. As stated earlier, the number of events limits extensive analysis. That said, these are nevertheless hard endpoints and the rule of 10 regarding multivariable analysis can be relaxed in these settings.²⁰¹ Whether ECV and pre contrast T1 – which are not entirely concordant - provide different pathological insights is at this stage unknown.

12.6 Conclusion:

1. ECV (ECV_b and ECV_i) tracks established disease, detects early cardiac involvement and independently correlates with survival.
2. The pre contrast T1 mapping method is shown to be almost as prognostic, providing options for patients in renal failure.

13. Pilot Study – Follow up EQ-CMR in Systemic AL Amyloidosis:

This preliminary study, led by me, assessed the change in ECV amongst a small number of AL patients who we were able to re-scan when they re-attended the National Amyloidosis Centre a few months after their 1st scan, for their follow up appointments. As the numbers were small at the time, this continues to be work in progress.

13.1 Introduction:

Change over time in cardiac amyloid is not well understood. The way myocytes hypertrophy or die and why such changes may be triggered by infiltration (or the free light chains) remain opaque. Treatment with chemotherapy or stem cell transplantation aims to reduce or eradicate abnormal circulating free light chains in order to reduce or stop further amyloid production; a CR is associated with improved morbidity and mortality.¹³⁵ The absence of systolic and diastolic dysfunction at presentation can carry a much more favourable prognosis than once thought.²⁰² If light chain production is switched off, NT-proBNP can fall nearly immediately despite no overt functional changes in the short term. Amyloid regression (well described in AA with inflammation switch off) does not occur substantially in the heart, although the liver and spleen may be more responsive.

Our knowledge has been hampered by poor measurement. Wall thickness and LV mass measure myocytes and interstitium: changes may be reflective of either compartment and compensatory processes clearly occur, impeding understanding. Cardiac biopsy has shown regression of cardiac amyloid histologically but this is invasive.²⁰³ We have demonstrated in this thesis how ECV can measure the interstitial expansion in multiple organs in systemic AL amyloidosis. We sought to explore therefore whether ECV could detect any significant changes in organ amyloid burden at different time points in the disease.

13.2 Hypothesis:

That ECV would change over time and with the success of therapy in AL amyloid.

13.3 Methods:

Of the 100 systemic AL patients, 26 were scanned a 2nd time as described in section 7.2 at one of their subsequent follow up appointments. As the patient follow up appointments are booked well in advance, it was not always possible to coincide an EQ-CMR scan as part of their next appointment because of the other clinically necessary investigations described in chapter 7. Hence, the follow up periods for each patient are different and their “starting points” are all at different stages of disease. The median duration of follow up was 12 months.

All 26 patients were scanned with the identical protocol to their first scan and the ECVs for heart, liver and spleen were calculated. The patients were then categorised as follows:

- (1) Complete responders - normal light chain levels (CR) throughout follow up (n=9)
- (2) Partial responders - normal light chain levels for part of follow up period (n=8)
 - e.g. (a) commenced 6 months of chemo to CR; (b) Relapsed
- (3) Non-responders - abnormal light chain levels throughout follow up (n=9)
 - e.g. (a) Failed to respond to chemo; (b) Stable PR

Mean difference in ECV for each organ was calculated for groups 1 to 3 and the results compared for statistically significant differences as described in section 7.11.

13.4 Results:

In group 1, there was a statistically significant improvement in LV mass, LA area and mean chest lead QRS voltage in patients who had normal light chains for the whole follow up period (see table 9). In terms of ECV, spleen ECV improved from 0.42 to 0.37 (P=0.02) but cardiac and liver ECV did not show any statistically significant changes.

In group 2, there were no statistically significant changes, whilst in group 3, the LVEDV showed an improvement from 115ml to 94ml (P=0.04). These results are summarised in table 11 on the next page:

	Responder group	Baseline	Follow up	P-Value
Myocardial T1 (msec)	1	1089	1084	0.219
	2	1159	1101	0.125
	3	1080	1089	0.688
Cardiac ECV	1	0.43	0.40	0.300
	2	0.48	0.54	0.125
	3	0.52	0.57	0.500
Liver ECV	1	0.33	0.31	0.313
	2	0.38	0.36	0.813
	3	0.37	0.35	0.578
Spleen ECV	1	0.42	0.37	0.039
	2	0.58	0.47	0.439
	3	0.44	0.46	0.813
ECG Limb Lead (mV)	1	4.0	3.6	0.355
	2	4.8	4.8	0.893
	3	3.5	3.5	0.866
ECG chest lead (mV)	1	12.4	11.4	0.016
	2	12.4	11.7	0.152
	3	11.4	11.3	0.915
LV mass (g)	1	182	159	0.004
	2	212	198	0.301
	3	222	219	0.997
Indexed LV mass (g/m²)	1	102	84	0.004
	2	103	97	0.310
	3	120	122	0.910
LA area (cm²)	1	24	22	0.050
	2	31	30	0.931
	3	25	25	0.281
Indexed LA area (cm²)	1	13	11	0.027
	2	15	15	0.930
	3	14	14	0.426

Table 11: Showing the change in value from baseline to follow up of various markers of systemic AL amyloidosis, split according the responder status. P-values also shown.

When the overall trend was considered, a scatter plot of cardiac ECV changes suggested that generally, there was an improvement in ECV in patients with normal light chains (group 1) and a gradual worsening of ECV in the incrementally worse responder groups 2 and 3 i.e. an apparent downward linear trend (see figure 47); however, this was not statistically significant on formal linear regression analysis ($P=0.132$). Additionally, the Kruskall Wallis test, used to assess the distribution of cardiac ECV changes across the responder groups, did not reveal a statistically significant result ($P=0.356$).

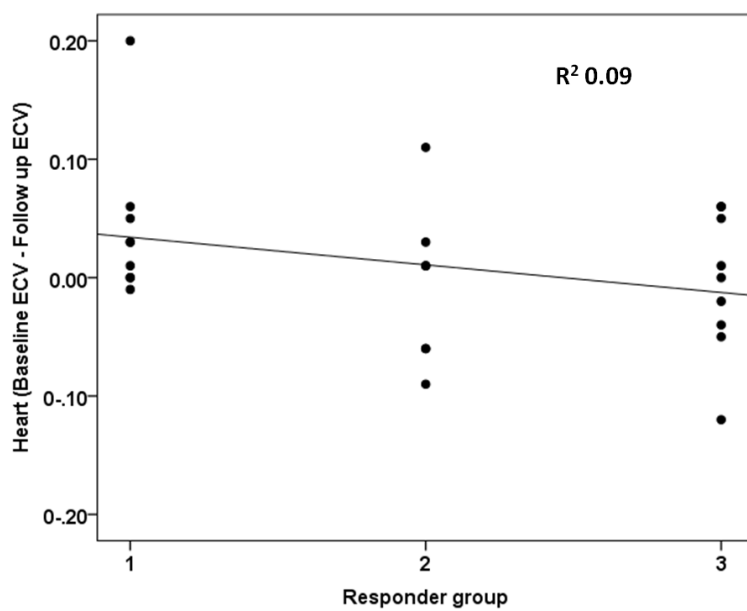


Figure 47: Scatter plot of individual results showing change in myocardial ECV (y-axis) against responder status (x-axis) in systemic AL amyloidosis. (NB: some patients had exactly the same ECV, but still displayed as 1 point on the graph).

Six patients in group 1, 7 in group 2 and all patients in group 3 had LGE at baseline. This did not qualitatively change at follow up ($P=0.107$).

Amyloid and cell mass were calculated as described in section 7.11 (baseline – follow up i.e. a **+ve value denotes a *decrease* at follow up**). Table 12 below shows the difference in amyloid mass and myocyte mass between the responder groups:

Responder group	Median amyloid mass difference in grams (IQ range)	Median cell mass difference in grams (IQ range)
1	+14.7 (+3 to +20)	+7.7 (+5 to +13)
2	-3.2 (-14 to +8)	+17.6 (+6 to +28)
3	-6.1 (-17 to +5)	+8.4 (0 to +11)

Table 12: Showing the median difference from baseline to follow up in amyloid mass and myocyte cell mass across the 3 responder groups.

When the trend across responder groups was analysed using the Kruskal Wallis test, the difference in amyloid mass only just reached statistical significance ($P=0.05$) while difference in cell mass did not ($P=0.305$).

13.5 Discussion:

In this pilot study, 26 patients underwent follow up EQ-CMR scans after a mean duration of 12 months and ECVs for heart, liver and spleen calculated. Group 1 demonstrated the most statistically significant changes, although other groups are confounded by a higher bias of death and therefore not reaching follow up, a limitation common to all studies assessing treatment response. There was a higher risk of death in group 3 compared to group 1 (HR 0.153, $P=0.014$ for group 1 by Cox regression analysis) in keeping with current knowledge. Group 2 showed no statistically significant results.

Spleen ECV showed an improvement from 0.42 to 0.37; cardiac and liver ECV changes did not reach statistical significance. These findings would suggest that the spleen may be a useful, early marker of disease response. This may be because of an intrinsic property of splenic tissue that enables it to recover more readily from disease processes, similar to the liver. Perhaps because embryologically-speaking, the spleen is a primarily haematological organ, the immune system is more readily able to clear amyloid deposited within it. Considering that splenic tissue shows a higher range of ECV than the other organs (0.24 – 0.85) and was a stronger correlator with SAP grade in chapter 9 than liver, this lends further

support to the theory that the spleen appears to be a more accurate marker of interstitial disease change systemic AL amyloidosis and this may be useful in pharmacological studies attempting to achieve amyloid regression. Histology would be necessary to confirm this.

Group 1 also showed a statistically significant reduction in LV mass and LA area, both indexed and non-indexed. One could speculate that this is due to a reduction in the interstitium as there is a concomitant decrease in cardiac ECV, though again, cardiac histology is required to corroborate these suspicions. The reduction in LA area may represent a crude marker of improved diastology.

Mean chest lead ECG voltage also showed a decrease from 12.4mV to 11.4mV in group 1 ($P=0.02$). This might be reflective of a reduction in LVH with a sustained complete haematological response as there is corresponding decrease in LV mass in this group. However, the long accepted theory has been that interstitial expansion explains the reduction in QRS voltages as electrical activity is “insulated” – therefore, any suspected amyloid regression should cause an increase in QRS voltage. So these findings raise questions about whether the interstitium truly insulates electrical activity or whether in fact surface ECG changes in amyloidosis reflect a balance between the source of the electrical activity (i.e. the myocytes) and the interstitium.

In group 3 (the non-responder group), cardiac ECV rose from 0.52 to 0.57. Although this did not reach statistical significance, we speculate that this may suggest continued interstitial expansion due to ongoing amyloid deposits in the heart when patients do not achieve a CR. Interestingly, LV mass showed little change in this group, which might suggest myocyte necrosis at the expense of interstitial expansion, a potential mechanism to explain the worsening clinical status in this group; this should be explored further with histological studies, although as mentioned earlier, follow up studies in this non-responder group are generally hampered by the higher incidence of death.

There was a borderline statistically significant trend towards a regression in actual gram mass of amyloid with improving light chains. Albeit without histological support, this is the first evidence of regression of the interstitial expansion seen in systemic amyloidosis and provides the framework for developing a highly accurate marker of measuring treatment response in the condition. Difference in cell mass did not reach statistical significance and it

was not possible to assess differences in extra cardiac organs as the mass of these organs was not known.

Clearly, the biggest limitation here is small numbers after categorising into 3 responder groups, as well as the bias towards death in the groups who do not achieve a complete haematological response. There is also the issue of lead time bias as the patients were not followed up for the same amount of time or from the same point in the disease process so it is difficult to draw many meaningful conclusions. A further limitation, common to the whole thesis, is the lack of corroborating evidence from histological studies. However, we are able to detect some changes in the different responder groups and these findings have potential to provide further insights into the biological mechanisms underlying the disease process in AL amyloid. The clinical relevance of these findings is once again emphasised when one considers the in vitro data and now the ongoing human trials of the dual CPHPC-monoclonal antibody trial.

13.6 Conclusion:

ECV may represent the initial stages of the first non-invasive tool to demonstrate amyloid regression and progression in systemic AL amyloidosis.

14. DISCUSSION AND CONCLUSIONS

14.1 Background and Hypotheses Explored:

Cardiac amyloidosis remains challenging to diagnose and to treat. Key 'red-flags' that should raise suspicion include clinical features indicating multisystem disease and concentric LV thickening on echocardiography in the absence of increased voltage on ECG; the pattern of gadolinium enhancement on CMR appears to be very characteristic. Confirmation of amyloid type is now possible in most cases through a combination of immunohistochemistry, DNA analysis and proteomics.

But whilst developments in chemotherapy have improved the outlook in AL amyloidosis, the prognosis of patients with cardiac involvement remains very poor and senile cardiac amyloidosis is probably greatly under-diagnosed. Although a variety of novel specific therapies are on the near horizon, with potential to both inhibit new amyloid formation and enhance clearance of existing deposits, current treatment remains mainly supportive, focussed on diuretic therapy.

The inability to reconcile advances in treatment strategies with improved outcomes reflects our incomplete understanding of the biology of the disease process. For example, whilst well recognised, it is not known why cardiac ATTR amyloidosis is better tolerated than cardiac AL amyloidosis, despite the much thicker hearts? Or why exactly ECGs show low voltages in the limb leads? A number of theories have been put forward e.g. myocyte necrosis in AL amyloidosis, or toxicity from circulating immunoglobulin light chains, or an acute (e.g. myocardial oedema) or chronic process in advanced stages of cardiac AL Amyloidosis, but none has ever been definitely proven.

This is likely because no technique has been thus far able to feasibly image or quantify the interstitium in this archetypal interstitial disease. Being able to do so would undoubtedly improve our knowledge of the differences between amyloid types and may allow therapy to be better targeted. Recently, MRI and more specifically, EQ-CMR has been shown to measure the interstitium in a variety of cardiac diseases.

As a result of the work during my MD:

- 1) I have demonstrated that ECV measurement in Systemic Amyloidosis is feasible and I have refined the technique as described in chapter 10 to make it clinically more applicable.
- 2) I have defined a reference range of ECVs that track increasing levels of cardiac disease within the amyloidosis population as well as in multiple other organs.
- 3) I have applied the pre contrast myocardial T1 technique to assess amyloid deposition in the heart, which will have a role in the 25-30% of AL amyloidosis patients with eGFR < 30ml/min where gadolinium administration would be relatively contraindicated.
- 4) I have shown how ECV and T1 correlate with mortality in this disease and demonstrated that clinical outcome may be changed by identifying those patients who may benefit the most from early treatment.

14.2 Refining Clinical Applicability of EQ-CMR in Systemic Amyloidosis:

Before the work in this thesis, measurement of the ECV technically required equilibration of contrast concentrations between blood and myocardium, which can be achieved precisely using a somewhat cumbersome primed contrast infusion (ECV_i).¹⁴⁷ The patient would have to undergo a 30 minute infusion of gadolinium contrast which was very disruptive to clinical workflow and quite tedious and cumbersome for a population of patients who are particularly unwell. We found that it was only possible to scan 6 patients per day using this method, whereas our clinical CMR list currently scans 10 patients in the same time frame – a significant financial burden. Additionally, the FLASH IR method of T1 measurement required 9 breath-holds before and after contrast administration, each lasting around 14 seconds to acquire a map of a single slice. It is also not an accurate method for evaluation of tissues with longer T1, particularly that of blood prior to contrast administration.

During my MD, we entered into a collaboration with the Oxford group, who had written a new T1 mapping sequence, the ShMOLLI. This allows a T1 map of a selected slice to be generated in a single breath-hold over 9 heart beats. We found it to be faster and more reproducible than the the FLASH IR method in amyloidosis. By applying this technique to EQ-CMR in chapter 10 and validating its use in calculating ECV in systemic amyloidosis, what

previously took 8-10 mins now takes under 1 minute as a result of my work. Similarly, I have shown in chapter 10 that ECV can be calculated sufficiently accurately through delayed study following administration of a bolus of gadolinium (ECV_b).¹⁸⁰ As a result of this work, the overall scan time is reduced by a further 30 minutes, making the scan clinically more applicable.

Both of these advances have made the assessment of ECV a much simpler “add on” to a clinical CMR scan, only requiring in addition, a haematocrit measurement.

14.3 ECV Measurement:

Before my work, there was no non-invasive quantifier of interstitial expansion in systemic amyloidosis. There had been some work assessing interstitial expansion in other disease using different models such as partition coefficients and dynamic contrast-enhanced MR.

My work has now demonstrated that ECV can be calculated in the basal to mid septum in cardiac AL amyloidosis and it shows a large increase in the myocardium. ECV Disease-specific correlations have been identified. The technique was also used to assess the liver, spleen and biceps ECV in amyloidosis patients healthy volunteers as well as a preliminary evaluation of its role in tracking disease progress or improvement at follow up.

Novel information has also been gained as a result of this work as I showed in chapter 8 that when ROIs are drawn in LGE positive and LGE negative areas in the same patient, the ECV, whilst lower in LGE negative areas, is still not normal.¹⁵⁰ Because of this, although T1 mapping is now more mature with sequences available on all platforms, it is difficult to compare ECV and T1 to LGE and PSIR imaging which can be helpful with LGE imaging in amyloid, is not available on all platforms.

14.4 Native Myocardial T1:

Prior to my work, there had been only case reports of T1 analysis using the Look-Locker method to assess T1 times in cardiac amyloidosis. The Look Locker method is prone to error because of long breath-hold times, T1 measurements in different phases of the cardiac cycle and being more T1 and heart-rate dependent.

My work has provided reference ranges for myocardial T1 times in cardiac amyloidosis using the more robust T1 mapping sequence, the ShMOLLI. We found a large increase in pre contrast T1 values in patients with increasing amyloid deposition. This work has opened up the door to non-invasive analysis of amyloid burden by cardiac MR in patients with renal failure which was hitherto not possible because of the risk of NSF from gadolinium. The combination of this with ECV has provided information on some of the biology in AL amyloid.

14.5 Clinical Insights and Potential:

Although trends are changing, assessment of cardiac amyloidosis currently relies predominantly on echocardiography which, as an imaging modality, has a much lower spatial resolution than MRI. The main determinants of severity are septal thickness and LV mass, which incompletely reflect the biology at work and systolic / diastolic dysfunction which likely represent more advanced stages of the disease.

The ECV shows the potential to fill this gap not only for the heart, but also the liver and spleen and may permit earlier identification of cardiac disease which may save lives. The pilot studies suggest possible biological explanations for some hitherto unexplained observations (e.g. low QRS voltages on ECG) and also speculate upon the role of ECV in monitoring response to therapy. But most importantly, it has the potential to be an independent predictor of survival, additive to current prognosticators such as the Mayo classification. This would save patient lives not only from the disease itself, but possibly even reduce some of the treatment-related mortality.

However, it is important to balance this with recognition of the current limitations. I have not been able to histologically validate the technique so the technique cannot yet be deemed to be a true non-invasive quantifier of cardiac amyloid burden. Removal of the need for a gadolinium infusion has made the technique more clinically applicable as a diagnostic tool. However, debate remains whether ECV_b would be sufficiently accurate for follow up and monitoring of disease progression.

Furthermore, although ECV has emerged as independently predictive of survival in multivariate analysis, it is unclear how much this will impact on and change current clinical management which relies heavily on Troponin T and NT-pro BNP; if one considers ECV as a

biomarker, it is more expensive than Troponin T and NT-pro BNP although if one considers the additional information gained from cardiac MRI as a whole with ECV as an add-on, this may represent a more cost-effective strategy overall – further studies are needed. There are also standardisation challenges yet to be addressed across different centres with MRI.

14.6 Future Work:

This thesis has looked at the diverse uses of CMR T1 mapping based methodology to assess systemic amyloidosis. Work is needed to establish histological validation of ECV with cardiac histology. This is challenging not only because of the obvious invasive nature of biopsy, but also because of the need to correlate the timing of biopsy within an acceptable time-frame of the EQ-CMR scan, something which is not easy when patients live so far away. The ideal staining method to differentiate amyloid from fibrosis in a manner which is still quantifiable by computer software remains an ongoing challenge too.

ECV measurements in extracardiac organs also requires standardising. The ideal method of T1 mapping the liver and spleen remains undetermined and where to draw ROIs in the liver requires universal agreement. Further work is also needed in evaluating the role of ECV and T1 in ATTR amyloidosis – this is already work in progress.

From an MRI perspective, the T1 mapping sequences are constantly improving e.g. the ShMOLLI sequence currently does not correct for any motion artefacts which makes it more likely to result in partial voluming with blood at the edges of a myocardial ROI – such sequences are work in progress.²⁰⁴ There has also been very little work comparing the reproducibility T1 and ECV across multiple sites and using MRI equipment from differing vendors.

From a more general perspective, myocardial T1 and ECV assessment is a new field and there is little agreement between groups as to what terminology should be used e.g. extracellular volume (ECV), extracellular volume fraction (ECVF), myocardial volume of distribution ($Vd_{(m)}$) have all been used by different groups to describe the same thing over the last 2-3 years. An initiative from this hospital (Prof. James Moon) has therefore set up a T1 mapping development group which has now met 7 times and has drafted proposed preliminary recommendations for everyone in the field to use as a baseline guide.

My work has triggered a number of key changes and progressions, specifically:

1. The NAC now routinely transfers patients to the Heart Hospital for CMR scanning and T1 mapping to calculate ECV which was not previously the case.
2. ECV results now play a key role in the weekly MDT meetings when determining the timing and choice of treatment.
3. My work comparing ECV to SAP scanning in AL amyloidosis has laid the groundwork for similar research in comparing ECV with DPD scanning in ATTR amyloidosis. This work has already begun and the preliminary findings were shortlisted at the Young Investigator Awards at the 2014 AHA scientific sessions in Chicago, USA.
4. My work with ECV in the liver and spleen in AL amyloidosis has attracted the attention of the pharmaceutical industry who are now using ECV of the liver and spleen as an endpoint for their first in man study of therapy in systemic AL amyloidosis, following my presentation of this data at the International Amyloidosis Symposium in 2012.

14.7 Conclusion:

This thesis has provided further insight into the field of myocardial T1 mapping and ECV assessment and highlighted their roles in detecting cardiac and systemic amyloidosis involvement at a much earlier stage and also more sensitively. It shows the huge potential of these techniques and lays a path for future work in the field to ultimately benefit and improve patient outcomes from this rare but fatal disease.

15. REFERENCES

1. Banypersad SM, Moon JC, Whelan C, Hawkins PN, Wechalekar AD. Updates in cardiac amyloidosis: a review. *J Am Heart Assoc.* 2012 Apr;1(2):e000364.
2. Westermark P, Benson MD, Buxbaum JN, Cohen AS, Frangione B, Ikeda S, Masters CL, Merlini G, Saraiva MJ, Sipe JD. A primer of amyloid nomenclature. *Amyloid.* 2007 Sep;14(3):179-83.
3. Bodin K, Ellmerich S, Kahan MC, Tennent GA, Loesch A, Gilbertson JA, Hutchinson WL, Mangione PP, Gallimore JR, Millar DJ, Minogue S, Dhillon AP, Taylor GW, Bradwell AR, Petrie A, Gillmore JD, Bellotti V, Botto M, Hawkins PN, Pepys MB. Antibodies to human serum amyloid P component eliminate visceral amyloid deposits. *Nature.* 2010 Nov 4;468(7320):93-7.
4. Sipe JD, Benson MD, Buxbaum JN, Ikeda S, Merlini G, Saraiva MJ, Westermark P. Amyloid fibril protein nomenclature: 2010 recommendations from the nomenclature committee of the International Society of Amyloidosis. *Amyloid.* 2010 Sep;17(3-4):101-4.
5. Kisilevsky R. The relation of proteoglycans, serum amyloid P and apo E to amyloidosis current status, 2000. *Amyloid.* 2000 Mar;7(1):23-5.
6. Woodrow SI, Stewart RJ, Kisilevsky R, Gore J, Young ID. Experimental AA amyloidogenesis is associated with differential expression of extracellular matrix genes. *Amyloid.* 1999 Mar;6(1):22-30.
7. Westermark GT, Norling B, Westermark P. Fibronectin and basement membrane components in renal amyloid deposits in patients with primary and secondary amyloidosis. *Clin Exp Immunol.* 1991 Oct;86(1):150-6.
8. Mysorekar VV, Rao SG, Satish NT, Kamath SM. Cardiac amyloidosis: report of an autopsy case with review of the literature. *Indian J Pathol Microbiol.* 2010 Oct-Dec;53(4):842-3.
9. Greene MJ, Sam F, Soo Hoo PT, Patel RS, Seldin DC, Connors LH. Evidence for a functional role of the molecular chaperone clusterin in amyloidotic cardiomyopathy. *Am J Pathol.* 2011 Jan;178(1):61-8.
10. Biolo A, Ramamurthy S, Connors LH, O'Hara CJ, Meier-Ewert HK, Soo Hoo PT, Sawyer DB, Seldin DC, Sam F. Matrix metalloproteinases and their tissue inhibitors in cardiac amyloidosis: relationship to structural, functional myocardial changes and to light chain amyloid deposition. *Circ Heart Fail.* 2008 Nov;1(4):249-57.

11. Dubrey SW, Cha K, Skinner M, LaValley M, Falk RH. Familial and primary (AL) cardiac amyloidosis: echocardiographically similar diseases with distinctly different clinical outcomes. *Heart*. 1997 Jul;78(1):74-82.
12. Falk RH. Diagnosis and management of the cardiac amyloidoses. *Circulation*. 2005 Sep 27;112(13):2047-60.
13. Gutierrez PS, Fernandes F, Mady C, Higuchi Mde L. Clinical, electrocardiographic and echocardiographic findings in significant cardiac amyloidosis detected only at necropsy: comparison with cases diagnosed in life. *Arq Bras Cardiol*. 2008 Mar;90(3):191-6.
14. Falk RH, Dubrey SW. Amyloid heart disease. *Prog Cardiovasc Dis*. 2010 Jan-Feb;52(4):347-61.
15. Brodarick S, Paine R, Higa E, Carmichael KA. Pericardial tamponade, a new complication of amyloid heart disease. *Am J Med*. 1982 Jul;73(1):133-5.
16. Navarro JF, Rivera M, Ortuno J. Cardiac tamponade as presentation of systemic amyloidosis. *Int J Cardiol*. 1992 Jul;36(1):107-8.
17. Chamarthi B, Dubrey SW, Cha K, Skinner M, Falk RH. Features and prognosis of exertional syncope in light-chain associated AL cardiac amyloidosis. *Am J Cardiol*. 1997 Nov 1;80(9):1242-5.
18. Padfield GJ, Maclay JD. Macroglossia and complete heart block in a woman with multiple myeloma. *QJM*. 2010 Apr;103(4):271-2.
19. Payne CE, Usher BW. Atrioventricular block in familial amyloidosis; revisiting an old debate. *J S C Med Assoc*. 2007 Jun;103(5):119-22.
20. Ridolfi RL, Bulkley BH, Hutchins GM. The conduction system in cardiac amyloidosis. Clinical and pathologic features of 23 patients. *Am J Med*. 1977 May;62(5):677-86.
21. Velazquez-Cecena JL, Lubell DL, Nagajothi N, Al-Masri H, Siddiqui M, Khosla S. Syncope from dynamic left ventricular outflow tract obstruction simulating hypertrophic cardiomyopathy in a patient with primary AL-type amyloid heart disease. *Tex Heart Inst J*. 2009;36(1):50-4.
22. Dinwoodey DL, Skinner M, Maron MS, Davidoff R, Ruberg FL. Light-chain amyloidosis with echocardiographic features of hypertrophic cardiomyopathy. *Am J Cardiol*. 2008 Mar 1;101(5):674-6.

23. Dubrey SW, Cha K, Anderson J, Chamarthi B, Reisinger J, Skinner M, Falk RH. The clinical features of immunoglobulin light-chain (AL) amyloidosis with heart involvement. QJM. 1998 Feb;91(2):141-57.
24. Morner S, Hellman U, Suhr OB, Kazzam E, Waldenstrom A. Amyloid heart disease mimicking hypertrophic cardiomyopathy. J Intern Med. 2005 Sep;258(3):225-30.
25. Mueller PS, Edwards WD, Gertz MA. Symptomatic ischemic heart disease resulting from obstructive intramural coronary amyloidosis. Am J Med. 2000 Aug 15;109(3):181-8.
26. Al Suwaidi J, Velianou JL, Gertz MA, Cannon RO, 3rd, Higano ST, Holmes DR, Jr., Lerman A. Systemic amyloidosis presenting with angina pectoris. Ann Intern Med. 1999 Dec 7;131(11):838-41.
27. Feng D, Edwards WD, Oh JK, Chandrasekaran K, Grogan M, Martinez MW, Syed IS, Hughes DA, Lust JA, Jaffe AS, Gertz MA, Klarich KW. Intracardiac thrombosis and embolism in patients with cardiac amyloidosis. Circulation. 2007 Nov 20;116(21):2420-6.
28. Zubkov AY, Rabinstein AA, Dispenzieri A, Wijdicks EF. Primary systemic amyloidosis with ischemic stroke as a presenting complication. Neurology. 2007 Sep 11;69(11):1136-41.
29. Poels MM, Ikram MA, van der Lugt A, Hofman A, Krestin GP, Breteler MM, Vernooij MW. Incidence of cerebral microbleeds in the general population: the Rotterdam Scan Study. Stroke. 2011 Mar;42(3):656-61.
30. Kisilevsky R, Young ID. Pathogenesis of amyloidosis. Baillieres Clin Rheumatol. 1994 Aug;8(3):613-26.
31. Kyle RA, Gertz MA. Primary systemic amyloidosis: clinical and laboratory features in 474 cases. Semin Hematol. 1995 Jan;32(1):45-59.
32. Merlini G, Stone MJ. Dangerous small B-cell clones. Blood. 2006 October 15, 2006;108(8):2520-30.
33. Dispenzieri A, Gertz MA, Kyle RA, Lacy MQ, Burritt MF, Therneau TM, Greipp PR, Witzig TE, Lust JA, Rajkumar SV, Fonseca R, Zeldenrust SR, McGregor CG, Jaffe AS. Serum cardiac troponins and N-terminal pro-brain natriuretic peptide: a staging system for primary systemic amyloidosis. J Clin Oncol. 2004 Sep 15;22(18):3751-7.
34. Jacobson DR, Pastore RD, Yaghoubian R, Kane I, Gallo G, Buck FS, Buxbaum JN. Variant-sequence transthyretin (isoleucine 122) in late-onset cardiac amyloidosis in black Americans. N Engl J Med. 1997 Feb 13;336(7):466-73.

35. Falk RH. The neglected entity of familial cardiac amyloidosis in African Americans. *Ethn Dis.* 2002 Winter;12(1):141-3.
36. Coelho T, Maurer MS, Suhr OB. THAOS - The Transthyretin Amyloidosis Outcomes Survey: initial report on clinical manifestations in patients with hereditary and wild-type transthyretin amyloidosis. *Curr Med Res Opin.* 2013 Jan;29(1):63-76.
37. Merlini G, Bellotti V. Molecular mechanisms of amyloidosis. *N Engl J Med.* 2003 Aug 7;349(6):583-96.
38. Dubrey SW, Hawkins PN, Falk RH. Amyloid diseases of the heart: assessment, diagnosis, and referral. *Heart.* 2011 Jan;97(1):75-84.
39. Westermark P, Sletten K, Johansson B, Cornwell GG, 3rd. Fibril in senile systemic amyloidosis is derived from normal transthyretin. *Proc Natl Acad Sci U S A.* 1990 Apr;87(7):2843-5.
40. Ng B, Connors LH, Davidoff R, Skinner M, Falk RH. Senile systemic amyloidosis presenting with heart failure: a comparison with light chain-associated amyloidosis. *Arch Intern Med.* 2005 Jun 27;165(12):1425-9.
41. Connors LH, Lim A, Prokaeva T, Roskens VA, Costello CE. Tabulation of human transthyretin (TTR) variants, 2003. *Amyloid.* 2003 Sep;10(3):160-84.
42. Dubrey SW, Falk RH. Amyloid heart disease. *Br J Hosp Med (Lond).* 2010 Feb;71(2):76-82.
43. Pinney JH, Whelan CJ, Petrie A, Dungu J, Banypersad SM, Sattianayagam P, Wechalekar A, Gibbs SD, Venner CP, Wassef N, McCarthy CA, Gilbertson JA, Rowczenio D, Hawkins PN, Gillmore JD, Lachmann HJ. Senile systemic amyloidosis: clinical features at presentation and outcome. *J Am Heart Assoc.* 2013 Apr;2(2):e000098.
44. Pinney JH, Smith CJ, Taube JB, Lachmann HJ, Venner CP, Gibbs SD, Dungu J, Banypersad SM, Wechalekar AD, Whelan CJ, Hawkins PN, Gillmore JD. Systemic amyloidosis in England: an epidemiological study. *Br J Haematol.* 2013 May;161(4):525-32.
45. Tanskanen M, Peuralinna T, Polvikoski T, Notkola IL, Sulkava R, Hardy J, Singleton A, Kiuru-Enari S, Paetau A, Tienari PJ, Myllykangas L. Senile systemic amyloidosis affects 25% of the very aged and associates with genetic variation in alpha2-macroglobulin and tau: a population-based autopsy study. *Ann Med.* 2008;40(3):232-9.
46. Ogiwara F, Koyama J, Ikeda S, Kinoshita O, Falk RH. Comparison of the strain Doppler echocardiographic features of familial amyloid polyneuropathy (FAP) and light-chain amyloidosis. *Am J Cardiol.* 2005 Feb 15;95(4):538-40.

47. Ariyarajah V, Steiner I, Hajkova P, Khadem A, Kvasnicka J, Apiyasawat S, Spodick DH. The association of atrial tachyarrhythmias with isolated atrial amyloid disease: preliminary observations in autopsied heart specimens. *Cardiology*. 2009;113(2):132-7.
48. Kaye GC, Butler MG, d'Ardenne AJ, Edmondson SJ, Camm AJ, Slavin G. Isolated atrial amyloid contains atrial natriuretic peptide: a report of six cases. *Br Heart J*. 1986 Oct;56(4):317-20.
49. Steiner I. The prevalence of isolated atrial amyloid. *J Pathol*. 1987 Dec;153(4):395-8.
50. Kristen AV, Schnabel PA, Winter B, Helmke BM, Longerich T, Hardt S, Koch A, Sack FU, Katus HA, Linke RP, Dengler TJ. High prevalence of amyloid in 150 surgically removed heart valves--a comparison of histological and clinical data reveals a correlation to atheroinflammatory conditions. *Cardiovasc Pathol*. 2010 Jul-Aug;19(4):228-35.
51. Iqbal S, Reehana S, Lawrence D. Unique type of isolated cardiac valvular amyloidosis. *J Cardiothorac Surg*. 2006;1:38.
52. Cheng ZW, Tian Z, Kang L, Chen TB, Fang LG, Cheng KA, Zeng Y, Fang Q. [Electrocardiographic and echocardiographic features of patients with primary cardiac amyloidosis]. *Zhonghua Xin Xue Guan Bing Za Zhi*. 2010 Jul;38(7):606-9.
53. Murtagh B, Hammill SC, Gertz MA, Kyle RA, Tajik AJ, Grogan M. Electrocardiographic findings in primary systemic amyloidosis and biopsy-proven cardiac involvement. *Am J Cardiol*. 2005 Feb 15;95(4):535-7.
54. Dungu J, Sattianayagam PT, Whelan CJ, Gibbs SD, Pinney JH, Banypersad SM, Rowczenio D, Gilbertson JA, Lachmann HJ, Wechalekar A, Gillmore JD, Hawkins PN, Anderson LJ. The electrocardiographic features associated with cardiac amyloidosis of variant transthyretin isoleucine 122 type in Afro-Caribbean patients. *Am Heart J*. 2012 Jul;164(1):72-9.
55. Rapezzi C, Merlini G, Quarta CC, Riva L, Longhi S, Leone O, Salvi F, Ciliberti P, Pastorelli F, Biagini E, Coccolo F, Cooke RM, Bacchi-Reggiani L, Sangiorgi D, Ferlini A, Cavo M, Zamagni E, Fonte ML, Palladini G, Salinaro F, Musca F, Obici L, Branzi A, Perlini S. Systemic cardiac amyloidoses: disease profiles and clinical courses of the 3 main types. *Circulation*. 2009 Sep 29;120(13):1203-12.
56. Takigawa M, Hashimura K, Ishibashi-Ueda H, Yamada N, Kiso K, Nanasato M, Yoshida Y, Hirayama H. Annual electrocardiograms consistent with silent progression of cardiac involvement in sporadic familial amyloid polyneuropathy: a case report. *Intern Med*. 2010;49(2):139-44.
57. Pinney J GJ, Lachmann H, Wechalekar A, Gibbs S, Banypersad SM, Dungu J, Rannigan L, Collins E, McCarthy C, Hawkins P, Whelan C. Disturbances of Cardiac Rhythm in AL Amyloidosis. 13th International Myeloma Workshop. 2011:426.

58. Kristen AV, Perz JB, Schonland SO, Hansen A, Hegenbart U, Sack FU, Goldschmidt H, Katus HA, Dengler TJ. Rapid progression of left ventricular wall thickness predicts mortality in cardiac light-chain amyloidosis. *J Heart Lung Transplant*. 2007 Dec;26(12):1313-9.
59. Koyama J, Falk RH. Prognostic significance of strain Doppler imaging in light-chain amyloidosis. *JACC Cardiovasc Imaging*. 2010 Apr;3(4):333-42.
60. Migrino RQ, Mareedu RK, Eastwood D, Bowers M, Harmann L, Hari P. Left ventricular ejection time on echocardiography predicts long-term mortality in light chain amyloidosis. *J Am Soc Echocardiogr*. 2009 Dec;22(12):1396-402.
61. Patel AR, Dubrey SW, Mendes LA, Skinner M, Cupples A, Falk RH, Davidoff R. Right ventricular dilation in primary amyloidosis: an independent predictor of survival. *Am J Cardiol*. 1997 Aug 15;80(4):486-92.
62. Porciani MC, Lilli A, Perfetto F, Cappelli F, Massimiliano Rao C, Del Pace S, Ciaccheri M, Castelli G, Tarquini R, Romagnani L, Pastorini T, Padeletti L, Bergesio F. Tissue Doppler and strain imaging: a new tool for early detection of cardiac amyloidosis. *Amyloid*. 2009;16(2):63-70.
63. Tsang W, Lang RM. Echocardiographic evaluation of cardiac amyloid. *Curr Cardiol Rep*. 2010 May;12(3):272-6.
64. Bellavia D, Pellikka PA, Abraham TP, Al-Zahrani GB, Dispenzieri A, Oh JK, Bailey KR, Wood CM, Lacy MQ, Miyazaki C, Miller FA, Jr. Evidence of impaired left ventricular systolic function by Doppler myocardial imaging in patients with systemic amyloidosis and no evidence of cardiac involvement by standard two-dimensional and Doppler echocardiography. *Am J Cardiol*. 2008 Apr 1;101(7):1039-45.
65. Park SJ, Miyazaki C, Bruce CJ, Ommen S, Miller FA, Oh JK. Left ventricular torsion by two-dimensional speckle tracking echocardiography in patients with diastolic dysfunction and normal ejection fraction. *J Am Soc Echocardiogr*. 2008 Oct;21(10):1129-37.
66. Porciani MC, Cappelli F, Perfetto F, Ciaccheri M, Castelli G, Ricceri I, Chiostri M, Franco B, Padeletti L. Rotational mechanics of the left ventricle in AL amyloidosis. *Echocardiography*. 2010 Oct;27(9):1061-8.
67. Kusunose K, Yamada H, Iwase T, Nishio S, Tomita N, Niki T, Yamaguchi K, Koshiba K, Taketani Y, Soeki T, Wakatsuki T, Akaike M, Shoichiro T, Harada M, Kagawa N, Kudo E, Sata M. Images in cardiovascular medicine. Cardiac magnetic resonance imaging and 2-dimensional speckle tracking echocardiography in secondary cardiac amyloidosis. *Circ J*. 2010;74(7):1494-6.
68. Sun JP, Stewart WJ, Yang XS, Donnell RO, Leon AR, Felner JM, Thomas JD, Merlino JD. Differentiation of hypertrophic cardiomyopathy and cardiac amyloidosis from other causes of

ventricular wall thickening by two-dimensional strain imaging echocardiography. Am J Cardiol. 2009 Feb 1;103(3):411-5.

69. Abdelmoneim SS, Bernier M, Bellavia D, Syed IS, Mankad SV, Chandrasekaran K, Pellikka PA, Mulvagh SL. Myocardial contrast echocardiography in biopsy-proven primary cardiac amyloidosis. Eur J Echocardiogr. 2008 Mar;9(2):338-41.

70. Feng D, Syed IS, Martinez M, Oh JK, Jaffe AS, Grogan M, Edwards WD, Gertz MA, Klarich KW. Intracardiac thrombosis and anticoagulation therapy in cardiac amyloidosis. Circulation. 2009 May 12;119(18):2490-7.

71. Palladini G, Campana C, Klersy C, Balduini A, Vadacca G, Perfetti V, Perlini S, Obici L, Ascari E, d'Erl GM, Moratti R, Merlini G. Serum N-terminal pro-brain natriuretic peptide is a sensitive marker of myocardial dysfunction in AL amyloidosis. Circulation. 2003 May 20;107(19):2440-5.

72. Wechalekar AD, Gillmore JD, Wassef N, Lachmann HJ, Whelan C, Hawkins PN. Abnormal N-terminal fragment of brain natriuretic peptide in patients with light chain amyloidosis without cardiac involvement at presentation is a risk factor for development of cardiac amyloidosis. Haematologica. 2011 May 23.

73. Takemura G, Takatsu Y, Doyama K, Itoh H, Saito Y, Koshiji M, Ando F, Fujiwara T, Nakao K, Fujiwara H. Expression of atrial and brain natriuretic peptides and their genes in hearts of patients with cardiac amyloidosis. J Am Coll Cardiol. 1998 Mar 15;31(4):754-65.

74. Dispenzieri A, Kyle RA, Gertz MA, Therneau TM, Miller WL, Chandrasekaran K, McConnell JP, Burritt MF, Jaffe AS. Survival in patients with primary systemic amyloidosis and raised serum cardiac troponins. Lancet. 2003 May 24;361(9371):1787-9.

75. Kristen AV, Giannitsis E, Lehrke S, Hegenbart U, Konstandin M, Lindenmaier D, Merkle C, Hardt S, Schnabel PA, Rocken C, Schonland SO, Ho AD, Dengler TJ, Katus HA. Assessment of disease severity and outcome in patients with systemic light-chain amyloidosis by the high-sensitivity troponin T assay. Blood. 2010 Oct 7;116(14):2455-61.

76. Palladini G, Barassi A, Klersy C, Pacciolla R, Milani P, Sarais G, Perlini S, Albertini R, Russo P, Foli A, Bragotti LZ, Obici L, Moratti R, Melzi d'Erl GV, Merlini G. The combination of high-sensitivity cardiac troponin T (hs-cTnT) at presentation and changes in N-terminal natriuretic peptide type B (NT-proBNP) after chemotherapy best predicts survival in AL amyloidosis. Blood. 2010 Nov 4;116(18):3426-30.

77. Dispenzieri A, Gertz MA, Kyle RA, Lacy MQ, Burritt MF, Therneau TM, McConnell JP, Litzow MR, Gastineau DA, Tefferi A, Inwards DJ, Micallef IN, Ansell SM, Porrata LF, Elliott MA, Hogan WJ, Rajkumar SV, Fonseca R, Greipp PR, Witzig TE, Lust JA, Zeldenrust SR, Snow DS, Hayman SR, McGregor CG, Jaffe AS. Prognostication of survival using cardiac troponins and N-

terminal pro-brain natriuretic peptide in patients with primary systemic amyloidosis undergoing peripheral blood stem cell transplantation. *Blood*. 2004 Sep 15;104(6):1881-7.

78. Palladini G, Russo P, Nuvolone M, Lavatelli F, Perfetti V, Obici L, Merlini G. Treatment with oral melphalan plus dexamethasone produces long-term remissions in AL amyloidosis. *Blood*. 2007 Jul 15;110(2):787-8.

79. Palladini G, Dispenzieri A, Gertz MA, Kumar S, Wechalekar A, Hawkins PN, Schonland S, Hegenbart U, Comenzo R, Kastritis E, Dimopoulos MA, Jaccard A, Klerys C, Merlini G. New criteria for response to treatment in immunoglobulin light chain amyloidosis based on free light chain measurement and cardiac biomarkers: impact on survival outcomes. *J Clin Oncol*. 2012 Dec 20;30(36):4541-9.

80. Tapan U, Seldin DC, Finn KT, Fennessey S, Shelton A, Zeldis JB, Sanchorawala V. Increases in B-type natriuretic peptide (BNP) during treatment with lenalidomide in AL amyloidosis. *Blood*. 2010 Dec 2;116(23):5071-2.

81. Dispenzieri A, Dingli D, Kumar SK, Rajkumar SV, Lacy MQ, Hayman S, Buadi F, Zeldenrust S, Leung N, Detweiler-Short K, Lust JA, Russell SJ, Kyle RA, Gertz MA. Discordance between serum cardiac biomarker and immunoglobulin-free light-chain response in patients with immunoglobulin light-chain amyloidosis treated with immune modulatory drugs. *Am J Hematol*. 2010 Oct;85(10):757-9.

82. Hawkins PN, Lavender JP, Pepys MB. Evaluation of systemic amyloidosis by scintigraphy with ¹²³I-labeled serum amyloid P component. *N Engl J Med*. 1990 Aug 23;323(8):508-13.

83. Minutoli F GM, Di Bella G, Crisafulli C, Murè G, Militano V, Brancati M, Di Leo R, Mazzeo A, Baldari S. Cardiac involvement in transthyretin familial amyloid polyneuropathy - comparison between ^{99m}Tc-DPD SPECT and magnetic resonance imaging. European Association of Nuclear Medicine. 2010(Cardiovascular: Cardiovascular disease and comorbidities):252.

84. Perugini E, Guidalotti PL, Salvi F, Cooke RM, Pettinato C, Riva L, Leone O, Farsad M, Ciliberti P, Bacchi-Reggiani L, Fallani F, Branzi A, Rapezzi C. Noninvasive etiologic diagnosis of cardiac amyloidosis using ^{99m}Tc-3,3-diphosphono-1,2-propanodicarboxylic acid scintigraphy. *J Am Coll Cardiol*. 2005 Sep 20;46(6):1076-84.

85. Antoni G, Lubberink M, Estrada S, Axelsson J, Carlson K, Lindsjo L, Kero T, Langstrom B, Granstrom SO, Rosengren S, Vedin O, Wassberg C, Wikstrom G, Westermark P, Sorensen J. In vivo visualization of amyloid deposits in the heart with ^{11C}-PIB and PET. *J Nucl Med*. 2013 Feb;54(2):213-20.

86. Hosch W, Bock M, Libicher M, Ley S, Hegenbart U, Dengler TJ, Katus HA, Kauczor HU, Kauffmann GW, Kristen AV. MR-relaxometry of myocardial tissue: significant elevation of T1 and T2 relaxation times in cardiac amyloidosis. *Invest Radiol.* 2007 Sep;42(9):636-42.
87. Sparrow P, Amirabadi A, Sussman MS, Paul N, Merchant N. Quantitative assessment of myocardial T2 relaxation times in cardiac amyloidosis. *J Magn Reson Imaging.* 2009 Nov;30(5):942-6.
88. Vogelsberg H, Mahrholdt H, Deluigi CC, Yilmaz A, Kispert EM, Greulich S, Klingel K, Kandolf R, Sechtem U. Cardiovascular magnetic resonance in clinically suspected cardiac amyloidosis: noninvasive imaging compared to endomyocardial biopsy. *J Am Coll Cardiol.* 2008 Mar 11;51(10):1022-30.
89. Maceira AM, Joshi J, Prasad SK, Moon JC, Perugini E, Harding I, Sheppard MN, Poole-Wilson PA, Hawkins PN, Pennell DJ. Cardiovascular magnetic resonance in cardiac amyloidosis. *Circulation.* 2005 Jan 18;111(2):186-93.
90. Austin BA, Tang WH, Rodriguez ER, Tan C, Flamm SD, Taylor DO, Starling RC, Desai MY. Delayed hyper-enhancement magnetic resonance imaging provides incremental diagnostic and prognostic utility in suspected cardiac amyloidosis. *Jacc.* 2009 Dec;2(12):1369-77.
91. Syed IS, Glockner JF, Feng D, Araoz PA, Martinez MW, Edwards WD, Gertz MA, Dispensieri A, Oh JK, Bellavia D, Tajik AJ, Grogan M. Role of cardiac magnetic resonance imaging in the detection of cardiac amyloidosis. *Jacc.* 2010 Feb;3(2):155-64.
92. Di Bella G, Minutoli F, Mazzeo A, Vita G, Oreto G, Carerj S, Anfuso C, Russo M, Gaeta M. MRI of cardiac involvement in transthyretin familial amyloid polyneuropathy. *AJR Am J Roentgenol.* 2010 Dec;195(6):W394-9.
93. Maceira AM, Prasad SK, Hawkins PN, Roughton M, Pennell DJ. Cardiovascular magnetic resonance and prognosis in cardiac amyloidosis. *J Cardiovasc Magn Reson.* 2008;10:54.
94. Sparrow PJ, Merchant N, Provost YL, Doyle DJ, Nguyen ET, Paul NS. CT and MR imaging findings in patients with acquired heart disease at risk for sudden cardiac death. *Radiographics.* 2009 May-Jun;29(3):805-23.
95. Kieninger B, Eriksson M, Kandolf R, Schnabel PA, Schonland S, Kristen AV, Hegenbart U, Lohse P, Rocken C. Amyloid in endomyocardial biopsies. *Virchows Arch.* 2010 May;456(5):523-32.
96. Benson MD, Breall J, Cummings OW, Liepnieks JJ. Biochemical characterisation of amyloid by endomyocardial biopsy. *Amyloid.* 2009 Mar;16(1):9-14.

97. Tian Z, Zeng Y, Cheng KA, Gao P, Zhao DC, Cui QC, Jiang XC, Chen LF, Fang Q. Importance of endomyocardial biopsy in unexplained cardiomyopathy in China: a report of 53 consecutive patients. *Chin Med J (Engl)*. 2010 Apr;123(7):864-70.
98. Sloan KP, Bruce CJ, Oh JK, Rihal CS. Complications of echocardiography-guided endomyocardial biopsy. *J Am Soc Echocardiogr*. 2009 Mar;22(3):324 e1-4.
99. Ardehali H, Qasim A, Cappola T, Howard D, Hruban R, Hare JM, Baughman KL, Kasper EK. Endomyocardial biopsy plays a role in diagnosing patients with unexplained cardiomyopathy. *Am Heart J*. 2004 May;147(5):919-23.
100. Gertz MA, Grogan M, Kyle RA, Tajik AJ. Endomyocardial biopsy-proven light chain amyloidosis (AL) without echocardiographic features of infiltrative cardiomyopathy. *Am J Cardiol*. 1997 Jul 1;80(1):93-5.
101. Vrana JA, Gamez JD, Madden BJ, Theis JD, Bergen HR, 3rd, Dogan A. Classification of amyloidosis by laser microdissection and mass spectrometry-based proteomic analysis in clinical biopsy specimens. *Blood*. 2009 Dec 3;114(24):4957-9.
102. Tam M, Seldin DC, Forbes BM, Connors LH, Skinner M, Oran B, Quillen K, Sanchorawala V. Spontaneous rupture of the liver in a patient with systemic AL amyloidosis undergoing treatment with high-dose melphalan and autologous stem cell transplantation: a case report with literature review. *Amyloid*. 2009;16(2):103-7.
103. Loss M, Ng WS, Karim RZ, Strasser SI, Koorey DJ, Gallagher PJ, Verran DJ, McCaughan GW. Hereditary lysozyme amyloidosis: spontaneous hepatic rupture (15 years apart) in mother and daughter. role of emergency liver transplantation. *Liver Transpl*. 2006 Jul;12(7):1152-5.
104. Higuchi K, Qian J, Yan J, Ge F, Zhang B, Fu X, Tomozawa H, Sawashita J, Mori M. Mouse apoA-II amyloid fibrils deposit in skeletal muscle and exhibit amyloidosis-enhancing activity. *Amyloid*. 2011 Jun;18 Suppl 1:42-4.
105. Qian J, Yan J, Ge F, Zhang B, Fu X, Tomozawa H, Sawashita J, Mori M, Higuchi K. Mouse senile amyloid fibrils deposited in skeletal muscle exhibit amyloidosis-enhancing activity. *PLoS Pathog*. 2010 May;6(5):e1000914.
106. Chuquelin M, Al-Lozi M. Primary amyloidosis presenting as "dropped head syndrome". *Muscle Nerve*. 2011 Jun;43(6):905-9.
107. Ohtsuka Y, Yasui N, Sekiguchi K, Kowa H, Nishino I, Kanda F, Toda T. [A case of amyloidosis with amyloid deposition detected only in skeletal muscles]. *Rinsho Shinkeigaku*. 2012;52(10):739-43.

108. Jeon CY, Jin SY, Jang JW, Kim US. A case of isolated primary amyloidosis in the medial rectus muscle. *Graefes Arch Clin Exp Ophthalmol*. 2013 Jan;251(1):395-6.
109. Keith J, Afshar-Ghotli Z, Rousset R, Ernst B, Young B, Bilbao JM. Myopathy as the initial manifestation of primary amyloidosis. *Can J Neurol Sci*. 2011 Jan;38(1):161-4.
110. Rubinow A, Skinner M, Cohen AS. Digoxin sensitivity in amyloid cardiomyopathy. *Circulation*. 1981 Jun;63(6):1285-8.
111. Gertz MA, Skinner M, Connors LH, Falk RH, Cohen AS, Kyle RA. Selective binding of nifedipine to amyloid fibrils. *Am J Cardiol*. 1985 Jun 1;55(13 Pt 1):1646.
112. Pollak A, Falk RH. Left ventricular systolic dysfunction precipitated by verapamil in cardiac amyloidosis. *Chest*. 1993 Aug;104(2):618-20.
113. Yamaguchi T. Syncope and sinus bradycardia from combined use of thalidomide and beta-blocker. *Pharmacoepidemiol Drug Saf*. 2008 Oct;17(10):1033-5.
114. Low PA. Autonomic neuropathies. *Curr Opin Neurol*. 2002 Oct;15(5):605-9.
115. Kristen AV, Dengler TJ, Hegenbart U, Schonland SO, Goldschmidt H, Sack FU, Voss F, Becker R, Katus HA, Bauer A. Prophylactic implantation of cardioverter-defibrillator in patients with severe cardiac amyloidosis and high risk for sudden cardiac death. *Heart Rhythm*. 2008 Feb;5(2):235-40.
116. Seethala S, Jain S, Ohori NP, Monaco S, Lacomis J, Crock F, Nemec J. Focal monomorphic ventricular tachycardia as the first manifestation of amyloid cardiomyopathy. *Indian Pacing Electrophysiol J*. 2010;10(3):143-7.
117. Dhoble A, Khasnis A, Olomu A, Thakur R. Cardiac amyloidosis treated with an implantable cardioverter defibrillator and subcutaneous array lead system: report of a case and literature review. *Clin Cardiol*. 2009 Aug;32(8):E63-5.
118. Bellavia D, Pellikka PA, Abraham TP, Al-Zahrani GB, Dispensieri A, Oh JK, Espinosa RE, Scott CG, Miyazaki C, Miller FA. 'Hypersynchronisation' by tissue velocity imaging in patients with cardiac amyloidosis. *Heart*. 2009 Mar;95(3):234-40.
119. Sattianayagam PT, Gibbs SD, Pinney JH, Wechalekar AD, Lachmann HJ, Whelan CJ, Gilbertson JA, Hawkins PN, Gillmore JD. Solid organ transplantation in AL amyloidosis. *Am J Transplant*. 2010 Sep;10(9):2124-31.
120. Gillmore JD, Goodman HJ, Lachmann HJ, Offer M, Wechalekar AD, Joshi J, Pepys MB, Hawkins PN. Sequential heart and autologous stem cell transplantation for systemic AL amyloidosis. *Blood*. 2006 Feb 1;107(3):1227-9.

121. Mignot A, Varnous S, Redonnet M, Jaccard A, Epailly E, Vermes E, Boissonnat P, Gandjbakhch I, Herpin D, Touchard G, Bridoux F. Heart transplantation in systemic (AL) amyloidosis: a retrospective study of eight French patients. *Arch Cardiovasc Dis.* 2008 Sep;101(9):523-32.
122. Sack FU, Kristen A, Goldschmidt H, Schnabel PA, Dengler T, Koch A, Karck M. Treatment options for severe cardiac amyloidosis: heart transplantation combined with chemotherapy and stem cell transplantation for patients with AL-amyloidosis and heart and liver transplantation for patients with ATTR-amyloidosis. *Eur J Cardiothorac Surg.* 2008 Feb;33(2):257-62.
123. Dey BR, Chung SS, Spitzer TR, Zheng H, Macgillivray TE, Seldin DC, McAfee S, Ballen K, Attar E, Wang T, Shin J, Newton-Cheh C, Moore S, Sanctorawala V, Skinner M, Madsen JC, Semigran MJ. Cardiac transplantation followed by dose-intensive melphalan and autologous stem-cell transplantation for light chain amyloidosis and heart failure. *Transplantation.* 2010 Oct 27;90(8):905-11.
124. Dubrey SW, Burke MM, Hawkins PN, Banner NR. Cardiac transplantation for amyloid heart disease: the United Kingdom experience. *J Heart Lung Transplant.* 2004 Oct;23(10):1142-53.
125. Barreiros AP, Post F, Hoppe-Lotichius M, Linke RP, Vahl CF, Schafers HJ, Galle PR, Otto G. Liver transplantation and combined liver-heart transplantation in patients with familial amyloid polyneuropathy: a single-center experience. *Liver Transpl.* 2010 Mar;16(3):314-23.
126. Hamour IM, Lachmann HJ, Goodman HJ, Petrou M, Burke MM, Hawkins PN, Banner NR. Heart transplantation for homozygous familial transthyretin (TTR) V122I cardiac amyloidosis. *Am J Transplant.* 2008 May;8(5):1056-9.
127. Wechalekar AD, Goodman HJ, Lachmann HJ, Offer M, Hawkins PN, Gillmore JD. Safety and efficacy of risk-adapted cyclophosphamide, thalidomide, and dexamethasone in systemic AL amyloidosis. *Blood.* 2007 Jan 15;109(2):457-64.
128. Dhodapkar MV, Hussein MA, Rasmussen E, Solomon A, Larson RA, Crowley JJ, Barlogie B. Clinical efficacy of high-dose dexamethasone with maintenance dexamethasone/alpha interferon in patients with primary systemic amyloidosis: results of United States Intergroup Trial Southwest Oncology Group (SWOG) S9628. *Blood.* 2004 Dec 1;104(12):3520-6.
129. Skinner M, Sanctorawala V, Seldin DC, Dember LM, Falk RH, Berk JL, Anderson JJ, O'Hara C, Finn KT, Libbey CA, Wiesman J, Quillen K, Swan N, Wright DG. High-dose melphalan and autologous stem-cell transplantation in patients with AL amyloidosis: an 8-year study. *Ann Intern Med.* 2004 Jan 20;140(2):85-93.
130. Cohen AD, Zhou P, Chou J, Teruya-Feldstein J, Reich L, Hassoun H, Levine B, Filippa DA, Riedel E, Kewalramani T, Stubblefield MD, Fleisher M, Nimer S, Comenzo RL. Risk-adapted

autologous stem cell transplantation with adjuvant dexamethasone +/- thalidomide for systemic light-chain amyloidosis: results of a phase II trial. Br J Haematol. 2007 Oct;139(2):224-33.

131. Comenzo RL. Managing systemic light-chain amyloidosis. J Natl Compr Canc Netw. 2007 Feb;5(2):179-87.

132. Wechalekar AD, Hawkins PN, Gillmore JD. Perspectives in treatment of AL amyloidosis. Br J Haematol. 2008 Feb;140(4):365-77.

133. Oliva L, Palladini G, Cerruti F, Pengo N, Cascio P, Merlini G, Sitia R, Cenci S. Assessing Proteostasis and Proteasome Stress In Light Chain Amyloidosis. ASH Annual Meeting Abstracts. 2010 November 19, 2010;116(21):3992.

134. Mikhael JR, Schuster SR, Jimenez-Zepeda VH, Bello N, Spong J, Reeder CB, Stewart AK, Bergsagel PL, Fonseca R. The Combination of Cyclophosphamide-Bortezomib-Dexamethasone (CYBOR-D) Is a Highly Effective and Well Tolerated Regimen that Produces Rapid and Complete Hematological Response In Patients with AL Amyloidosis. ASH Annual Meeting Abstracts. 2010 November 19, 2010;116(21):3063-.

135. Wechalekar AD, Kastritis E, Merlini G, Hawkins PN, Dimopoulos MA, Gillmore JD, Gibbs SD, Palladini G. A European Collaborative Study of Treatment Outcomes In 428 Patients with Systemic AL Amyloidosis. ASH Annual Meeting Abstracts. 2010 November 19, 2010;116(21):988-.

136. Zonder JA, Sanchorawala V, Snyder RM, Matous J, Terebelo H, Janakiraman N, Mapara MY, Lalo S, Tageja N, Webb C, Monsma D, Sellers C, Abrams J, Gasparetto C. Melphalan and Dexamethasone Plus Bortezomib Induces Hematologic and Organ Responses in AL-Amyloidosis with Tolerable Neurotoxicity. ASH Annual Meeting Abstracts. 2009 November 20, 2009;114(22):746-.

137. Ihse E, Suhr OB, Hellman U, Westermark P. Variation in amount of wild-type transthyretin in different fibril and tissue types in ATTR amyloidosis. J Mol Med. 2011 Feb;89(2):171-80.

138. Tomas MT, Santa-Clara H, Bruno PM, Monteiro E, Carrolo M, Barroso E, Sardinha LB, Fernhall B. The impact of exercise training on liver transplanted familial amyloidotic polyneuropathy (FAP) patients. Transplantation. 2013 Jan 27;95(2):372-7.

139. Benson MD, Kluwe-Beckerman B, Zeldenrust SR, Siesky AM, Bodenmiller DM, Showalter AD, Sloop KW. Targeted suppression of an amyloidogenic transthyretin with antisense oligonucleotides. Muscle Nerve. 2006 May;33(5):609-18.

140. Sekijima Y, Dendale MA, Kelly JW. Orally administered diflunisal stabilizes transthyretin against dissociation required for amyloidogenesis. Amyloid. 2006 Dec;13(4):236-49.

141. Tojo K, Sekijima Y, Kelly JW, Ikeda S. Diflunisal stabilizes familial amyloid polyneuropathy-associated transthyretin variant tetramers in serum against dissociation required for amyloidogenesis. *Neurosci Res.* 2006 Dec;56(4):441-9.
142. Kolstoe SE, Mangione PP, Bellotti V, Taylor GW, Tennent GA, Deroo S, Morrison AJ, Cobb AJ, Coyne A, McCammon MG, Warner TD, Mitchell J, Gill R, Smith MD, Ley SV, Robinson CV, Wood SP, Pepys MB. Trapping of palindromic ligands within native transthyretin prevents amyloid formation. *Proc Natl Acad Sci U S A.* 2010 Nov 23;107(47):20483-8.
143. Dember LM, Hawkins PN, Hazenberg BP, Gorevic PD, Merlini G, Butrimiene I, Livneh A, Lesnyak O, Puechal X, Lachmann HJ, Obici L, Balshaw R, Garceau D, Hauck W, Skinner M. Eprodisate for the treatment of renal disease in AA amyloidosis. *N Engl J Med.* 2007 Jun 7;356(23):2349-60.
144. Messroghli DR, Radjenovic A, Kozerke S, Higgins DM, Sivananthan MU, Ridgway JP. Modified Look-Locker inversion recovery (MOLLI) for high-resolution T1 mapping of the heart. *Magn Reson Med.* 2004 Jul;52(1):141-6.
145. Piechnik SK, Ferreira VM, Dall'Armellina E, Cochlin LE, Greiser A, Neubauer S, Robson MD. Shortened Modified Look-Locker Inversion recovery (ShMOLLI) for clinical myocardial T1-mapping at 1.5 and 3 T within a 9 heartbeat breathhold. *J Cardiovasc Magn Reson.* 2010;12:69.
146. Chow K, Flewitt JA, Green JD, Pagano JJ, Friedrich MG, Thompson RB. Saturation recovery single-shot acquisition (SASHA) for myocardial T mapping. *Magn Reson Med.* 2013 Jul 23.
147. Flett AS, Hayward MP, Ashworth MT, Hansen MS, Taylor AM, Elliott PM, McGregor C, Moon JC. Equilibrium contrast cardiovascular magnetic resonance for the measurement of diffuse myocardial fibrosis: preliminary validation in humans. *Circulation.* 2010 Jul 13;122(2):138-44.
148. Sado DM, Flett AS, Banypersad SM, White SK, Maestrini V, Quarta G, Lachmann RH, Murphy E, Mehta A, Hughes DA, McKenna WJ, Taylor AM, Hausenloy DJ, Hawkins PN, Elliott PM, Moon JC. Cardiovascular magnetic resonance measurement of myocardial extracellular volume in health and disease. *Heart.* 2012 Oct;98(19):1436-41.
149. Gertz MA, Comenzo R, Falk RH, Fermand JP, Hazenberg BP, Hawkins PN, Merlini G, Moreau P, Ronco P, Sanchorawala V, Sezer O, Solomon A, Grateau G. Definition of organ involvement and treatment response in immunoglobulin light chain amyloidosis (AL): a consensus opinion from the 10th International Symposium on Amyloid and Amyloidosis, Tours, France, 18-22 April 2004. *Am J Hematol.* 2005 Aug;79(4):319-28.
150. Banypersad SM, Sado DM, Flett AS, Gibbs SD, Pinney JH, Maestrini V, Cox AT, Fontana M, Whelan CJ, Wechalekar AD, Hawkins PN, Moon JC. Quantification of myocardial

extracellular volume fraction in systemic AL amyloidosis: an equilibrium contrast cardiovascular magnetic resonance study. *Circ Cardiovasc Imaging*. 2013 Jan 1;6(1):34-9.

151. Hundley WG, Bluemke D, Bogaert JG, Friedrich MG, Higgins CB, Lawson MA, McConnell MV, Raman SV, van Rossum AC, Flamm S, Kramer CM, Nagel E, Neubauer S. Society for Cardiovascular Magnetic Resonance guidelines for reporting cardiovascular magnetic resonance examinations. *J Cardiovasc Magn Reson*. 2009;11:5.

152. ATS statement: guidelines for the six-minute walk test. *Am J Respir Crit Care Med*. 2002 Jul 1;166(1):111-7.

153. Borg GA. Psychophysical bases of perceived exertion. *Med Sci Sports Exerc*. 1982;14(5):377-81.

154. Nagueh SF, Appleton CP, Gillebert TC, Marino PN, Oh JK, Smiseth OA, Waggoner AD, Flachskampf FA, Pellikka PA, Evangelista A. Recommendations for the evaluation of left ventricular diastolic function by echocardiography. *J Am Soc Echocardiogr*. 2009 Feb;22(2):107-33.

155. Harris PA, Taylor R, Thielke R, Payne J, Gonzalez N, Conde JG. Research electronic data capture (REDCap)--a metadata-driven methodology and workflow process for providing translational research informatics support. *J Biomed Inform*. 2009 Apr;42(2):377-81.

156. Heagerty PJ, Lumley T, Pepe MS. Time-dependent ROC curves for censored survival data and a diagnostic marker. *Biometrics*. 2000 Jun;56(2):337-44.

157. Perlini S, Salinaro F, Cappelli F, Perfetto F, Bergesio F, Alogna A, Mussinelli R, Boldrini M, Raimondi A, Musca F, Palladini G, Merlini G. Prognostic value of fragmented QRS in cardiac AL amyloidosis. *Int J Cardiol*. 2012 Jun 27.

158. Miller F, Jr., Bellavia D. Comparison of right ventricular longitudinal strain imaging, tricuspid annular plane systolic excursion, and cardiac biomarkers for early diagnosis of cardiac involvement and risk stratification in primary systematic (AL) amyloidosis: a 5-year cohort study: reply. *Eur Heart J Cardiovasc Imaging*. 2013 Jan;14(1):91-2.

159. Bellavia D, Pellikka PA, Al-Zahrani GB, Abraham TP, Dispenzieri A, Miyazaki C, Lacy M, Scott CG, Oh JK, Miller FA, Jr. Independent predictors of survival in primary systemic (AL) amyloidosis, including cardiac biomarkers and left ventricular strain imaging: an observational cohort study. *J Am Soc Echocardiogr*. 2010 Jun;23(6):643-52.

160. Carroll JD, Gaasch WH, McAdam KP. Amyloid cardiomyopathy: characterization by a distinctive voltage/mass relation. *Am J Cardiol*. 1982 Jan;49(1):9-13.

161. Sado D FA, White S, Banypersad SM, Maestrini V, Mehta A, Hawkins PN, Hausenloy DJ, Elliott P, Moon JC. Interstitial expansion in health and disease - an equilibrium contrast CMR

study. *Journal of cardiovascular Magnetic Resonance*. 2012 Feb 2012; Abstracts of the 15th Annual SCMR Scientific Sessions: 2012(14(Suppl 1)):1.

162. Roberts WC, Waller BF. Cardiac amyloidosis causing cardiac dysfunction: analysis of 54 necropsy patients. *Am J Cardiol*. 1983 Jul;52(1):137-46.

163. Monia BP AE, Guo S, Benson MD. Clinical Development of an antisense therapy for the treatment of TTR-associated polyneuropathy. 8th International Symposium on Familial Amyloid polyneuropathy. 2011 2011;S2-8(S2-8):S2-8.

164. Messroghli DR, Greiser A, Frohlich M, Dietz R, Schulz-Menger J. Optimization and validation of a fully-integrated pulse sequence for modified look-locker inversion-recovery (MOLLI) T1 mapping of the heart. *J Magn Reson Imaging*. 2007 Oct;26(4):1081-6.

165. Ugander M, Oki AJ, Hsu LY, Kellman P, Greiser A, Aletras AH, Sibley CT, Chen MY, Bandettini WP, Arai AE. Extracellular volume imaging by magnetic resonance imaging provides insights into overt and sub-clinical myocardial pathology. *Eur Heart J*. 2012 Jan 24.

166. Bandula S, Banypersad SM, Sado D, Flett AS, Punwani S, Taylor SA, Hawkins PN, Moon JC. Measurement of Tissue Interstitial Volume in Healthy Patients and Those with Amyloidosis with Equilibrium Contrast-enhanced MR Imaging. *Radiology*. 2013 May 14.

167. Gilmore IT, Burroughs A, Murray-Lyon IM, Williams R, Jenkins D, Hopkins A. Indications, methods, and outcomes of percutaneous liver biopsy in England and Wales: an audit by the British Society of Gastroenterology and the Royal College of Physicians of London. *Gut*. 1995 Mar;36(3):437-41.

168. Ronot M, Asselah T, Paradis V, Michoux N, Dorvilliers M, Baron G, Marcellin P, Van Beers BE, Vilgrain V. Liver fibrosis in chronic hepatitis C virus infection: differentiating minimal from intermediate fibrosis with perfusion CT. *Radiology*. 2010 Jul;256(1):135-42.

169. Friedrich-Rust M, Ong MF, Martens S, Sarrazin C, Bojunga J, Zeuzem S, Herrmann E. Performance of transient elastography for the staging of liver fibrosis: a meta-analysis. *Gastroenterology*. 2008 Apr;134(4):960-74.

170. Loustaud-Ratti VR, Cypierre A, Rousseau A, Yagoubi F, Abraham J, Fauchais AL, Carrier P, Lefebvre A, Bordessoule D, Vidal E, Sautereau D, Jaccard A. Non-invasive detection of hepatic amyloidosis: FibroScan, a new tool. *Amyloid*. 2011 Mar;18(1):19-24.

171. Huwart L, Sempoux C, Salameh N, Jamart J, Annet L, Sinkus R, Peeters F, ter Beek LC, Horsmans Y, Van Beers BE. Liver fibrosis: noninvasive assessment with MR elastography versus aspartate aminotransferase-to-platelet ratio index. *Radiology*. 2007 Nov;245(2):458-66.

172. Levitt DG. The pharmacokinetics of the interstitial space in humans. *BMC Clin Pharmacol*. 2003 Jul 30;3:3.

173. Benjaminsen IC, Brurberg KG, Ruud EB, Rofstad EK. Assessment of extravascular extracellular space fraction in human melanoma xenografts by DCE-MRI and kinetic modeling. *Magn Reson Imaging*. 2008 Feb;26(2):160-70.
174. Li SP, Padhani AR. Tumor response assessments with diffusion and perfusion MRI. *J Magn Reson Imaging*. 2012 Apr;35(4):745-63.
175. Orton MR, Miyazaki K, Koh DM, Collins DJ, Hawkes DJ, Atkinson D, Leach MO. Optimizing functional parameter accuracy for breath-hold DCE-MRI of liver tumours. *Phys Med Biol*. 2009 Apr 7;54(7):2197-215.
176. Padhani AR, Hayes C, Landau S, Leach MO. Reproducibility of quantitative dynamic MRI of normal human tissues. *NMR Biomed*. 2002 Apr;15(2):143-53.
177. Calvaruso V, Burroughs AK, Standish R, Manousou P, Grillo F, Leandro G, Maimone S, Pleguezuelo M, Xirouchakis I, Guerrini GP, Patch D, Yu D, O'Beirne J, Dhillon AP. Computer-assisted image analysis of liver collagen: relationship to Ishak scoring and hepatic venous pressure gradient. *Hepatology*. 2009 Apr;49(4):1236-44.
178. Standish RA, Cholongitas E, Dhillon A, Burroughs AK, Dhillon AP. An appraisal of the histopathological assessment of liver fibrosis. *Gut*. 2006 Apr;55(4):569-78.
179. Fontana M, White SK, Banypersad SM, Sado DM, Maestrini V, Flett AS, Piechnik SK, Neubauer S, Roberts N, Moon JC. Comparison of T1 mapping techniques for ECV quantification. Histological validation and reproducibility of ShMOLLI versus multibreath-hold T1 quantification equilibrium contrast CMR. *J Cardiovasc Magn Reson*. 2012;14:88.
180. White SK, Sado DM, Fontana M, Banypersad SM, Maestrini V, Flett AS, Piechnik SK, Robson MD, Hausenloy DJ, Sheikh AM, Hawkins PN, Moon JC. T1 Mapping for Myocardial Extracellular Volume Measurement by CMR: Bolus Only Versus Primed Infusion Technique. *JACC Cardiovasc Imaging*. 2013 Apr 5.
181. Schelbert EB, Testa SM, Meier CG, Ceyrolles WJ, Levenson JE, Blair AJ, Kellman P, Jones BL, Ludwig DR, Schwartzman D, Shroff SG, Wong TC. Myocardial extravascular extracellular volume fraction measurement by gadolinium cardiovascular magnetic resonance in humans: slow infusion versus bolus. *J Cardiovasc Magn Reson*. 2011;13:16.
182. Kawel N, Nacif M, Zavodni A, Jones J, Liu S, Sibley CT, Bluemke DA. T1 mapping of the myocardium: intra-individual assessment of post-contrast T1 time evolution and extracellular volume fraction at 3T for Gd-DTPA and Gd-BOPTA. *J Cardiovasc Magn Reson*. 2012;14:26.
183. Wong TC, Piehler KM, Kang IA, Kadakkal A, Kellman P, Schwartzman DS, Mulukutla SR, Simon MA, Shroff SG, Kuller LH, Schelbert EB. Myocardial extracellular volume fraction quantified by cardiovascular magnetic resonance is increased in diabetes and associated with mortality and incident heart failure admission. *Eur Heart J*. 2013 Jun 11.

184. Wong TC, Piehler K, Meier CG, Testa SM, Klock AM, Aneizi AA, Shakesprere J, Kellman P, Shroff SG, Schwartzman DS, Mulukutla SR, Simon MA, Schelbert EB. Association between extracellular matrix expansion quantified by cardiovascular magnetic resonance and short-term mortality. *Circulation*. 2012 Sep 4;126(10):1206-16.
185. Karamitsos TD, Piechnik SK, Banypersad SM, Fontana M, Ntusi NB, Ferreira VM, Whelan CJ, Myerson SG, Robson MD, Hawkins PN, Neubauer S, Moon JC. Noncontrast t1 mapping for the diagnosis of cardiac amyloidosis. *JACC Cardiovasc Imaging*. 2013 Apr;6(4):488-97.
186. Banypersad SM, Moon JC, Whelan C, Hawkins PN, Wechalekar AD. Updates in Cardiac Amyloidosis: A Review. *J Am Heart Assoc*. 2012;1:e000364.
187. Dall'Armellina E, Piechnik SK, Ferreira VM, Si QL, Robson MD, Francis JM, Cuculi F, Kharbanda RK, Banning AP, Choudhury RP, Karamitsos TD, Neubauer S. Cardiovascular magnetic resonance by non contrast T1-mapping allows assessment of severity of injury in acute myocardial infarction. *J Cardiovasc Magn Reson*. 2012;14:15.
188. Dass S, Suttie J, Piechnik SK, Ferreira V, Holloway C, Robson MD, Watkins H, Karamitsos T, Neubauer S. Non-contrast T1 mapping characterizes the myocardium beyond that achieved by late gadolinium enhancement in both hypertrophic and dilated cardiomyopathy. *J Cardiovasc Magn Reson*. 2012;14(Suppl 1):O27.
189. Bull S, White SK, Piechnik SK, Flett A, Ferreira V, Loudon M, Francis JM, Neubauer S, Moon JC, Myerson S. Pre-contrast T1 mapping for detection of myocardial fibrosis in asymptomatic and symptomatic aortic stenosis. *J Cardiovasc Magn Reson*. 2012;14(Suppl 1):P93.
190. Ferreira VM, Piechnik SK, Dall'Armellina E, Karamitsos TD, Francis JM, Choudhury RP, Friedrich MG, Robson MD, Neubauer S. Non-contrast T1-mapping detects acute myocardial edema with high diagnostic accuracy: a comparison to T2-weighted cardiovascular magnetic resonance. *J Cardiovasc Magn Reson*. 2012;14:42.
191. Benson L, Hemmingsson A, Ericsson A, Jung B, Sperber G, Thuomas KA, Westermark P. Magnetic resonance imaging in primary amyloidosis. *Acta Radiol*. 1987 Jan-Feb;28(1):13-5.
192. Liu D, Niemann M, Hu K, Herrmann S, Stork S, Knop S, Ertl G, Weidemann F. Echocardiographic evaluation of systolic and diastolic function in patients with cardiac amyloidosis. *Am J Cardiol*. 2011 Aug 15;108(4):591-8.
193. Bergesio F, Ciciani AM, Santostefano M, Brugnano R, Manganaro M, Palladini G, Di Palma AM, Gallo M, Tosi PL, Salvadori M. Renal involvement in systemic amyloidosis--an Italian retrospective study on epidemiological and clinical data at diagnosis. *Nephrol Dial Transplant*. 2007 Jun;22(6):1608-18.

194. Krombach GA, Hahn C, Tomars M, Buecker A, Grawe A, Gunther RW, Kuhl HP. Cardiac amyloidosis: MR imaging findings and T1 quantification, comparison with control subjects. *J Magn Reson Imaging*. 2007 Jun;25(6):1283-7.
195. Robbers LF, Baars EN, Brouwer WP, Beek AM, Hofman MB, Niessen HW, van Rossum AC, Marcu CB. T1 mapping shows increased extracellular matrix size in the myocardium due to amyloid depositions. *Circ Cardiovasc Imaging*. 2012 May 1;5(3):423-6.
196. Piechnik SK, Ferreira VM, Dall'Armellina E, Cochlin LE, Greiser A, Neubauer S, Robson MD. Shortened Modified Look-Locker Inversion recovery (ShMOLLI) for clinical myocardial T1-mapping at 1.5 and 3 T within a 9 heartbeat breathhold. *J Cardiovasc Magn Reson*. 2010 Nov 19;12(1):69.
197. Banypersad SM, Fontana M, Maestrini V, Sado DM, Captur G, Petrie A, Piechnik SK, Whelan CJ, Herrey AS, Gillmore JD, Lachmann HJ, Wechalekar AD, Hawkins PN, Moon JC. T1 mapping and survival in systemic light-chain amyloidosis. *Eur Heart J*. 2015 Jan 21;36(4):244-51.
198. Banypersad SM MJ, Whelan C, Hawkins PN, Wechalekar AD. Updates in Cardiac Amyloidosis : A Review. *Journal of the American Heart Association*. 2012;1 (2); e000364.
199. Wong TC, Piehler KM, Kang IA, Kadakkal A, Kellman P, Schwartzman DS, Mulukutla SR, Simon MA, Shroff SG, Kuller LH, Schelbert EB. Myocardial extracellular volume fraction quantified by cardiovascular magnetic resonance is increased in diabetes and associated with mortality and incident heart failure admission. *Eur Heart J*. 2014 Mar;35(10):657-64.
200. Kumar S, Dispenzieri A, Lacy MQ, Hayman SR, Buadi FK, Colby C, Laumann K, Zeldenrust SR, Leung N, Dingli D, Greipp PR, Lust JA, Russell SJ, Kyle RA, Rajkumar SV, Gertz MA. Revised prognostic staging system for light chain amyloidosis incorporating cardiac biomarkers and serum free light chain measurements. *J Clin Oncol*. 2012 Mar 20;30(9):989-95.
201. Vittinghoff E, McCulloch CE. Relaxing the rule of ten events per variable in logistic and Cox regression. *Am J Epidemiol*. 2007 Mar 15;165(6):710-8.
202. Finocchiaro G, Merlo M, Pinamonti B, Barbatì G, Santarossa E, Doimo S, Bussani R, Sinagra G. Long term survival in patients with cardiac amyloidosis. Prevalence and characterisation during follow-up. *Heart Lung Circ*. 2013 Feb 25.
203. Nelson MR, Lanza LA, Reeder CB, Scott RL, McCullough AE, Chandrasekaran K, Click RL. Histologic remission of cardiac amyloidosis: a case report. *Amyloid*. 2012 Jun;19(2):106-9.
204. Kellman P, Wilson JR, Xue H, Ugander M, Arai AE. Extracellular volume fraction mapping in the myocardium, part 1: evaluation of an automated method. *J Cardiovasc Magn Reson*. 2012;14:63.

16. APPENDIX

16.1 Acknowledgements:

A list of collaborators for this work is provided below. There are many people I would like to thank for their help with this work. First and foremost, I thank Dr. James Moon for his supervision and for spearheading the collaboration between the Heart Hospital and the Royal Free Hospital. I would like to thank Sarah Anderson, Dr. Daniel Sado and Dr. Derek Hausenloy for teaching me how to perform clinical CMR and Dr. Daniel Sado and Dr. Andrew Flett for teaching me how to perform T1 mapping based CMR. I am also thankful to Dr. Viviana Maestrini, Dr. Marianna Fontana and all the other fellows for their assistance during the scans during my 3 years at the unit. My thanks also to Sandy Gardner and Neelu Jauffur for booking the patients in for scans and for their patience when frequently rearranging their slots... and a special thank you to Neelu who also became my wife during this time.

At the Royal Free Hospital, I would like to thank Prof. Philip Hawkins for his supervision and support in creating this collaboration and getting the project off the ground. I also thank Drs. Gillmore, Wechalekar and Lachmann for teaching me about systemic amyloidosis over this last 3 years. I am grateful to the nursing staff, in particular Thirusha Lane, Lisa Rannigan and Darren Foard for their help in coordinating the MRI scans with the multiple investigations at the National Amyloidosis Centre. I must also thank Ramon Lamarca for rearranging patient bookings and slots in order to coincide with free MRI slots, as well Sherla Isaacs and Christianne Guillotte for arranging all the transport for the patients.

More distantly, I thank Prof. Sir Mark Pepys whose academic prowess was responsible for attracting the attention of industry to the department. I must also thank Mr. Duncan Richards for constantly supporting the project and for remaining actively involved in directing the project through regular meetings at the National Amyloidosis Centre.

Lastly, I would like to thank my parents and my brother Dr. Vishal Banypersad for their support over this 3 years.

List of Collaborators:

- James Moon,^{1,2} Reader and honorary Consultant in Cardiology: Primary supervisor.
- Prof. Philip Hawkins,³ Clinical Lead National Amyloidosis Centre: Secondary supervisor.
- Dr. Viviana Maestrini,¹ Clinical Research Fellow: Technical Development
- Dr. Marianna Fontana,^{1,3} Clinical Research Fellow: Technical Development
- Dr. Daniel Sado,¹ Clinical Research Fellow: Technical Development
- Dr. Jennifer Pinney,³ Clinical Research Fellow: Cardiac and extracardiac ECV
- Dr. Simon Gibbs,³ Clinical Research Fellow: Cardiac and extracardiac ECV
- Dr. Chris Venner,³ Clinical Research Fellow: Cardiac and extracardiac ECV
- Dr. Jason Dungu,³ Clinical Research Fellow: Pilot ATTR
- Dr. Ashutosh Wechalekar,³ Consultant Haematologist: Cardiac and extracardiac ECV
- Dr. Julian Gillmore,³ Consultant Nephrologist: Cardiac and extracardiac ECV
- Dr. Helen Lachmann,³ Consultant Nephrologist: Cardiac and extracardiac ECV
- Dr. Stefan Piechnik,⁴ Physicist: Pre contrast T1, Technical Development
- Dr. Matthew Robson,⁴ Physicist: Technical Development
- David Hutt,³ Nuclear Physicist: Pilot ATTR
- Dorothea Gopaul,³ Nuclear Physicist: Pilot ATTR
- Dr. Vanessa Ferreira,⁴ Clinical Research Fellow: Technical Development
- Dr. Theodoros Karamitsos,⁴ Clinical Research Fellow: Pre-contrast T1
- Prof. Stefan Neubauer,⁴ Professor of Cardiology: Technical Development
- Dr. Steve Bandula,⁵ Clinical Research Fellow: Extracardiac ECV
- Dr. Shonit Punwani,⁵ Consultant Radiologist: Extracardiac ECV
- Dr. Stuart Taylor,⁵ Consultant Radiologist: Extracardiac ECV
- Sarah Anderson, Sandy Gardner, Neelu Jauffur, Paula Campbell, Jodee Cooper, Queen's Square Enterprises Staff: CMR Logistics⁶
- Ramon Lamarca, Sherla Morris, Sam Ramiz, Christianne Guillotte, Leon Peet, Thirusha Lane, Annie Hughes, Alicia Bangova: National Amyloidosis Centre Logistics³
- Aviva Petrie,⁷ Head of Biostatistics: Statistical Analysis
- All the patients who took part in the research programme

1. The Heart Hospital, 16-18 Westmoreland Street, London, W1G 8PH.
2. Institute of Cardiovascular Science, University College London, London, WC1E 6BT.
3. Centre for Amyloidosis and Acute Phase Proteins and National Amyloidosis Centre, Royal Free Campus, University College London, Rowland Hill Street, London, NW3 2PF.
4. Oxford Centre for Clinical Magnetic Resonance Research, Department of Cardiovascular Medicine, University of Oxford, Oxford, OX3 9DU.
5. University College Hospital, Department of Radiology, Gower Street London, WC1E 6BT.
6. QSE, The heart Hospital Imaging Centre, The Heart Hospital, 16-18 Westmoreland Street, London, W1G 8PH.
7. Biostatistics Unit, UCL Eastman Dental Institute, 256 Grays Inn Road, London WC1X 8LD.

16.2 List of Original Findings:

1. T1 and ECV are measurable in cardiac amyloid
2. T1 and ECV track disease and early disease is detected prior to other changes
3. Cardiac, liver, spleen and skeletal muscle ECV are all raised in systemic AL amyloidosis compared to normal and are easily quantified using EQ-CMR
4. ECV and pre contrast myocardial T1 predict survival in systemic AL Amyloidosis
5. Change over time can be detected
6. ECV and T1 track disease burden in ATTR amyloidosis and provide insights into biology
7. Technically, the EQ-CMR technique using the FLASH IR method is reproducible but the ShMOLLI method of T1 mapping is superior for calculating ECV and pre contrast T1
8. The bolus only approach is sufficient and is equally prognostic as the infusion method

16.3 Location of Research:

All of the CMR imaging was performed at the Heart Hospital Imaging centre (16-18 Westmoreland Street, London, W1G 8PH). All nuclear imaging, Echocardiography, ECG, blood tests and 6 minute walk testing were all performed at the National Amyloidosis Centre.

16.4 Personal Contribution:

My contribution to this work is documented below:

- 1) Obtained minor ethics amendment.
- 2) Recruited, personally scanned, clinically reported and performed the research post processing on all of the patients.
- 3) Took preliminary hypotheses, proved them, developed new hypotheses and followed the science as it developed
- 4) Taught the technique to Dr. Marianna Fontana and played second author roles in the subsequent ATTR studies.
- 5) Performed most of the statistical analysis presented in this thesis.
- 6) Wrote this thesis.

16.5 Supervision:

Primary supervisor: Dr James Moon

Secondary supervisor: Prof. Philip Hawkins

16.6 Funding:

This work was funded by GlaxoSmithKline.

16.7 Prizes / Awards:

- May 2012 – Won €1000 as Young Investigator Award winner, International Symposium for Amyloidosis, Groningen, The Netherlands.
- Nov 2013 – Won \$500 as AHA Young Investigator Award finalist, Dallas, USA.
- Jan 2014 – SCMR Young Investigator Award finalist, SCMR, New Orleans, USA.

16.8 Publications:

1. **Banypersad SM, Fontana M, Maestrini V, Sado DM, Captur G, Petrie A, Piechnik SK, Whelan CJ, Herrey AS, Gillmore JD, Lachmann HJ, Wechalekar AD, Hawkins PN, Moon JC.** “T1 mapping and survival.” *European Heart Journal* (2015); 36(4): 244-51.

2. Sado DM, Maestrini V, Piechnik SK, **Banypersad SM**, White SK, Flett AS, Robson MD, Neubauer S, Ariti C, Arai A, Kellman P, Yamamura J, Schoennagel BP, Shah F, Davis B, Trompeter S, Walker M, Porter J, Moon JC. "Non-contrast myocardial T₁ mapping using cardiovascular magnetic resonance for iron overload." *J Magn Reson Imaging*. 2014 Aug 8. doi: 10.1002.
3. Fontana M, **Banypersad SM**, Treibel TA, Maestrini V, Sado DM, White SK, Pica S, Castaletti S, Piechnik SK, Robson MD, Gilbertson JA, Rowczenio D, Hutt DF, Lachmann HJ, Wechalekar AD, Whelan CJ, Gillmore JD, Hawkins PN, Moon JC. "Native T1 Mapping in Transthyretin Amyloidosis." *JACC Cardiovascular Imaging*. 2014; 7(2), 157-65
4. Pinney JH, Smith CJ, Taube JB, Lachmann HJ, Venner CP, Gibbs SD, Dungu J, **Banypersad SM**, Wechalekar AD, Whelan CJ, Hawkins PN, Gillmore JD. "Systemic amyloidosis in England: An Epidemiological study." *Br J Haem* 2013 May;161(4):525-32. doi: 10.1111/bjh.12286.
5. Bandula S, **Banypersad SM**, Sado D, Flett AS, Punwani S, Taylor SA, Hawkins PN, Moon JC. Measurement of Tissue Interstitial Volume in Healthy Patients and Those with Amyloidosis with Equilibrium Contrast-enhanced MR Imaging. *Radiology*. 2013 May 14
6. Pinney JH, Whelan CJ, Petrie A, Dungu J, **Banypersad SM**, Sattianayagam P, Wechalekar A, Gibbs SD, Venner CP, Wassef N, McCarthy CA, Gilbertson JA, Rowczenio D, Hawkins PN, Gillmore JD, Lachmann HJ. "Senile systemic amyloidosis: clinical features at presentation and outcome." *J Am Heart Assoc*. 2013 Apr 22;2(2):e000098
7. White SK, Sado DM, Fontana M, **Banypersad SM**, Maestrini V, Flett AS, Piechnik SK, Robson MD, Hausenloy DJ, Sheikh AM, Hawkins PN, Moon JC. "T1 Mapping for Myocardial Extracellular Volume Measurement by CMR: Bolus Only Versus Primed Infusion Technique." *JACC Cardiovasc Imaging*. 2013 Apr 5
8. Sado DM, White SK, Piechnik SK, **Banypersad SM**, Treibel T, Captur G, Fontana M, Maestrini V, Flett AS, Robson MD, Lachmann RH, Murphy E, Mehta A, Hughes D, Neubauer S, Elliott PM, Moon JC. "The Identification and Assessment of Anderson Fabry Disease by Cardiovascular Magnetic Resonance Non-Contrast Myocardial T1 Mapping." *Circ Cardiovasc Imaging*. 2013 1;6(3), 392-8.

9. Karamitsos TD, Piechnik SK, **Banypersad SM**, Fontana M, Ntusi NB, Ferreira VM, Whelan CJ, Myerson SG, Robson MD, Hawkins PN, Neubauer S, Moon JC. "Noncontrast t1 mapping for the diagnosis of cardiac amyloidosis." *JACC Cardiovasc Imaging*. 2013 Apr;6(4):488-97
10. **Banypersad SM**, Sado DM, Flett AS, Gibbs SD, Pinney JH, Maestrini V, Cox AT, Fontana M, Whelan CJ, Wechalekar AD, Hawkins PN, Moon JC. "Quantification of myocardial extracellular volume fraction in systemic AL amyloidosis: an equilibrium contrast cardiovascular magnetic resonance study." *Circ Cardiovasc Imaging*. 2013 Jan 1;6(1):34-9
11. Fontana M, White SK, **Banypersad SM**, Sado DM, Maestrini V, Flett AS, Piechnik SK, Neubauer S, Roberts N, Moon JC. "Comparison of T1 mapping techniques for ECV quantification. Histological validation and reproducibility of ShMOLLI versus multibreath-hold T1 quantification equilibrium contrast CMR." *J Cardiovasc Magn Reson*. 2012 Dec 28; 14: 88-96
12. **Banypersad SM**, Moon JC, Whelan C, Hawkins PN, Wechalekar AD. Updates in cardiac amyloidosis: a review. *J Am Heart Assoc*. 2012 Apr;1(2):e000364
13. Sado DM, Flett AS, **Banypersad SM**, White SK, Maestrini V, Quarta G, Lachmann RH, Murphy E, Mehta A, Hughes DA, McKenna WJ, Taylor AM, Hausenloy DJ, Hawkins PN, Elliott PM, Moon JC. Cardiovascular magnetic resonance measurement of myocardial extracellular volume in health and disease. *Heart*. 2012 Oct;98(19):1436-41
14. Dungu J, Sattianayagam PT, Whelan CJ, Gibbs SD, Pinney JH, **Banypersad SM**, Rowczenio D, Gilbertson JA, Lachmann HJ, Wechalekar A, Gillmore JD, Hawkins PN, Anderson LJ. The electrocardiographic features associated with cardiac amyloidosis of variant transthyretin isoleucine 122 type in Afro-Caribbean patients. *Am Heart J*. 2012 Jul;164(1):72-9

16.9 Abstract Presentations:

16.9.1 Oral Presentations:

1. Cardiac Amyloid Burden Assessment by T1 Mapping Predicts Survival in Systemic AL Amyloidosis: A 2 year follow up study

- *SCMR Young Investigator Award, SCMR, New Orleans, USA, Jan 2014*

2. T1 Mapping and Survival in Systemic Amyloidosis

- *AHA Young Investigator Award, AHA, Dallas, USA, Nov 2013*

3. Assessment of Organ Dysfunction in Systemic AL Amyloidosis using Equilibrium MRI to calculate Extracellular Volume Fraction

- *EuroCMR, Florence, Italy, May 2013*

4. Multi-Organ ECV as Measured by Eq-MRI in Systemic Amyloidosis

- *SCMR, San Francisco, USA, Feb 2013*

5. Cardiac Disease in Systemic Amyloidosis as Measured by Eq-CMR

- *Young Investigator Award, International Amyloidosis Symposium, Groningen, Holland, May 2012*

6. Pre-Contrast ShMOLLI T1 mapping in Cardiac AL Amyloidosis

- *SCMR, Orlando, USA, Feb 2012*

16.9.2 Poster Presentations:

1. Cardiac Disease in Systemic AL Amyloidosis as measured by EQ-CMR

- *SCMR, Orlando, Feb 2012*

2. Cardiac Involvement in Systemic AL Amyloidosis as measured by EQ-CMR

- *BCS, Manchester, June 2012*

16.9.3 Named-author Abstracts Presented by Others:

1. Mahmood S, Venner CP, Lane T, Rannigan L, Foard D, Pinney J, **Banypersad SM**, Dungu J, Whelan C, Lachmann HJ, Gillmore JD, Hawkins PN, Wechalekar A, "Continuous Therapy with Lenalidomide Correlates with Improved Progression Free Survival in Heavily Pre-Treated Patients with AL Amyloidosis." Blood (2012); 120(21), 2978
2. Venner CP, Lane T, Foard D, Rannigan L, Mahmood S, Gibbs SDJ, Pinney J, **Banypersad SM**, Dungu J, Whelan C, Lachmann H, Gillmore JD, Hawkins PN, Wechalekar A, "A Matched Comparison of Cyclophosphamide, Bortezomib and Dexamethasone (CVD) Versus Cyclophosphamide, Thalidomide and Dexamethasone (CTD) in the Treatment of Mayo Cardiac Stage III Patients with AL Amyloidosis." Blood (2012); 120(21), 2966
3. Lane T, Rannigan L, Foard D, Wechalekar A, Gibbs S, Pinney J, Venner CP, **Banypersad SM**, Lachmann H, Hawkins PN, Gillmore JD, "ALchemy - A Large Prospective 'Real World' Study of Chemotherapy in AL Amyloidosis" Blood (2011); 118(21), 453
4. Pinney JH, Lachmann HJ, Gillmore JG, Wechalekar A, Gibbs SD, Sattianayagam P, **Banypersad SM**, Dungu J, Wassef N, McCarthy CA, Hawkins PN, Whelan CJ. Senile Systemic Amyloidosis: A common cause of heart failure in the elderly? Heart (2011); 97(Suppl 1), 59-60